UNIVERSITY OF SOUTHAMPTON

FACULTY OF NATURAL AND ENVIRONMENTAL SCIENCES

SCHOOL OF OCEAN AND EARTH SCIENCE

The Biogeochemical Role of *Coccolithus pelagicus*

by

Chris James Daniels

Thesis for the degree of Doctor of Philosophy

June 2015

UNIVERSITY OF SOUTHAMPTON

ABSTRACT

FACULTY OF NAUTRAL AND ENVIRONMENTAL SCIENCES
SCHOOL OF OCEAN AND EARTH SCIENCE

Doctor of Philosophy

THE BIOGEOCHEMICAL ROLE OF *COCCOLITHUS PELAGICUS*

by Chris James Daniels

Coccolithophores are a biogeochemically important group of phytoplankton, responsible for around half of oceanic carbonate production through the formation of calcite coccoliths. Globally distributed, *Emiliania huxleyi* is generally perceived to be the key calcite producer, yet it has a relatively low cellular calcite content (~ 0.4 – 0.7 pmol C cell^{-1}) compared to heavily calcified species such as *Coccolithus pelagicus* (~ 15 – 21 pmol C cell^{-1}). This study set out to test the central hypothesis that *C. pelagicus* has a significant biogeochemical role, dominating calcite production within mixed communities in the North Atlantic. Cultures of *Coccolithus* species *(C. pelagicus, C. braarudii)* and *E. huxleyi* were grown in parallel to examine relative growth rates, and relative calcite production was modelled. While *E. huxleyi* grew faster than *C. pelagicus*, it was estimated that at the average relative growth rate observed, *C. pelagicus* calcified at a rate equivalent to 34 cells of *E. huxleyi*. This was compared to field samples of abundances from the North Atlantic, where *C. pelagicus* was found to be the major calcite producer in 69 % of the samples. At two sites in the North Atlantic (Iceland Basin, Norwegian Sea), repeat samples were collected during the early stages of the spring bloom to examine phytoplankton community dynamics and the role of coccolithophores. The two sites had contrasting communities with diatoms dominant in the Iceland Basin, but absent in the Norwegian Basin. The coccolithophore community was generally similar, with *E. huxleyi* dominating abundance and *C. pelagicus* dominating coccolithophore calcite. In situ growth rates found that *C. pelagicus* grew faster than *E. huxleyi*. In the Arctic and North Atlantic, species-specific calcite production was determined from measurements of calcite production and community composition. The results of this study indicated that *C. pelagicus* dominated calcite production despite forming only a small fraction (< 2 %) of the community. In the synthesis, the seasonal contribution of *C. pelagicus* to calcite production was determined, using measured growth rates to estimate calcite production in spring. *Coccolithus pelagicus* was found to be the major source of calcite in the North Atlantic throughout the early to late spring and summer. When *C. pelagicus* was absent, other heavily calcified species, such as *Coronosphaera mediterranea* and *Helicosphaera carteri*, were important sources of calcite.

Table of Contents

List of Figures

List of Tables

Declaration of Authorship

I, Chris Daniels, declare that this thesis entitled "The Biogeochemical Role of *Coccolithus pelagicus*" and the work presented in it are my own and has been generated by me as the result of my own original research. I confirm that:

- This work was done wholly or mainly while in candidature for a research degree at this University;
- Where any part of this thesis has previously been submitted for a degree or any other qualification at this University or any other institution, this has been clearly stated;
- Where I have consulted the published work of others, this is always clearly attributed;
- Where I have quoted from the work of others, the source is always given. With the exception of such quotations, this thesis is entirely my own work;
- I have acknowledged all main sources of help;
- Where the thesis is based on work done by myself jointly with others, I have made clear exactly what was done by others and what I have contributed myself;
- Parts of this work have been published as:

Daniels, C. J., Poulton, A. J., and Sheward, R. M.: Biogeochemical implications of comparative growth rates of Emiliania huxleyi and Coccolithus species, Biogeosciences, 11, 6915-6925, 2014.

Daniels, C. J., Poulton, A. J., Esposito, M., Paulsen, M. L., Bellerby, R., St. John, M., and Martin, A. P.: Phytoplankton dynamics in contrasting early stage North Atlantic spring blooms: composition, succession, and potential drivers, Biogeosciences, 12, 2395-2409, 2015.

Signed .....

Date.....

Acknowledgements

Firstly I would like to thank my supervisor Alex Poulton for your guidance, knowledge and ability to rein me in my overly-complicated ideas. I hope I have repaid the faith you put in me when I unintentionally did my best not to get this PhD. Thank you for the significant chunk of your time that you have dedicated towards me over the last 5 years. To Toby Tyrrell, thank you for getting me interested in coccolithophores, I haven't looked back since. To Jeremy Young, thank you for your advice and expertise.

A big thank you to Ian Probert for giving up your time to allow me to visit Roscoff and learn how to culture. Your knowledge and invaluable advice helped me enormously with everything related to culturing. A further thanks goes to John Gittins for your help and putting up with my forgetfulness when it comes to emptying autoclaves.

Thank you to all those involved in the UK-OA project that allowed me to participate in the Arctic and Southern Ocean cruises. Thanks to the crew of the RRS James Clark Ross. Thank you also to those involved in the EuroBASIN project, particularly the crew of the R/V Meteor for coping with my poor to non-existent German.

I am indebted to many people at NOC for their time and help. Richard Pearce spent hours helping to capture the perfect image on the SEM. Thanks to Darryl Green and Matt Cooper for running the PIC analysis, Mark Stinchcombe for the BSi analysis, running nutrients and patiently teaching me to be a nutrient chemist, Stuart Painter for helping with ^{13}C calculations, Sharon McNeil for POC and ^{13}C analysis.

Thank you Jason for your sage wisdom throughout our PhDs. You proved an excellent sounding board and our discussions proved very useful. Thank you to Rosie for your expert eye on the microscope. To my many office mates: Simon, Sam, Sian, Katsia, Rose, Erik and Steph, thank-you for putting up with me. Thank you for Matthew for being a great housemate and my go to carbonate chemist.

My biggest thanks must go to my family, who have supported me completely throughout the course of my studies, and for pretending to be interested in coccolithophores. Finally, thank you to Lucie for being the only person other than my supervisors and myself to read my entire thesis.

List of Abbreviations

AMpS	Automated Marine pH Sensor
A_T	Total Alkalinity
BCP	Biological Carbon Pump
$bSiO_2$	Particulate Silicate
C	Cellular Calcite
Chl *a*	Chlorophyll *a*
CP	Calcite Production
CP_{bulk}	Total Calcite Production
CP_{sp}	Species-Specific Calcite Production
CRM	Certified Reference Material
C_T	Dissolved Inorganic Carbon
CTD	Conductivity Temperature Depth
dSi	Silicic Acid
EGC	East Greenland Current
HOL	Holococcolithophore
ICB	Iceland Basin
K_d	Vertical Diffuse Attenuation Coefficient of PAR
k_s	Coccolith Shape Factor
MDT	Micro-diffusion Technique
MODIS	Moderate Resolution Image Spectroradiometer
N	Abundance
N*	$NO_x - 16 \times PO_4$
NC	Norwegian Current
NO_3	Nitrate
NO_x	Nitrate + Nitrite
NWB	Norwegian Basin
OWSM	Ocean Weather Station Mike
PAR	Photosynthetically Active Radiation
PC	Principal Component
PCA	Principal Component Analysis

$pCO2^{sw}$	Seawater Partial Pressure of CO_2
pH_T	pH on the Total Scale
PIC	Particulate Inorganic Carbon / Calcite
PO_4	Phosphate
POC	Particulate Organic Carbon
PON	Particulate Organic Nitrogen
POP	Particulate Organic Phosphorus
PP	Primary Production
RCC	Roscoff Culture Collection
SEM	Scanning Electron Microscope
Si*	dSi - NO_x
SSS	Sea Surface Salinity
SST	Sea Surface Temperature
WMLD	Winter Mixed Layer Depth
Z_{eup}	Depth of the Euphotic Zone
$\Delta\sigma_t$	Change in Density with Temperature
μ	Growth Rate
μ_{Chl}	Growth Rate by Change in Chlorophyll
Ω_c	Calcite Saturation State
$\%CP_{sp}$	Species-Specific Calcite Production as a Percentage of Total Calcite Production

Chapter 1: General Introduction

1.1 Phytoplankton

Phytoplankton are photosynthetic microscopic organisms, responsible for the majority of primary production in the ocean. Despite forming less than 1 % of the photosynthetic biomass on Earth, phytoplankton perform around 50 % of the photosynthesis, and are vital in shaping the ecology and biogeochemistry of life on Earth (Falkowski and Raven, 2007). In the process of photosynthesis (Eq. 1.1), phytoplankton take up dissolved carbon dioxide (CO_2) and water and through the absorption of light by photosynthetic pigments (primarily chlorophyll a [Chl *a*]), fix carbon into organic compounds (Falkowski and Raven, 2007). In converting light energy into organic matter, phytoplankton form the base of nearly all marine food webs, sustaining marine ecosystems and influencing biological and biogeochemical processes (Falkowski and Raven 2007; Sanders et al. 2014).

$$2H_2O + CO_2 + Light \xrightarrow{Chl\ a} (CH_2O) + H_2O + O_2 \quad (1.1)$$

The phytoplankton community is very diverse, thought to number at least 5000 individual species (Tett and Barton, 1995; Guiry, 2012), and consisting of several major groups including cyanobacteria, diatoms, dinoflagellates, and coccolithophores. In addition to a large species diversity, phytoplankton have a huge variability in cell size, ranging over nine orders of magnitude, from the < 2µm picoplankton, through the 2 – 20 µm nanoplankton, the 20 – 200 microplankton, upto the > 200 µm macroplankton (Finkel et al., 2009). While how such diversity is able to coexist in the oceans has perplexed scientists for over 50 years, (Hutchinson, 1961; Kenitz et al., 2013), the significant role of phytoplankton in global carbon cycling is well understood.

1.2 Carbon cycle

The cycling of carbon on Earth plays a critical role in controlling the climate. The concentration of atmospheric CO_2 is an important regulator of the Earth's temperature (Falkowski et al., 2000). Over the last 200 years, anthropogenic emissions of CO_2 have resulted in an unprecedented increase in atmospheric CO_2, exceeding 400 ppm for the first time in 2013 (https://scripps.ucsd.edu/programs/keelingcurve/). The ocean is the largest reservoir of actively cycling carbon on Earth (> 38,000 Gt C, Falkowski et al., 2000) and has taken up nearly a third of the anthropogenic CO_2 released into the atmosphere (Sabine et al., 2004). The air-sea exchange of CO_2 is rapid, resulting in an equilibrium between the atmosphere and the surface ocean. The transport of carbon to depth away from the rapidly equilibrating surface layer is a vital process in the carbon cycle, with approximately 96 % of the oceanic carbon pool in the deep ocean (Falkowski et al. 2000).

Three processes drive the transport of carbon to depth: the solubility pump, the biological carbon pump and the carbonate counter pump (Volk and Hoffert 1985). The solubility pump, responsible for the largest turnover of carbon between the surface and deep ocean (~ 100 Gt C, Ciais et al., 2013), is driven by both the increased solubility of CO_2 in colder waters and the thermohaline circulation. Cold deep water formation at high latitudes, particularly in the North Atlantic and the Southern Ocean, is transported into the interior of the ocean, carrying CO_2 to depth (Fig. 1.1). Through ventilation and upwelling, these waters will be transported throughout the oceans eventually returning to surface waters several hundred years later and re-equilibrating with atmospheric CO_2. The main focus of the following sections will be on the biologically driven pumps, the biological carbon pump and the carbonate counter pump.

1.2.1 Biological carbon pump

The biological carbon pump (BCP) is the process whereby particulate organic carbon (POC) is transported, mostly as sinking particles, from the surface ocean to the deep

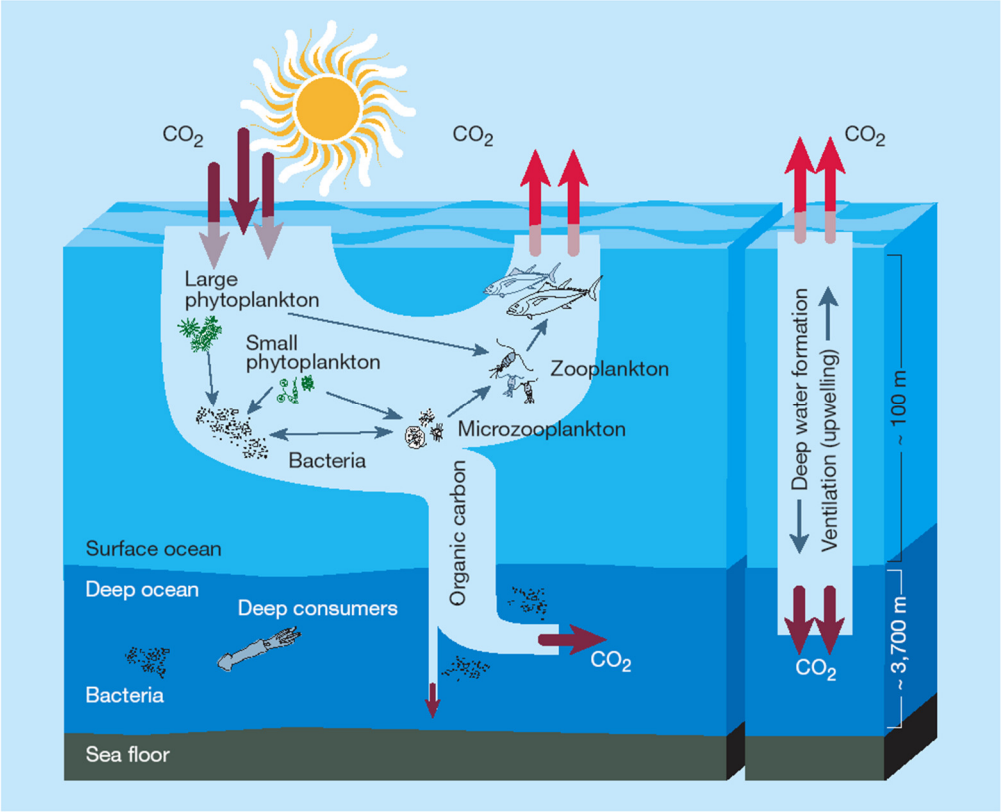

Fig. 1.1: A schematic of the biological carbon pump and the solubility pump (Chisholm, 2000)

ocean (Sanders et al., 2014). In the euphotic zone of the ocean, phytoplankton receive enough light to photosynthesise, fixing carbon into POC (Fig. 1.1). From the formation of such POC, a number of processes can occur that result in the transport of the phytoplankton POC to depth. Zooplankton grazing of the plankton community produces dense faecal pellets, facilitating rapid export, aggregation of phytoplankton cells into marine snow, or negatively buoyant phytoplankton cells may individually be exported (Boyd and Trull, 2007).

The BCP is an inefficient process; as POC sinks through the twilight zone (defined as beginning at the base of the euphotic zone down to ~ 1000m), up to 95 % of it may be remineralised (Boyd and Trull, 2007; Henson et al., 2011) into inorganic carbon by bacteria or zooplankton (Giering et al., 2014; Sanders et al., 2014). Sequestration of POC only occurs if the POC is exported below the winter mixed layer, operationally defined as ~ 1000m (Sanders et al., 2014). Below this depth, it is assumed that organic

carbon will not be immediately mixed back up to the surface ocean but instead will be sequestered for decades or longer (Sanders et al., 2014). Of the total primary production occurring in the surface ocean, only ~ 1 % reaches abyssal depths (3000 m, Poulton et al., 2006).

As the initial stage in the BCP, the phytoplankton community can significantly influence the BCP. Small changes in primary production can significantly affect the magnitude of the exported material (Boyd and Newton, 1995), while a change in the composition of the plankton community structure can affect sinking rates of the exported material and thus the efficiency of the BCP (Sanders et al., 2014). Changes in the magnitude or efficiency of the BCP could significantly impact the climate system; it is estimated that the atmospheric CO_2 concentration would be approximately 50 % higher if the BCP did not function (Parekh et al., 2006).

The phytoplankton community structure can further influence the BCP through the production of biominerals; POC is ballasted by denser biominerals, increasing the transfer of POC to the deep ocean with the biominerals potentially protecting the sinking POC from remineralisation within the twilight zone (Armstrong et al., 2001; Sanders et al., 2014). The two major biominerals involved in the ballasting of POC are calcite and opal (Armstrong et al., 2001). Opal is a silicic mineral predominately produced by diatoms, while calcite is the most stable form of calcium carbonate, produced in the pelagic ocean mainly by coccolithophores and foraminifera (Broecker and Clark, 2009).

1.3 Coccolithophores

Coccolithophores are a diverse group of single celled phytoplankton belonging to the division Haptophyta. They are distinguished from other phytoplankton in that during at least part of their life cycle (Billard and Inouye, 2004), they produce extracellular calcite plates (coccoliths) to form a complete test (coccosphere) around their cell (Fig 1.2). Of the approximately 300 species of haptophyte in the modern ocean, about 200

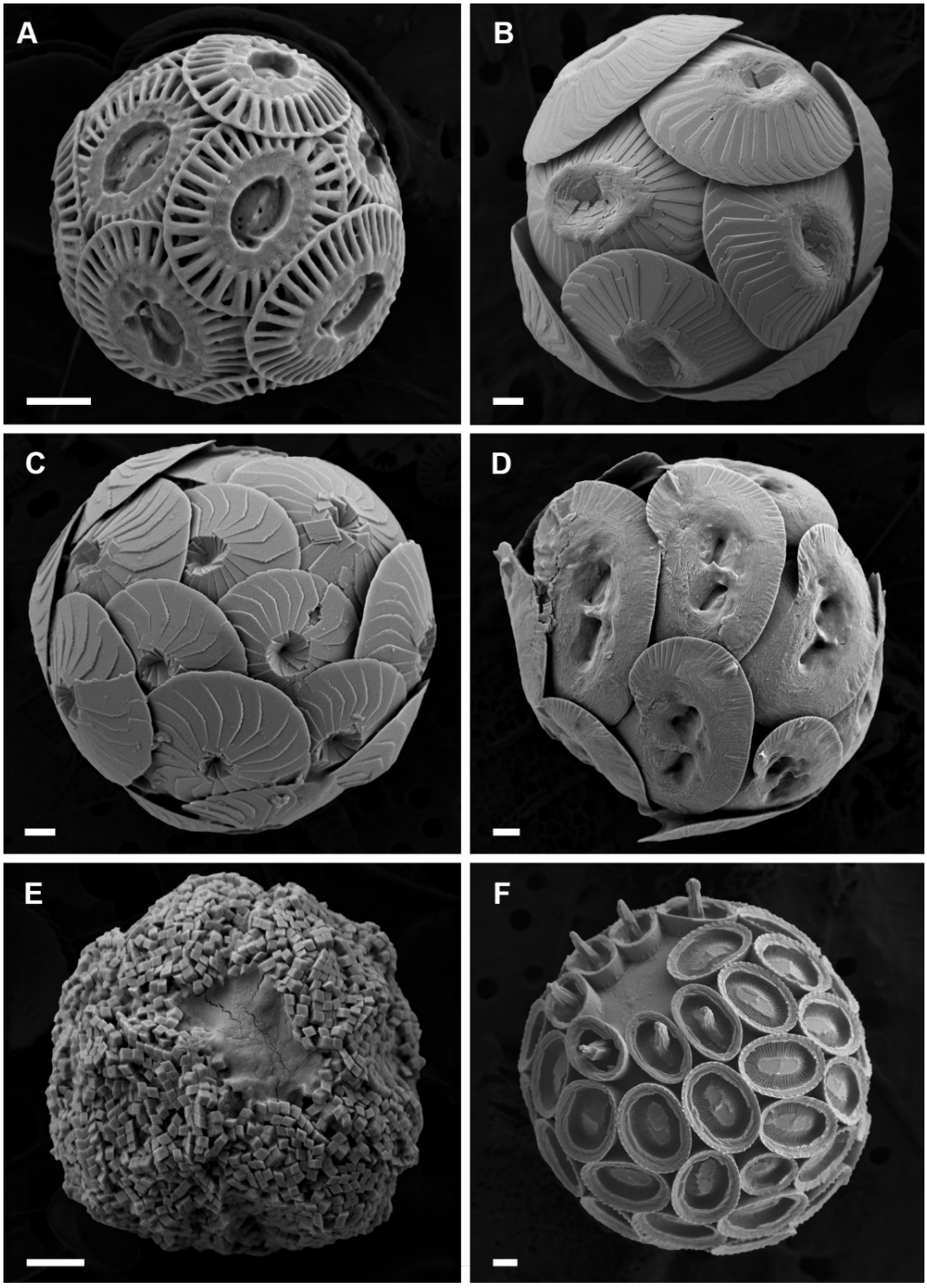

Fig. 1.2: SEM images of coccolithophores. A) *Emiliania huxleyi*. B) *Coccolithus pelagicus*. C) *Calcidiscus leptoporus*. D) *Helicosphaera carteri*. E) *Coccolithus pelagicus* HOL. F) *Coronosphaera mediterranea*. Scale bars represent 1 µm in each image. Image credit Martine Couapel.

of these are calcifying coccolithophores (Young et al., 2003; Billard and Inouye, 2004). With a long lineage, dating back to at least 225 Ma to the Upper Triassic period, and forming one of the most abundant and stratigraphically complete fossil groups (Bown et al., 2004), coccolithophores are a key group for paleontological research (Cachao and Moita, 2000; Gibbs et al., 2013). In the modern ocean, *Emiliania huxleyi* is the most widespread and abundant species of coccolithophore, capable of forming intensive blooms that turn surface waters milky white and can be detected by satellite (Holligan et al., 1983; Holligan et al., 1993).

Many species of coccolithophore are heteromorphic; their life-cycle consists of haploid and diploid phases (Houdan et al., 2004), both of which are capable of asexual reproduction (Billard and Inouye, 2004). The different phases bear different coccoliths or organic scales (Billard and Inouye, 2004). In the diploid phase, coccolithophores produce heterococcoliths intracellularly and consist of an array of complex crystal units (Young et al., 2003). In contrast, the haploid phase is either non-calcifying, in species such as *E. huxleyi*, or produces holococcoliths formed of many small (~ 0.1 μm) euhedral crystals (Young et al., 2003). The holococcoliths and heterococcoliths are so different that in almost all species the separate phases were originally described as different species (Young and Henriksen, 2003). Through flow cytometric analysis (Houdan et al., 2004), identification of combination coccospheres bearing both heterococcoliths and holococcoliths (Geisen et al., 2002), and observations of life-cycle transitions within cultures (Parke and Adams, 1960), diploid-haploid pairs have been identified for many species, resulting in a revised taxonomic system of nomenclature (Young et al., 2003). Natural communities of coccolithophores tend to be dominated by the heterococcolith bearing diploid phase (e.g., Okada and Mcintyre, 1979; Poulton et al., 2010; Frada et al., 2012), as does coccolithophore export (Ziveri et al., 2007).

With multiple impacts on the carbon cycle, coccolithophores are a biogeochemically important group of phytoplankton, through the production of both particulate inorganic and organic carbon. Coccolithophores photosynthesise and although they

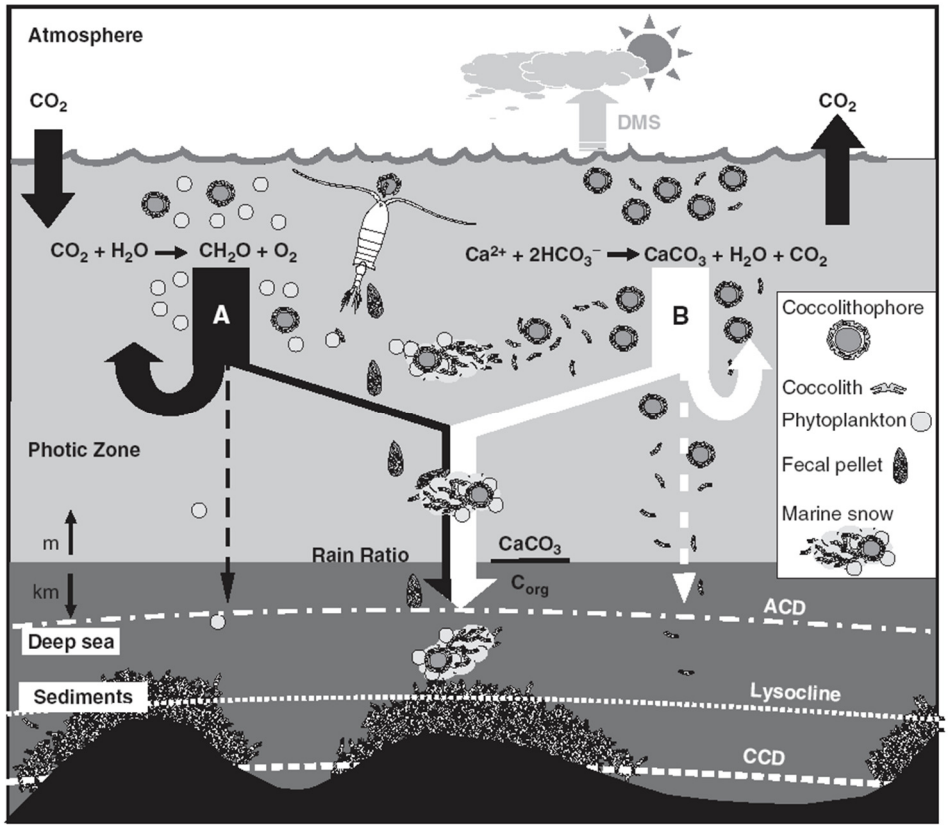

Fig. 1.3: A schematic of A) the biological carbon pump, and B) the carbonate counter pump (De Vargas et al., 2007).

rarely dominate the phytoplankton community (Poulton et al., 2013; Poulton et al., 2014), they constitute up to 20 % of primary production in certain oceanic regions (Poulton et al., 2006; Poulton et al., 2007; Poulton et al., 2010). Therefore coccolithophore-derived POC significantly contributes to the BCP. The production of particulate inorganic carbon by coccolithophores through the process of calcification has both direct and indirect effects on carbon cycling.

1.3.1 Coccolithophore calcification and the carbonate pump

Calcification in diploid cells of coccolithophores takes place intracellularly within a specialised Golgi-derived vesicle (Young and Henriksen, 2003). An organic scale or baseplate forms within the vesicle, followed by nucleation of calcite crystals to form the coccolith. The process of calcite crystal formation is highly precise and is dependent on calcium binding proteins and polysaccharides (Taylor et al., 2007). Post-

formation, the coccoliths, complete with an organic coating (Young and Henriksen, 2003) are secreted through the cell membrane to form the coccosphere, in a process not well understood (Paasche, 2002; Young et al., 2003). The process of coccolith formation has been studied mainly in *E. huxleyi* and *Pleurochrysis carterae*, a coastal species of coccolithophore (Young and Henriksen, 2003). However, observations of coccolith formation in other species, including *Coccolithus pelagicus* (Taylor et al., 2007), *Umbilicosphaera sibogae* and *Syracosphaera pulchra* (Young and Henriksen, 2003), found that although there is significant inter-species variability in the process of coccolith formation, in all species examined, heterococcoliths are formed within a Golgi-derived vesicle in all species examined.

The process of calcification involves the uptake of calcium and bicarbonate ions to produce calcium carbonate (Eq. 1.2). Although theoretically correct, this reaction equation is an oversimplification as calcite production occurs within the upper ocean where the carbonate system exists in equilibrium and acts to buffer changes (Wolf-Gladrow et al., 2007). The precipitation of 1 mole of calcite results in the decrease in the total alkalinity (A_T) by 2 moles and dissolved inorganic carbon (C_T) by 1 mole. The resulting shift in the system causes an increase in the seawater partial pressure of CO_2 (pCO_2^{sw}), such that calcification is a source of CO_2 (Wolf-Gladrow et al., 2007).

$$Ca^{2+} + 2HCO_3^- \longrightarrow CaCO_3 + H_2O + CO_2 \qquad (1.2)$$

The production of calcium carbonate works in opposition to the photosynthetic production of organic carbon (Fig. 1.3). This process is known as the carbonate counter pump (Rost and Riebesell, 2004) and is the third main process within the oceanic carbon cycle (Falkowski et al., 2000). However, while on short time scales (centuries) the carbonate pump acts as a source of CO_2, over geological time scales (millions of years) the formation, export, and burial of carbonate is a significant sink for CO_2 as the Ca supply from weathering matches the removal of carbonates (Broecker and Peng, 1987; Falkowski et al., 2000). Sedimentary carbonates, including calcium carbonate form the largest reservoir of carbon on Earth (Falkowski et al., 2000). Coccolithophores are responsible for around half of oceanic carbonate production (Broecker and Clark,

2009) and form a major component of the carbonate pump. Together with their significant role in the BCP through both the export of their organic material, and the ballast effect that their coccoliths provide, coccolithophores play a key role in the biogeochemical cycling of carbon in the ocean.

Despite the biogeochemical importance of coccolith formation, the function of coccoliths is unclear (Young, 1994). Calcification is an energy intensive process (Brownlee and Taylor, 2004) and thus from an evolutionary perspective, should have a beneficial function. The proposed functions include protection from predation, regulation of light, buoyancy control and a beneficial by-product of photosynthesis (Young, 1994). The huge diversity of coccolithophores (Young et al., 2003) suggests that coccoliths may have different functions depending on the ecological niche of the species (Young, 1994).

1.3.2 Ocean acidification

While the uptake of anthropogenic CO_2 into the ocean has reduced the concentration of atmospheric CO_2 and slowed the rate of climate change, it has had an adverse effect on the ocean itself. The increase of pCO_2^{sw} causes a decrease in pH as the CO_2 reacts with water to form carbonic acid (H_2CO_3) which dissociates into bicarbonate (HCO_3^-) and carbonate (CO_3^{2-}) ions thus increasing the concentration of H^+ (Doney et al., 2009). In an increasingly acidic ocean, marine calcifiers are expected to find it harder to produce and maintain their calcite shells (Society, 2005). The response of coccolithophores to ocean acidification is unclear, culture experiments have produced conflicting responses (summarised in Raven and Crawfurd, 2012). Reduced calcite production at high pCO_2^{sw} was observed in *E. huxleyi* and *Gephyrocapsa oceanica* (Riebesell et al., 2000), yet the opposite response was observed by Iglesias-Rodriguez et al. (2008) with increased calcification at high pCO_2^{sw}. The response of coccolithophores to ocean acidification is strain-specific (Iglesias-Rodriguez et al., 2008; Langer et al., 2009; Hoppe et al., 2011), thus culture experiments may not realistically represent the in situ response. The response to ocean acidification appears to be species-specific (Langer et al., 2006; Fiorini et al., 2011), suggesting that the

structure of natural multi-species coccolithophore communities may shift in a high CO_2 world.

1.4 Species-specific biogeochemical roles of coccolithophores

Coccolithophores are a highly diverse group, with ~ 200 extant species of varying size, shape and cellular calcite quota (Young and Ziveri, 2000; Young et al., 2003). *Emiliania huxleyi* is considered to be the most widespread and abundant species of coccolithophore (Paasche, 2002). It is responsible for the seasonally occurring satellite detectable coccolithophore blooms (Holligan et al., 1983; Holligan et al., 1993), and is relatively easy to grow in culture. Thus the majority of our understanding about coccolithophores is based on studies of *E. huxleyi*, whether through in situ studies (e.g. Holligan et al., 1993; Poulton et al., 2013) or from culture experiments (e.g. Balch et al., 1993; Iglesias-Rodriguez et al., 2008; Hoffman et al., 2015).

However, *E. huxleyi* is considered an atypical coccolithophore species in terms of its genetic lineage, physiology and ecology (De Vargas et al., 2007). Molecular phylogeny suggests that the Noelaerhabdaceae family (of which *E. huxleyi* belongs to) branched at the base of the Calcihaptophycidae tree (of which the coccolithophores belong to), making *E. huxleyi* genetically dissimilar to most other species (De Vargas et al., 2007). *Emiliania huxleyi* is the only species known to produce multiple layers of coccoliths (Gibbs et al., 2013; Hoffman et al., 2015), and with their ability to bloom in high densities it has been suggested they inhabit a different ecological niche than other coccolithophore species (Balch, 2004). Therefore, the physiology and ecology of *E. huxleyi* may not be fully applicable to other coccolithophore species, particularly as inter-species differences have been observed in the response to carbonate chemistry changes (Langer et al., 2006; Langer et al., 2009), photo-physiology of haploid and diploid life stages (Houdan et al., 2006), and patterns of coccosphere construction during reduced growth rate (Gibbs et al., 2013).

The key biogeochemical role of coccolithophores is the production of calcite. *Emiliania huxleyi* is a relatively small species of coccolithophore (~ 5 µm) with a relatively low cellular calcite content (0.22 – 1.1 pmol C cell^{-1}, Fritz and Balch, 1996; Paasche, 2002; Hoppe et al., 2011), and is a minor contributor to calcite export (Ziveri et al., 2007). In contrast, other more heavily calcified species such as *Coccolithus pelagicus*, *Calcidiscus leptoporus* and *Helicosphaera carteri* are major calcite exporters despite having a lower relative abundance (Ziveri et al., 2000; Ziveri et al., 2007; Hurst, 2011). Therefore, these heavily calcified but less abundant coccolithophore species may be the biogeochemically key calcite producers, rather than *E. huxleyi*.

1.4.1 *Coccolithus pelagicus*

Coccolithus pelagicus is one of the oldest extant species of coccolithophore, appearing in the Palaeocene over 60 Ma (Cachao and Moita, 2000), although this very long fossil record is based on a very broad species concept (Geisen et al., 2004). In the modern ocean, through analysis of heterococcolith size (Baumann et al., 2000b), holococcolith morphology (Geisen et al., 2002) and genetic sequencing (Sáez et al., 2003), two species of *Coccolithus* have been identified: *C. pelagicus* and *C. braarudii*.

In the fossil record, *C. pelagicus* was a widely distributed temperate species of coccolithophore (Cachao and Moita, 2000; Sato et al., 2004). However, the distribution of *C. pelagicus* and *C. braarudii* in the modern ocean is more limited. *Coccolithus pelagicus*, the smaller of the two species of *Coccolithus* with coccoliths 6 – 10 µm in length (Baumann et al., 2000b; Young and Ziveri, 2000; Young et al., 2003), is an arctic/subarctic species. Particularly prevalent in the subarctic North Atlantic, the distribution of *C. pelagicus* covers the Arctic Ocean and the subarctic regions of the Atlantic and the Pacific (Mcintyre and Bé, 1967; Mcintyre et al., 1970). Recorded in temperatures as low as -1.7 °C (Braarud, 1979), *C. pelagicus* is thought to be limited by a 14 °C seasonal isotherm (Mcintyre and Bé, 1967), with a temperature optimum of 8 °C based on its distribution (Baumann et al., 2000a). *Coccolithus pelagicus* is capable of dominating the coccolithophore community in the North Atlantic (Okada and

Mcintyre, 1979), with reported blooms of ~ 1000 cells mL^{-1} (Milliman, 1980; Tarran et al., 2001).

In contrast to *C. pelagicus*, *C. braarudii* is a larger (9 – 15 µm coccoliths) temperate species of coccolithophore (Young et al., 2003). The distribution of *C. braarudii* is more limited than *C. pelagicus*, generally confined to coastal regions around the English Channel and Bay of Biscay (Daniels et al., 2012), upwelling regions in the North Atlantic (Blasco et al., 1980; Cachao and Moita, 2000; Cabeçadas and Oliveira, 2005), the Benguela upwelling (Giraudeau et al., 1993), the Agulhas current (Mitchell-Innes and Winter, 1987) and the Great Australian Bight (Hallegraeff, 1984; Cubillos et al., 2012).

Coccolithus species produce the largest and heaviest common coccoliths in the modern ocean (Young and Ziveri, 2000; Ziveri et al., 2004). A coccolith of *C. pelagicus* (~ 1 pmol C $coccolith^{-1}$, Young and Ziveri, 2000) is estimated to have over 40 times more calcite than a coccolith of *E. huxleyi* (~ 0.023 pmol C $coccolith^{-1}$, Young and Ziveri, 2000), while a coccolith of *C. braarudii* (~ 4 pmol C $coccolith^{-1}$, Young and Ziveri, 2000) may have more than 100 times the calcite. The relative cellular calcite quota of *E. huxleyi* and *Coccolithus* is important as it will determine the contribution of *Coccolithus* to calcite production relative to *E. huxleyi*. However, the cellular calcite quota of *C. pelagicus* is poorly constrained. Very few culture studies of *Coccolithus* have used a strain of *C. pelagicus* (Sáez et al., 2003; Gibbs et al., 2013; Gerecht et al., 2014), with most studies using a strain of *C. braarudii* (e.g., Stoll et al., 2002; Langer et al., 2006; Krug et al., 2011). Gerecht et al. (2014) report a cellular calcite quota of 26 pmol C $cell^{-1}$; although there is an uncertainty in this value as cellular calcite quota of *C. braarudii* in this study was lower (17 pmol C $cell^{-1}$), this would suggest the cellular calcite content of *C. pelagicus* to be ~ 24 – 120 times greater than *E. huxleyi*. Therefore, although the cellular quotas are poorly constrained, it is possible that even if present in low abundances relative to *E. huxleyi*, *C. pelagicus* may be a greater calcite producer than *E. huxleyi*, and the dominant calcite producer within a mixed community.

1.5 Motivations, aims and hypotheses

The key motivation for this thesis was to establish whether the assumption that *E. huxleyi* is the keystone species of coccolithophore in terms of calcite production is valid or whether other species such as *C. pelagicus* could be potentially greater calcite producers than *E. huxleyi* in mixed communities of coccolithophores. Specifically, the main aim of this thesis was to establish whether *C. pelagicus* has a significant biogeochemical role in the production of calcite in the North Atlantic: will it dominate calcite production within a mixed community?

The study aimed to combine culture experiments providing detailed information about *C. pelagicus* with field studies in regions where *C. pelagicus* was expected to inhabit. The individual focussed hypotheses tested in the thesis were:

1. "Under identical growth conditions, *E. huxleyi* would grow at a significantly faster rate than either of the *Coccolithus* species, *C. pelagicus* and *C. braarudii*"
2. "Coccolithophores will be present in the North Atlantic spring bloom and increase in abundance with the bloom progression. *Coccolithus pelagicus* will be the major source of calcite."
3. "*C. pelagicus* is the major calcifier in the Arctic Ocean"

1.6 Thesis Outline

Chapter 2 is a culture based investigation into the relative growth rates of *E. huxleyi*, *C. pelagicus* and *C. braarudii* under a range of growth conditions (light, temperature) and their biogeochemical implications. The effect of relative growth rates on calcite production is examined using a simplistic two species model. The importance of relative abundance to species calcite production is considered by combining the model results with field data on the abundance of *E. huxleyi* and *C. pelagicus*. This chapter has been published as:

Daniels, C. J., Sheward, R. M., and Poulton, A. J.: Biogeochemical implications of comparative growth rates of *Emiliania huxleyi* and *Coccolithus* species, Biogeosciences, 11, 6915-6925, doi:10.5194/bg-11-6915-2014, 2014.

Chapter 3 is an investigation into the dynamics and evolution of the phytoplankton community during the early stage of a North Atlantic spring bloom. The overall phytoplankton community structure is compared to the physical environment to examine the drivers of the phytoplankton bloom. The role of individual diatom species in the production of particulate silicate is determined and the contrasting patterns examined. The biogeochemistry and dynamics of the coccolithophore community are also assessed in terms of species-specific growth rates and cellular calcite. This chapter has been published as:

Daniels, C. J., Poulton, A. J., Esposito, M., Paulsen, M. L., Bellerby, R., St. John, M., and Martin, A. P.: Phytoplankton dynamics in contrasting early stage North Atlantic spring blooms: composition, succession, and potential drivers, Biogeosciences, 12, 2395-2409, doi:10.5194/bg-12-2395-2015, 2015.

Chapter 4 determines species-specific calcite production rates of individual coccolithophore species in the Arctic and Iceland Basin. The abundance and cellular calcite content of individual species are combined with measurements of total calcite production to assess which species are the major calcifiers. Finally, species-specific calcite production was compared to a set of environmental variables.

Chapter 5 brings together the results of Chapter 2, 3, and 4, and discusses the biogeochemical role of *C. pelagicus* in calcite production. The influence of seasonality on species-specific calcite production is discussed in the context of the results, expanding on the field data of Chapter 2. The wider implications of the main findings, along with the limitations and future directions of the study are also considered.

Chapter 2: Biogeochemical implications of comparative growth rates of *Emiliania huxleyi* and *Coccolithus* species

Published as: Daniels, C. J., Poulton, A. J., and Sheward, R. M.: Biogeochemical implications of comparative growth rates of *Emiliania huxleyi* and *Coccolithus* species, Biogeosciences, 11, 6915-6925, doi:10.5194/bg-11-6915-2014, 2014.

Abstract

Coccolithophores, a diverse group of phytoplankton, make important contributions to pelagic calcite production and export, yet the comparative biogeochemical role of species other than the ubiquitous *Emiliania huxleyi* is poorly understood. The contribution of different coccolithophore species to total calcite production is controlled by inter-species differences in cellular calcite, growth rate and relative abundance within a mixed community. In this study I examined the relative importance of *E. huxleyi* and two *Coccolithus* species in terms of daily calcite production. Culture experiments compared growth rates and cellular calcite content of *E. huxleyi* (Arctic and temperate strains), *Coccolithus pelagicus* (novel Arctic strain) and *Coccolithus braarudii* (temperate strain). Despite assumptions that *E. huxleyi* is a fast growing species, growth rates between the three species were broadly comparable (0.16-0.85 d^{-1}) under identical temperature and light conditions. *Emiliania huxleyi* grew only 12 % faster on average than *C. pelagicus*, and 28 % faster than *C. braarudii*. As the cellular calcite content of *C. pelagicus* and *C. braarudii* is typically 30-80 times greater

than *E. huxleyi*, comparable growth rates suggest that *Coccolithus* species have the potential to be major calcite producers in mixed populations.

To further explore these results I devised a simplistic model comparing daily calcite production from *Coccolithus* and *E. huxleyi* across a realistic range of relative abundances and a wide range of relative growth rates. Using the relative differences in growth rates from culture studies I found that *C. pelagicus* would be a larger source of calcite if abundances of *E. huxleyi* to *C. pelagicus* were below 34:1. Relative abundance data collected from North Atlantic field samples (spring and summer 2010) suggest that with a relative growth rate of 88 %, *C. pelagicus* dominated calcite production at 69 % of the sites sampled. With a more extreme difference in growth rates, where *C. pelagicus* grows at a tenth of the rate of *E. huxleyi*, *C. pelagicus* still dominated calcite production in 14 % of the field.

These results demonstrate the necessity of considering interactions between inter-species differences in growth rates, cellular calcite and relative abundances when evaluating the contribution of different coccolithophores to pelagic calcite production. In the case of *C. pelagicus*, I find that there is strong potential for this species to make major contributions to calcite production in the North Atlantic, although estimates of relative growth rates from the field are needed to confirm these conclusions, and will be examined in Chapter 3.

2.1 Introduction

Coccolithophores are a diverse and biogeochemically important group of phytoplankton; through the production and subsequent export of their calcite coccoliths, they form a key component of the global carbon cycle (De Vargas et al., 2007). *Emiliania huxleyi* is considered the keystone species of the coccolithophores due to its global dominance, propensity to form large-scale blooms and its perceived relatively fast growth rates (Paasche, 2002). Assumptions on the comparative physiology and ecology of the other ~ 200 extant species are often poorly addressed, although studies have examined intra- and inter-species differences in response to

Table 2.1: Coccolithophore strain-specific values of cell diameter, cellular calcite, cellular particulate organic carbon (POC), cellular chlorophyll (Chl) and cellular calcite:POC. Values reported are averaged over experiments, with ± 1 standard deviation. [a] measured from light microscopy, calculated following Young and Ziveri (2000). [b] measured from SEM, calculated following Young and Ziveri (2000). [c] calculated following Menden-Deuer and Lessard (2000).

Species	Strain	Cell diameter (μm)	Cell calcite (pmol C cell^{-1})	Cell POC (pmol C cell^{-1})	Cell Chl (pg Chl cell^{-1})	Cell calcite:POC
C. pelagicus	RCC4092	12.9 (± 1.8)	16.6[a] (± 3.9)	13.8[c] (± 5.1)	5.1 (± 1.0)	1.2
E. huxleyi	RCC3533	4.47 (± 0.52)	0.43[b] (± 0.14)	0.67[c] (± 0.24)	0.31 (± 0.06)	0.64
C. braarudii	RCC1198	15.9 (± 2.4)	38.7[a] (± 6.2)	25.0[c] (± 8.9)	7.8 (± 1.4)	1.5
E. huxleyi	RCC1228	4.52 (± 0.58)	0.52[b] (± 0.14)	0.69[c] (± 0.26)	0.32 (± 0.07)	0.75

carbonate chemistry changes (Langer et al., 2006; Langer et al., 2009), photo-physiological differences between haploid and diploid life stages (Houdan et al., 2006), and patterns of coccosphere construction during reduced growth rate (Gibbs et al., 2013). However, the often stated (e.g., Tyrrell and Merico, 2004) assumption that *E. huxleyi* is a fast growing species relative to other coccolithophores has been largely un-tested.

Understanding whether different species grow at comparable or vastly different rates is key to understanding the relative calcification of these species within natural communities. *Emiliania huxleyi* has a relatively low cellular calcite content (~ 0.4 – 0.5 pmol C cell^{-1}; Table 2.1 and Fig. 2.1) compared with larger, more heavily calcified species such as *Coccolithus pelagicus* (~ 16.6 pmol C cell^{-1}; Table 2.1 and Fig. 2.1). With a similar growth rate (e.g., 0.7 d^{-1}), at a cellular level *C. pelagicus* would have a calcification rate approximately 30 – 40 times greater (11.6 pmol C cell^{-1} d^{-1}) than *E. huxleyi* (0.28 – 0.35 pmol C cell^{-1} d^{-1}). Alternatively, if *C. pelagicus* grew at only a tenth of the growth rate of *E. huxleyi* (e.g., 0.07 d^{-1}), then the difference in calcification between the two would be greatly reduced to around 3 – 4 times (although *C. pelagicus* would still represent ~ 75 % of the total calcite production).

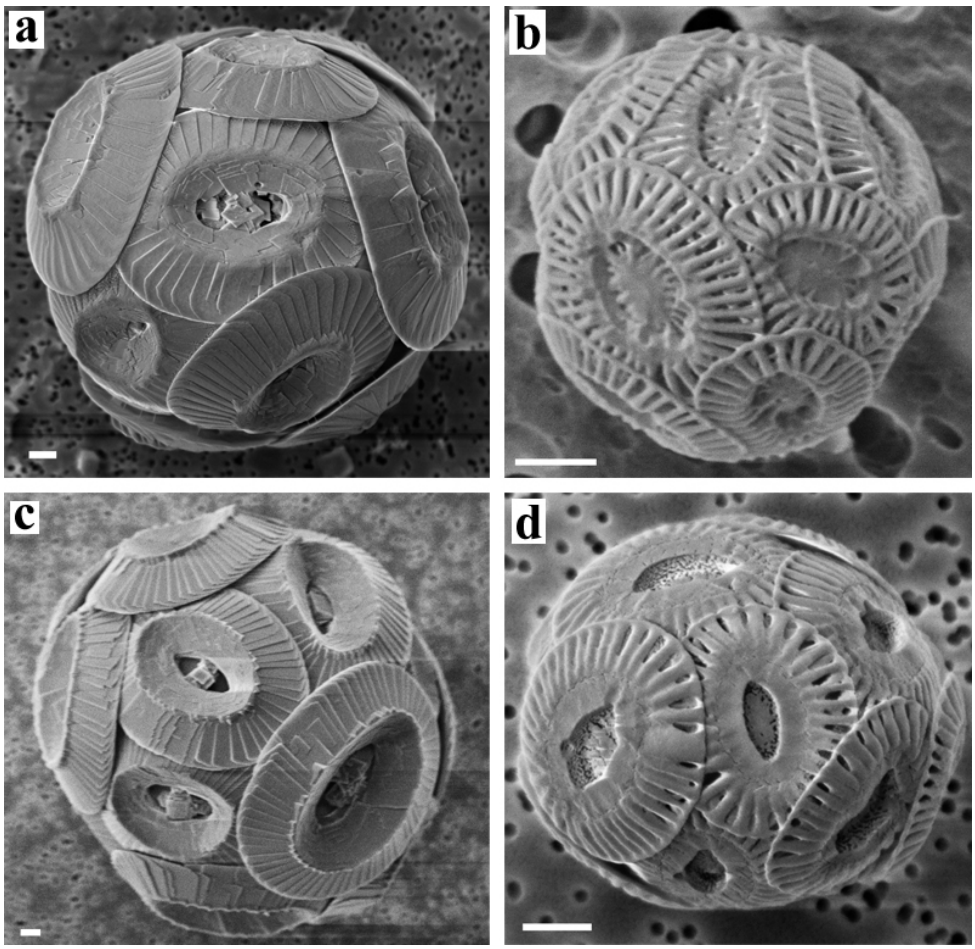

Fig. 2.1: SEM images. A) *Coccolithus pelagicus* RCC4092. B) *Emiliania huxleyi* RCC3533. C) *Coccolithus braarudii* RCC1198. D) *Emiliania huxleyi* RCC1228. Scale bars represent 1 µm in each image.

Besides relative growth rates (the growth rate of *Coccolithus* relative to *E. huxleyi*), the distribution and relative abundance of the different species are important factors in determining whether *Coccolithus* will dominate calcite production. While *E. huxleyi* is ubiquitously distributed throughout the oceans, the biogeography of *C. pelagicus* only covers the Arctic Ocean and the sub-polar northern hemisphere (Mcintyre and Bé, 1967; Mcintyre et al., 1970), with a particular prevalence in the sub-polar North Atlantic (Milliman, 1980; Tarran et al., 2001). As such, *C. pelagicus* has the potential to be a major oceanic calcite producer in this region. *Coccolithus braarudii*, a closely related taxa of *C. pelagicus* with an even greater cellular calcite content (39.1 pmol C cell^{-1}; Table 2.1 and Fig. 2.1), has a more limited range, restricted to coastal and upwelling areas (Giraudeau et al., 1993; Cachao and Moita, 2000; Ziveri et al., 2004;

Cubillos et al., 2012). However, where present, *C. braarudii* also has the potential to dominate calcite production.

Although studies concerning coccolithophore growth and calcite production have concentrated mainly on *E. huxleyi*, the potential for other species to be biogeochemically important has been previously highlighted in studies concerning coccolith export (Broerse et al., 2000; Ziveri et al., 2000; Baumann et al., 2004; Ziveri et al., 2007). *Coccolithus pelagicus* is a major contributor to the downwards flux of calcite in the northern North Atlantic (Ziveri et al., 2000), while other larger coccolithophore species such as *Calcidiscus leptoporus*, *Helicosphaera carteri* and *Gephyrocapsa oceanica* are significant contributors in other regions (Ziveri et al., 2007). The relative abundance of *C. pelagicus* in the downward flux has been shown to increase with depth, which is likely to be due to the greater susceptibility of smaller coccospheres, such as those of *E. huxleyi,* to disintegration and remineralisation (Ziveri et al., 2000). Therefore, *C. pelagicus* can dominate coccolith calcite export despite relatively low abundances in surface waters.

I set about to experimentally test the basic hypothesis that under identical growth conditions (light, nutrients, temperature) *E. huxleyi* would grow at a significantly faster rate than either of the *Coccolithus* species, *C. pelagicus* and *C. braarudii*. Furthermore, I also collected a number of ancillary cellular parameters (e.g., cell size, cell chlorophyll content) and examine these in a comparative sense between the different species. Lastly, the biogeochemical implications of growth rates and relative cell abundances are assessed using model and field data.

2.2 Materials and Methods

2.2.1 Experimental Design

Monoclonal cultures of *Coccolithus pelagicus* (RCC4092) and an Arctic strain of *Emiliania huxleyi* (RCC3533) were obtained in June 2012 through single cell isolations from surface water samples collected in the Greenland Sea (67.83 °N, 16.42 °W and

66.79 °N, 25.14 °W respectively) during the 2012 UK Ocean Acidification Arctic cruise (JR271). These cultures have been deposited into the Roscoff Culture Collection (RCC). North Atlantic Ocean strains of *Coccolithus braarudii* (RCC1198) and *E. huxleyi* (RCC1228) were obtained from the RCC.

Cultures were grown in sterile-filtered (0.2 µm) modified K/20 medium (modified from Keller et al., 1987; following Gerecht et al., 2014); aged natural seawater was enriched with 28.8 µM nitrate and 1.8 µM phosphate. Experiments on parallel cultures of either the Arctic strains (*C. pelagicus* and *E. huxleyi* RCC3533) or the Atlantic strains (*C. braarudii* and *E. huxleyi* RCC1228) were carried out over a range of temperature and light conditions, under a 12/12 h light/dark cycle.

To reflect a realistic *in situ* environment (Poulton et al., 2010; Ryan-Keogh et al., 2013), different experimental conditions were used for the Arctic and Atlantic cultures. The Arctic strain experiments were carried out at 6, 9 and 12 °C, with a daily photon flux ranging from 1.30-8.21 mol photons m^{-2} d^{-1} (30 – 190 µmol photons m^{-2} s^{-1}) between experiments, while the Atlantic strain experiments were carried out at 12, 14, 16 and 19 °C, with a daily photon flux ranging from 1.94 – 10.54 mol photons m^{-2} d^{-1} (45 – 244 µmol photons m^{-2} s^{-1}). Cells were acclimated to experimental conditions for approximately 10 generations and grown in dilute batch cultures in duplicate. Cultures were grown in ventilated flasks and to low cell densities to avoid biological effects on the carbonate system (150,000 – 470,000 cells mL^{-1}, 4,500 – 8,700 cells mL^{-1} and 5,300 – 16,000 cells mL^{-1}, for *E. huxleyi*, *C. braarudii* and *C. pelagicus* respectively) and sampled during the mid-exponential phase to avoid nutrient limitation (Langer et al., 2009; Hoffman et al., 2015).

For determination of cell density, samples were taken daily or every other day and counted immediately in triplicate using either a Sedgwick rafter cell for *C. braarudii* and *C. pelagicus* (Langer et al., 2006), or a Coulter Multisizer™ III (Beckman Coulter) for *E. huxleyi* (Langer et al., 2009). Cell density was plotted against time and growth rates (μ) were calculated by exponential regression (Langer et al., 2006).

Biometric measurements of coccolithophores were made on samples collected on cellulose nitrate (0.8 µm) and polycarbonate (0.8 µm) filters, and prepared following Poulton et al. (2010) and Daniels et al. (2012), respectively. Light microscopy was used for all biometric measurements of *Coccolithus* (Gibbs et al., 2013), and was carried out by Rosie Sheward, while a combination of light microscopy and scanning electron microscopy (SEM) was used to study *E. huxleyi*. Measurements of coccolith size and the number of coccoliths per coccosphere were used to estimate cellular calcite content following the relationship of Young and Ziveri (2000). Cellular particulate organic carbon (POC) was estimated from measured internal cell diameters and cell biovolume following Menden-Deuer and Lessard (2000). Samples for determination of cellular chlorophyll *a* (Chl *a*) were collected on Fisherbrand MF300 filters (effective pore size 0.7 µm), extracted in 8 mL of 90 % acetone (HPLC grade, Sigma) for 24 h and analysed on a Turner Designs Trilogy Fluorometer calibrated using a solid standard and a chlorophyll-*a* extract. All experimental data included in this chapter are available from the data repository PANGAEA via Sheward et al. (2014).

2.2.2 Field samples

Samples for coccolithophore abundance were collected from three RRS *Discovery* cruises spanning the Irminger and Iceland Basins of the North Atlantic during the period of April to August 2010, by Stuart Painter, Martine Couapel and Mike Lucas. Two cruises (D350, D354) were part of the (UK) Irminger Basin Iron Study (IBIS), while the third cruise (D351) occupied the Extended Ellett Line. In all three cruises, surface water samples (0.2 – 1 L) were filtered through cellulose nitrate (0.8 µm) and polycarbonate (0.45 µm or 0.8 µm) filters, oven dried (30 – 40 °C, 6 – 12 h) and stored in Millipore PetriSlides. The filters were examined using a Leo 1450VP scanning electron microscope, with coccolithophores identified following Young et al. (2003), and enumerated from 225 fields of view (Daniels et al., 2012). The detection limit was estimated to be 0.2 – 1.1 cells mL^{-1}. All field data included in this chapter are available from the British Oceanographic Data Centre (BODC) via Daniels et al. (2014a).

2.3 Results and Discussion

2.3.1 Growth rates

Through manipulation of experimental conditions (temperature and irradiance), a wide range of growth rates was achieved, ranging from 0.16 – 0.85 d^{-1} (Fig. 2.2). *Emiliania huxleyi* RCC1228 (0.50 – 0.85 d^{-1}) grew significantly faster (Student's t-test, t = 6.8, df = 10, $p < 0.001$) than *C. braarudii* (0.32 – 0.58 d^{-1}). For the Arctic strains, the growth rate of *E. huxleyi* (0.16 – 0.58 d^{-1}) was significantly different (Student's t-test, t = 3.5, df = 6, $p < 0.02$) to that of *C. pelagicus* (0.18 – 0.49 d^{-1}), growing faster in all but the experiment with the slowest growth rates (Fig. 2.2).

Although *E. huxleyi* always grew faster than *C. braarudii*, and was generally faster than *C. pelagicus*, the differences in growth rates were smaller than previously reported, with *E. huxleyi* growing on average only 12 % (-11 % to 26 %) faster than *C. pelagicus*, and 28 % (12 – 49 %) faster than *C. braarudii*. In contrast, Buitenhuis et al. (2008) observed that when grown in conditions comparable to mine (12 – 15 °C, 14/10 L/D, 4.20 mol photons m^{-2} d^{-1}), the growth rate of *C. braarudii* was 42 – 51 % that of *E. huxleyi*, although the strain of *E. huxleyi* used by Buitenhuis et al. (2008) was a non-calcifying mutant, which have been observed to have higher growth rates (Paasche, 2002).

While my maximum growth rate of *E. huxleyi* (0.85 d^{-1}) was lower than in some recent studies (e.g., 0.98 – 1.64 d^{-1}, Langer et al., 2009), they are well within the range of reported growth rates (0.4 – 1.9 d^{-1}, Paasche, 2002). Strain-specific variability is likely to partly contribute to this large range in growth rates (e.g., Langer et al., 2009). However, it is also likely that my lower maximum growth rates are due to the effect of the day length used in my study (12 L / 12 D), as day lengths shorter than 16 hours have been observed to reduce phytoplankton growth rates (Paasche, 1967). Although my *E. huxleyi* growth rates were lower than those obtained in 16 hour day length studies (e.g. Langer et al., 2009; Hoppe et al., 2011), they were similar to another 12 hour day length study (0.6 – 1 d^{-1}, Iglesias-Rodriguez et al., 2008). This is also the case

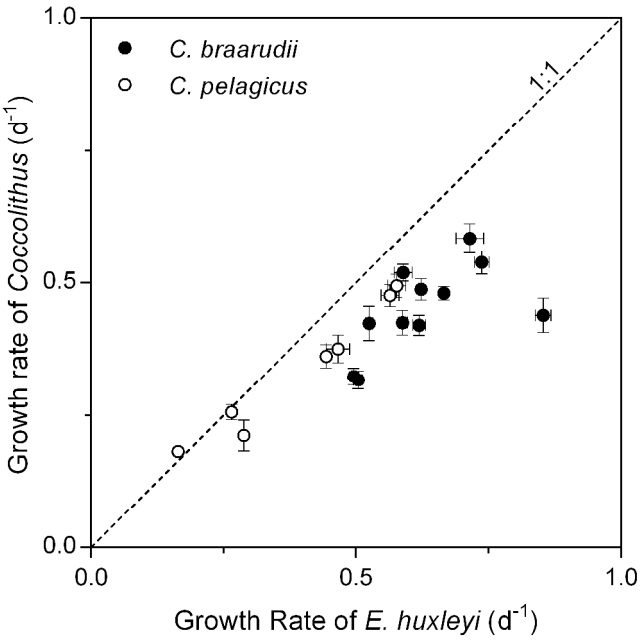

Fig. 2.2: Growth rates (d^{-1}) of *Coccolithus pelagicus* RCC4092 and *Coccolithus braarudii* RCC1198 against corresponding growth rates of *Emiliania huxleyi* RCC3533 and RCC1228 respectively. Dashed line indicates a 1:1 ratio. Error bars are ± 1 standard deviation.

for *C. braarudii* and *C. pelagicus*; the maximum growth rate of *C. braarudii* (0.58 d^{-1}) was below that observed in 16 hour day length studies (0.73 – 0.82 d^{-1}, Langer et al., 2006; Gibbs et al. 2013), but above both 12 hour (0.42 – 0.5 d^{-1}, Taylor et al., 2007; Gerecht et al., 2014) and 14 hour (0.4 d^{-1}, Buitenhuis et al., 2008) day length experiments. Although there are few studies of *C. pelagicus*, my maximum growth rate (0.49 d^{-1}) was greater than the 12 hour day length study (0.36 d^{-1}) by Gerecht et al. (2014) but lower than a 16 hour day length experiment (0.58 d^{-1}) by Gibbs et al. (2013). Given these differences between experiments, and no literature consensus on recommended day length (Probert and Houdan, 2004), I am therefore confident that my growth rates are representative of these coccolithophore species.

Both temperature and irradiance had a measurable effect on growth rates (Table 2.2, Appendix Fig. A.1). Temperature was the primary driver of growth rates for both *E. huxleyi* (r^2 = 0.84, p < 0.001, n = 18) and *Coccolithus* (r^2 = 0.62, p < 0.001, n = 18), while irradiance had a secondary, but significant, effect on both *E. huxleyi* (r^2 = 0.33, p < 0.02, n = 18) and *Coccolithus* (r^2 = 0.23, p = 0.04, n = 18). The growth rate of *C. braarudii*

declined between 16 °C and 19 °C, suggesting that 19 °C was above the optimum temperature for *C. braarudii*. No such decline was observed in the temperature range experienced by *C. pelagicus* (6-12 °C).

In general, a decrease in absolute growth rates was coupled with a smaller difference in the relative growth rates of *E. huxleyi* and *Coccolithus* (Fig. 2.2). As the variability in growth rate was primarily driven by temperature, this suggests that growth rates of *Coccolithus* and *E. huxleyi* may be most comparable in cold waters (< 10 °C), while the growth rate of *E. huxleyi* will become increasingly greater relative to *Coccolithus* in temperate waters. As a cold water species (Winter et al., 1994), with a biogeography spanning the Arctic and sub-polar northern hemisphere (Mcintyre and Bé, 1967; Mcintyre et al., 1970), *C. pelagicus* could therefore potentially dominate calcite production in this region. As a more temperate species, seemingly present only in coastal waters of the North Atlantic (Cachao and Moita, 2000; Daniels et al., 2012) and upwelling pockets (Giraudeau et al., 1993; Cubillos et al., 2012), I expect the difference in growth rate between *C. braarudii* and *E. huxleyi* to be greater in areas where they are both present. However, as a heavily calcified species, where the coccosphere calcite of one cell is equivalent to ~ 78 cells of *E. huxleyi* (Table 2.1), *C. braarudii* still has the potential to dominate calcite production in these regions.

2.3.2 Modelling relative calcite production

The potential for *C. pelagicus* and *C. braarudii* to dominate calcite production in their respective environments is dependent on both their relative growth rates and cellular calcite inventories, as well as the relative abundance of these species compared to other coccolithophores. In the context of this chapter, I consider daily contributions to calcite production, as this is the minimal time-length over which I can realistically expect relative abundances to be least variable. Also, much of the work measuring calcite production by natural field communities is based on daily integrals (e.g., Poulton et al., 2010; Poulton et al., 2013).

Table 2.2: Experiment culture strains, temperature, daily irradiance and growth rates, with ± 1 standard deviation for the experiments. Atlantic = RCC1198 and RCC1228, Arctic = RCC4092 and RCC3533.

Experiment Strains	Temperature (°C)	Daily Irradiance (mol photons m^{-2} d^{-1})	Growth Rate (d^{-1})	
			E. huxleyi	*Coccolithus*
Atlantic	16	9.07	0.59 (± 0.02)	0.52 (± 0.02)
	16	8.64	0.72 (± 0.03)	0.58 (± 0.03)
	16	8.64	0.74 (± 0.01)	0.54 (± 0.02)
	16	4.97	0.62 (± <0.01)	0.49 (± 0.02)
	16	3.20	0.53 (± 0.01)	0.42 (± 0.03)
	14	8.64	0.62 (± 0.01)	0.42 (± 0.02)
	14	5.62	0.59 (± 0.01)	0.43 (± 0.02)
	12	8.21	0.50 (± 0.01)	0.32 (± 0.02)
	12	5.18	0.50 (± 0.01)	0.32 (± 0.02)
	19	10.54	0.85 (± 0.02)	0.44 (± 0.03)
	19	1.94	0.67 (± <0.01)	0.48 (± 0.01)
Arctic	6	3.89	0.27 (± 0.01)	0.26 (± 0.02)
	6	1.30	0.16 (± <0.01)	0.18 (± <0.01)
	12	8.21	0.58 (± 0.02)	0.49 (± 0.02)
	12	5.18	0.56 (± 0.02)	0.48 (± 0.02)
	9	8.21	0.47 (± 0.02)	0.38 (± 0.03)
	9	5.18	0.44 (± 0.01)	0.36 (± 0.02)
	6	6.05	0.29 (± 0.01)	0.21 (± 0.03)

I examine the potential relative daily calcite production by modelling a simplified community comprised of just *E. huxleyi* and either *C. pelagicus* or *C. braarudii*. Assuming steady state in terms of the cellular quota across a day, calcite production for a given species is the product of its growth rate (μ), cellular calcite (C) and abundance (N) (Leynaert et al., 2001; Poulton et al., 2010). Therefore, I can calculate the percentage of calcite production by a specific species ($\%CP_{sp}$), such as *Coccolithus,* within a mixed community, using the following equation:

$$\%CP_{sp} = \frac{\mu_{sp} C_{sp} N_{sp}}{\sum_{i=1}^{n} \mu_i C_i N_i} \times 100 \quad (2.1)$$

The model was parameterised using a range of relative growth rates that spans the range measured in my culture experiments (Fig. 2.2, Table 2.2), but has also been extended down to 10 % to investigate the effect of *Coccolithus* having a much lower relative growth rate. The relative abundance of *Coccolithus* and *E. huxleyi* in my simple model community is represented as the ratio of *E. huxleyi* to *Coccolithus* and was varied from 0 to 80. Cellular calcite values for each species were experimentally determined (Table 2.1). The percentage calcite production by *Coccolithus* is linearly related to the relative growth rate, relative cellular calcite and relative abundance. As the ratio of *E. huxleyi* to *Coccolithus* increases, or the relative growth rate of *Coccolithus* decreases, a decrease in the percentage calcite production by *Coccolithus* is observed (Fig. 2.3).

Coccolithus braarudii is the major source (> 50 %) of calcite production in 56 % of the model, and 64 % of the model when considering only the range of relative growth rates of *C. braarudii* observed in this study (51 – 88 %, Fig. 2.3A). At its average relative growth rate (72 %), *C. braarudii* will dominate (> 50 %) calcite production if the ratio of *E. huxleyi* to *C. braarudii* is less than 53:1, whilst with the same growth rates, *C. braarudii* calcifies at a rate equivalent to 74 cells of *E. huxleyi*. However, if *C. braarudii* is only able to grow at a relative growth rate of 10 % that of *E. huxleyi*, its calcite production is reduced to only 7 times that of an *E. huxleyi* cell. Therefore, unless *C. braarudii* is both in a very low relative abundance and has a very low relative growth rate, I would expect *C. braarudii* to be a major source of calcite compared to *E. huxleyi*.

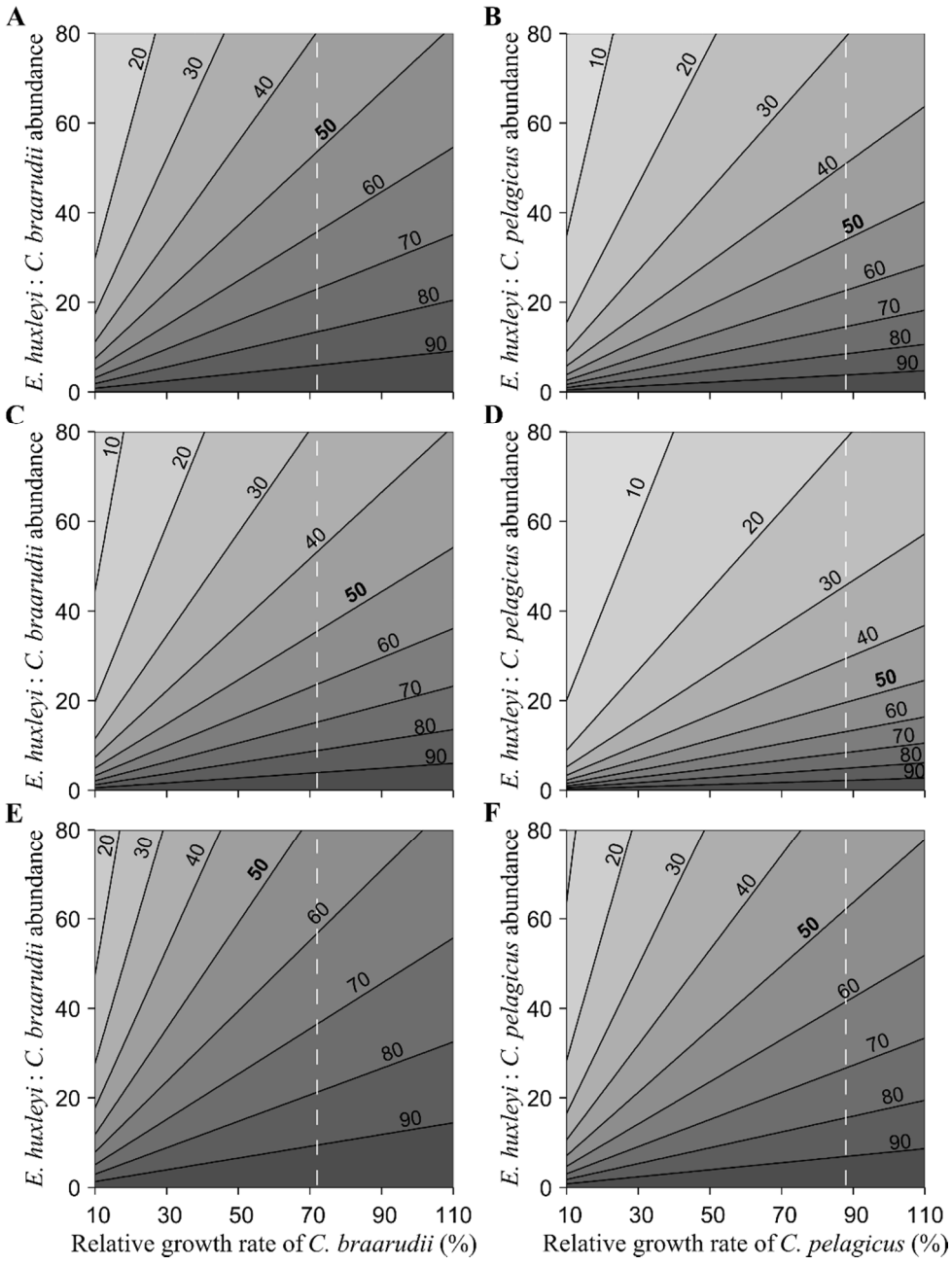

Fig. 2.3: Contour plots of how percentage calcite production by *Coccolithus* varies with the abundance ratio of *Emiliania huxleyi* to *Coccolithus* and the growth rate of *Coccolithus* relative to *E. huxleyi*, for modelled communities of *Coccolithus braarudii* and *E. huxleyi* (A, C, E) *and Coccolithus pelagicus* and *E. huxleyi* (B, D, F). Plots A and B show model with input using calcite quotas from Table 2.1, C and D have increased *E. huxleyi* and decreased *Coccolithus* calcite content by one standard deviation from average values in Table 2.1, while E and F have decreased *E. huxleyi* and increased *Coccolithus* calcite by one standard deviation away from average values given in Table 2.1. Dotted lines indicate the average relative growth rate as determined from the culture experiments.

Coccolithus pelagicus has a lower cellular calcite content than *C. braarudii* (16.6 and 38.7 pmol C cell^{-1} respectively, Table 2.1), thus only dominates 29 % of its total model, and 44 % of the model when constrained to observed relative growth rates (74 – 110 %). When growing at its average observed relative growth rate (88 %), *C. pelagicus* dominates calcite production when the ratio of *E. huxleyi* to *C. pelagicus* is less than 34:1 (Fig. 2.3B). Equivalent growth rates require a ratio less than 39:1 for *C. pelagicus* to dominate cellular calcite production, whilst a growth rate of only 10 % that of *E. huxleyi* results in calcite production from *C. pelagicus* being only 3.5 times that of an *E. huxleyi* cell. Although a greater relative abundance of *C. pelagicus* is required to dominate calcite production compared to *C. braarudii*, I still find that it would also be a large source of calcite unless both relative growth rates and abundances are low.

Although I have modelled the effect of growth rate and relative abundance on the role of *Coccolithus* as a calcite producer, the relative calcite production of the two species in these models are highly dependent on the cellular calcite quotas attributed to both *E. huxleyi* and *Coccolithus* (Table 2.1), as calcite production is the product of growth rate and cellular calcite. Estimates of the cellular calcite content of *E. huxleyi* varies significantly between studies (Balch et al., 1996a; Paasche, 2002; Langer et al., 2009; Poulton et al., 2010), which is likely due to both ecophysiological and methodological differences (Young and Ziveri, 2000; Poulton et al., 2010; Poulton et al., 2013; Hoffman et al., 2015). My estimates of *E. huxleyi* cellular calcite (0.43 – 0.52 pmol C cell^{-1}) are similar to recent estimates based on similar biometric measurements (Hoffman et al., 2015), and are within the range of literature values (0.22 – 1.1 pmol C cell^{-1} Fritz and Balch, 1996; Paasche, 2002; Hoppe et al., 2011). My value for *C. braarudii* cellular calcite is greater than previously measured (28 pmol C cell^{-1}, Langer et al. 2006; 17 pmol C cell^{-1}, Gerecht et al., 2014), while the value for *C. pelagicus* cellular calcite is lower (26 pmol C cell^{-1}, Gerecht et al., 2014).

To address the impact of variability in cellular calcite on calcite production I have varied the parameters of my model by concurrently increasing the calcite content of *E. huxleyi* and decreasing that of *Coccolithus*, by one standard deviation each (Table 2.1), or vice versa (Figs. 3C-F). In doing this, I capture most of the reported range of *E.*

huxleyi calcite as it is the equivalent of varying *E. huxleyi* RCC3533 calcite by 0.23-0.75 pmol C cell^{-1} and RCC1228 by 0.33-0.79 pmol C cell^{-1}, while the value for *Coccolithus* is held constant. Reducing the calcite content of *C. pelagicus* (12.7 pmol C cell^{-1}) and *C. braarudii* (32.5 pmol C cell^{-1}) and increasing that of *E. huxleyi* (0.57 – 0.66 pmol C cell^{-1}) reduces the dominance of *Coccolithus* in the model (Fig. 2.3C-D). Thus *C. braarudii* dominates only 37 % of the total model (Fig. 2.3C), 43 % of the model when constrained to observed relative growth rates, and calcifies at a rate equivalent to 49 cells of *E. huxleyi* when growth rates are the same. With the same reductions in cellular calcite content, *C. pelagicus* is the major calcite producer in only 17 % of the total model (Fig. 2.3D), 26 % of the model when constrained to observed relative growth rates, and with the same growth rate will dominate calcite production if the ratio of *E. huxleyi* to *C. pelagicus* is less than 22:1.

An increase in the calcite content of *C. pelagicus* (20.5 pmol C cell^{-1}) and *C. braarudii* (44.9 pmol C cell^{-1}), coupled with a decrease in that of *E. huxleyi* (0.29 – 0.38 pmol C cell^{-1}), results unsurprisingly in an increased dominance of both *C. braarudii* (Fig. 2.3E) and *C. pelagicus* (Fig. 2.3F). *Coccolithus braarudii* dominates 75 % of the total model and 93 % of the observation-constrained model, while *C. pelagicus* dominates 53 % of the total model and 81 % of the observation-constrained model.

Cellular calcite clearly has a significant influence on my calculation of percentage calcite production, and therefore needs to be constrained more tightly, particularly in the case of *Coccolithus*. However, I still observe notable levels of calcite production deriving from *Coccolithus* rather than *E. huxleyi* in the models using even the lowest values of cellular calcite for *Coccolithus*.

2.3.3 The importance of relative abundance

The model scenarios clearly highlight the importance of relative cellular calcite quotas, relative growth rates and relative abundances when determining the relative role of *E. huxleyi* and *Coccolithus* in calcite production. While cellular calcite and growth rates will affect relative calcite production at a cellular level, it is the relative abundance of *E. huxleyi* and *Coccolithus* within a population that will determine the proportion of

calcite production that derives from *Coccolithus*. Using data from field communities I can examine whether populations exist where *C. pelagicus* has the potential to be a significant calcite producer.

Coccolithophore abundances were determined from samples collected on three cruises in the Irminger and Iceland Basins of the North Atlantic, a region in which both *E. huxleyi* and *C. pelagicus* are present (Mcintyre and Bé, 1967). A physicochemical description of the region is available in Ryan-Keogh et al. (2013), which indicates nutrient replete conditions for the phytoplankton community in spring and nutrient depleted (iron and/or nitrate) conditions in summer. Although other species of coccolithophore were present, I have extracted only the abundances of *E. huxleyi* and *C. pelagicus*, so that the data is comparable to my model scenarios in Section 3.2. Of the 37 samples analysed, *E. huxleyi* and *C. pelagicus* were observed in 29 samples, with *E. huxleyi* present in a further 6 samples in which *C. pelagicus* was absent (Fig. 2.4). When present, concentrations of *E. huxleyi* ranged from 2-980 cells mL^{-1}, while *C. pelagicus* ranged from 0.1 – 74 cells mL^{-1}. The relative abundance of *E. huxleyi* to *C. pelagicus* (0.7 – 85) was generally comparable to my modelled range, with a relatively low median average of 12.7. However, in 2 samples (Appendix Table A.1), the relative abundance was much higher (155 – 212), such that *C. pelagicus* was unlikely to be a significant calcite producer in these samples.

Assuming the original model scenario of measured cellular calcite (Table 2.1, Figs. 3A and 3B) and the average relative growth rate for *C. pelagicus* of 88 %, the minimum relative abundance of *E*. *huxleyi* to *C. pelagicus* required for *E*. *huxleyi* to dominate calcite production (34:1) was exceeded in only 5 out of 29 samples. Taking into account those samples in which *C. pelagicus* was absent, *C. pelagicus* is a greater calcite producer than *E. huxleyi* in 69 % of the samples. If equivalent growth rates are assumed, then *C. pelagicus* remains the major calcite producer in 69 % of the samples.

Under the more conservative model scenario (Fig. 2.3D), with a relative growth rate of 88 %, *C. pelagicus* remains the major calcite producer in 57 % of the samples, which is reduced to 46 % if the lowest measured relative growth rate (74 %) is used. If *C. pelagicus* has a higher nutrient requirement and lower nutrient affinity than *E. huxleyi*,

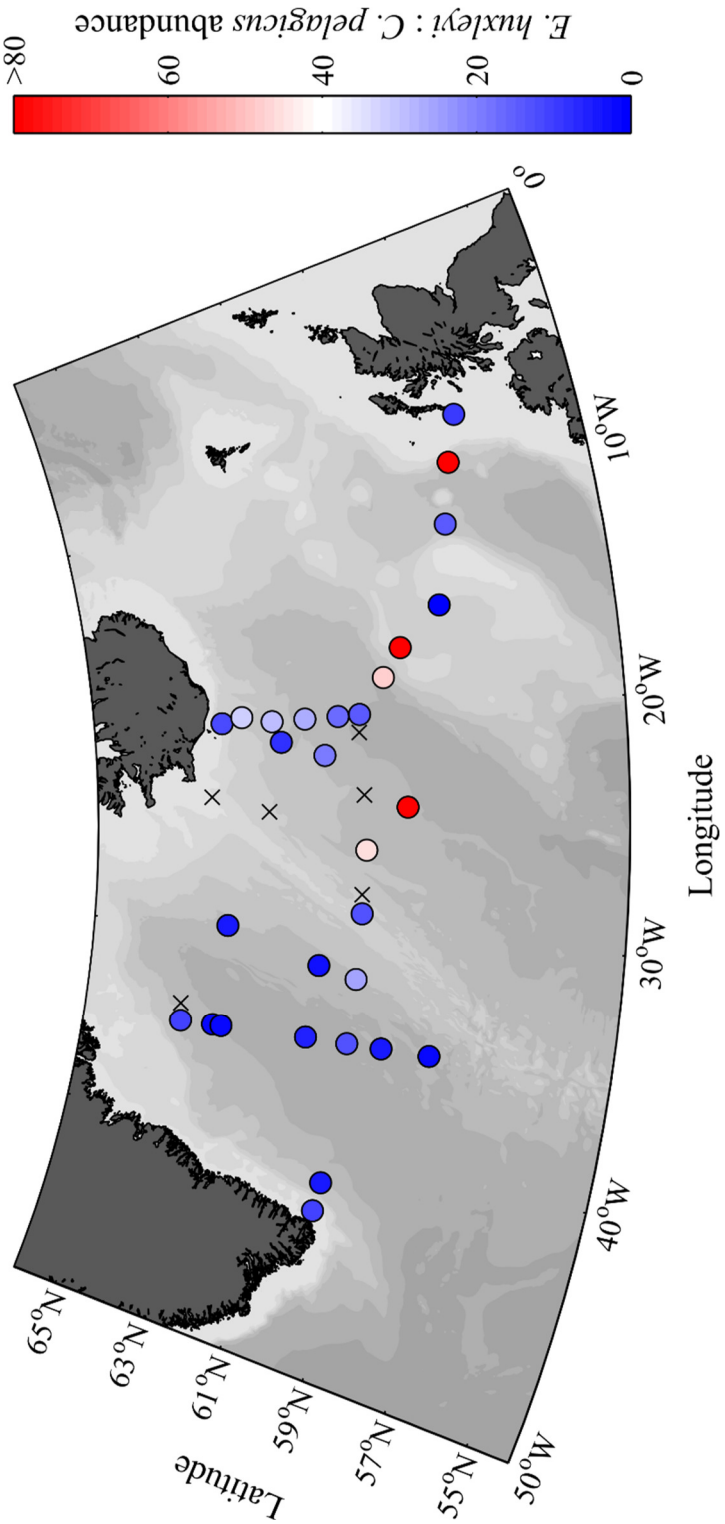

Fig. 2.4: Relative cellular abundance of *Emiliania huxleyi* to *Coccolithus pelagicus* in the North Atlantic in 2010 (April - August). Crossed symbols indicate samples where *C. pelagicus* was absent.

then in low nutrient conditions, I would expect a lower relative growth rate. As I do not know the relative nutrient affinities, I have used an extreme in my original model where *C. pelagicus* has a relative growth rate of 10 %. Under this scenario, *C. pelagicus* is the major calcite producer in 9 % of the samples, although it would still form a significant component of the total calcite production (7 – 49%) in other samples when present.

Using experimentally determined relative growth rates and cellular calcite quotas, in conjunction with relative abundances from field populations, I have shown that *C. pelagicus* is likely to be a major source of calcite in the sub-polar North Atlantic. Data on relative abundances of *E. huxleyi* and *C. braarudii* in field communities were not available for an equivalent comparison study.

2.3.4 Implications of cell size differences

While the difference in growth rates between *E. huxleyi* and *Coccolithus* is comparatively small, the difference in cell volume of *C. pelagicus* (~ 1100 μm^3) and *C. braarudii* (~ 2100 μm^3) compared to *E. huxleyi* (~ 50 μm^3) is relatively large. These differences are reflected in their cellular Chl *a* and cellular calcite:POC (Table 2.1), with the species having similar ratios of Carbon:Chl *a* (25-36 g g^{-1}) across the experimental conditions. Larger cells have a lower surface area to volume ratio, which reduces the diffusive nutrient uptake per unit volume of the cell (Lewis, 1976; Finkel et al., 2009) and thus maximal growth rates generally increase with decreasing cell size (Sarthou et al., 2005). Hence, although I expect *E. huxleyi* maximal (optimal) growth rates to be higher than *Coccolithus*, the relatively small difference in growth rate (Fig. 2.2) compared to cell volume (Table 2.1) implies that *Coccolithus* must have efficient (competitive) nutrient uptake pathways, or that these experimental conditions are less optimal for *E. huxleyi* than *Coccolithus*.

It is also worth considering the implications of relative differences in cell size and surface area to volume for nutrient requirements to support growth. From my estimates of cellular POC (Table 2.1) and assuming Redfield stoichiometry (Redfield, 1958), I can also estimate that the cellular particulate organic nitrogen (PON) and

particulate organic phosphorus (POP) content of *E. huxleyi*, *C. pelagicus* and *C. braarudii* is respectively 0.10, 2.0 and 3.6 pmol N $cell^{-1}$, and 0.006, 0.12 and 0.22 pmol P $cell^{-1}$. My estimates of cellular quotas for *E. huxleyi* are similar to Langer et al. (2013), who measured cellular quotas of 0.69 pmol C $cell^{-1}$, 0.12 pmol N $cell^{-1}$, and 0.003 pmol P $cell^{-1}$. Cellular quotas of both *C. pelagicus* and *C. braarudii* have recently been measured by Gerecht et al. (2014). While the cellular PON (1.9 pmol N $cell^{-1}$) and POP (0.19 pmol P $cell^{-1}$) of *C. pelagicus* were generally similar to my study, the value for cellular POC was slightly larger (20 pmol C $cell^{-1}$), suggesting a lower nutrient requirement per unit POC. However, Gerecht et al. (2014) report *C. braarudii* cellular quotas of POC (13 pmol C $cell^{-1}$) and PON (1.5 pmol N $cell^{-1}$) that are much lower than their values for *C. pelagicus*. This is unexpected, as it is generally accepted that *C. braarudii* is a larger species of coccolithophore than *C. pelagicus* (Geisen et al., 2004) and I would therefore expect a higher POC content for *C. braarudii* than *C. pelagicus* (Table 2.1) if POC scales with cell size. Clearly further cellular measurements of POC, PON and POP for different coccolithophore species are needed to fully examine cellular nutrient requirements.

For culture media with a given nitrate concentration of 10 µmol N L^{-1}, the maximum cumulative cell concentration that could be supported using my estimated cellular PON would therefore be ~ 1 x 10^5, ~ 5,000 and ~ 2,800 cells mL^{-1}, respectively for *E. huxleyi*, *C. pelagicus* and *C. braarudii*. This corresponds to cumulative calcite concentrations, using cellular calcite quotas from Table 2.1, of ~ 50, ~ 80 and ~ 110 µmol C L^{-1}. Therefore despite lower cell densities, for a given nutrient concentration, a population of *C. pelagicus* and *C. braarudii* would be a greater source of calcite than *E. huxleyi.*

Emiliania huxleyi regularly forms seasonal blooms in excess of 1000 cells mL^{-1}, particularly in the high latitudes of the Northern and Southern hemispheres (Tyrrell and Merico, 2004; Poulton et al., 2013). For a bloom with a magnitude of 1000 cells mL^{-1}, this would require a nitrate concentration of only ~ 0.1 µmol N L^{-1}. Comparatively, although rare, *C. pelagicus* has also been reported in concentrations exceeding 1000 cells mL^{-1} in the high latitude North Atlantic (Milliman, 1980), requiring

a much larger nitrate concentration of 2 µmol N L^{-1}. The seasonal drawdown of nitrate in the North Atlantic is estimated be ~ 10 µmol N L^{-1} (Sanders et al., 2005; Ryan-Keogh et al., 2013), and thus a *C. pelagicus* bloom of 1000 cells mL^{-1} represents the utilization of a significant amount of the available nutrients. For a bloom of this magnitude to occur, I would expect *C. pelagicus* to be a significant proportion of the total phytoplankton community with a relatively low mortality rate, as nutrient drawdown will be related to gross production by the total phytoplankton community. Reduced mortality has also been discussed as a possible factor in the formation and persistence of *E. huxleyi* blooms in the southeast Bering Sea (Olson and Strom, 2002).

The function of coccoliths is not well understood, but may have a significant role in reducing mortality by providing a certain level of protection from zooplankton grazing (Young, 1994; Tyrrell and Young, 2009). If this is the case, then I would speculate that *C. pelagicus* has a relatively lower mortality then *E. huxleyi* due to both its larger cell size and it's much larger and heavier coccosphere. A lower mortality may explain how *C. pelagicus* is able to form high density populations, while the large nutrient requirement would restrict *C. pelagicus* blooms to populations where it heavily dominates the plankton community and this may explain the scarcity of reported *C. pelagicus* blooms.

2.4 Conclusion

The data I have presented shows that when grown in parallel under identical experimental conditions, the relative difference in growth rates between *E. huxleyi* and *Coccolithus* species was generally small (12 % and 28 % respectively for *C. pelagicus* and *C. braarudii*), although *E. huxleyi* generally grew significantly faster than both *C. pelagicus* and *C. braarudii.* Using relative growth rates and estimates of cellular calcite to model relative calcite production, I have also shown that when in a suitable relative abundance to *E. huxleyi*, both *C. pelagicus* and *C. braarudii* have the potential to dominate relative and absolute calcite production.

The relative abundance of *E. huxleyi* and *C. pelagicus* was determined from samples collected from the Irminger and Iceland Basins in the North Atlantic. This showed that using my standard model scenario with *C. pelagicus* growing at 88 % of the growth rate of *E. huxleyi*, I would expect *C. pelagicus* to be the major calcite producer in 69 % of the field samples. Using a more conservative model reduced this to 57 %, while the scenario of an extreme difference in growth rates led to *C. pelagicus* only dominating 14% of the samples. Therefore, I would expect *C. pelagicus* to be a major source of calcite in the sub-polar North Atlantic across a spectrum of relative growth rates. With a present-day distribution constrained to the polar and sub-polar northern hemisphere, *C. pelagicus* is unlikely to be a dominant calcite producer on a global scale. However, the fossil record of *C. pelagicus* shows that it has remained a major contributor to sedimentary calcite for the last 65 million years (Gibbs et al., 2013) and therefore there is the strong potential that it was also a major producer in the surface ocean in the past. There are a number of other extant coccolithophore species that have high cellular calcite content relative to *E. huxleyi* (e.g. *Calcidiscus leptoporus*, *Helicosphaera carteri*) and are known to have high contributions to deep sea calcite fluxes, and therefore may similarly make significant contributions to pelagic calcite production.

Further studies elucidating the relative growth rates of these species compared to *E. huxleyi*, in culture and in the field, as well as their relative abundances in mixed coccolithophore communities are therefore needed to fully examine their potential to dominate calcite production; this will be partly addressed in Chapter 3. Lastly, investigations of community composition and calcification rates are also needed to examine the contribution of different species to total calcite production, and will be addressed in Chapter 4.

Despite a small relative difference in growth rates, there were large differences in cell size. Estimates of the cellular nutrient requirements suggest that for a given nutrient concentration, despite a much smaller maximum cell density, both *C. pelagicus* and *C. braarudii* would be a greater source of calcite than *E. huxleyi*. These results have significant implications for how we view calcite production in natural coccolithophore

communities and which coccolithophores are keystone species for oceanic biogeochemical cycles.

Chapter 3: Phytoplankton dynamics in contrasting early stage North Atlantic spring blooms: composition, succession, and potential drivers

Adapted from: Daniels, C. J., Poulton, A. J., Esposito, M., Paulsen, M. L., Bellerby, R., St. John, M., and Martin, A. P.: Phytoplankton dynamics in contrasting early stage North Atlantic spring blooms: composition, succession, and potential drivers, Biogeosciences, 12, 2395-2409, doi:10.5194/bg-12-2395-2015, 2015.

Abstract

The spring bloom is a key annual event in the phenology of pelagic ecosystems, making a major contribution to the oceanic biological carbon pump through the production and export of organic carbon. However, there is little consensus as to the main drivers of spring bloom formation, exacerbated by a lack of in situ observations of the phytoplankton community composition and its evolution during this critical period.

I investigated the dynamics of the phytoplankton community structure at two contrasting sites in the Iceland and Norwegian Basins during the early stage (25th March – 25th April) of the 2012 North Atlantic spring bloom. The plankton composition and characteristics of the initial stages of the bloom were markedly different between the two basins. The Iceland Basin (ICB) appeared well mixed to > 400 m, yet surface chlorophyll *a* (0.27-2.2 mg m^{-3}) and primary production (0.06-0.66 mmol C m^{-3} d^{-1}) were elevated in the upper 100 m. Although the Norwegian Basin (NWB) had a persistently shallower mixed layer (< 100 m), chlorophyll *a* (0.58-0.93 mg m^{-3}) and

primary production (0.08-0.15 mmol C m^{-3} d^{-1}) remained lower than the in the ICB, with picoplankton (< 2 μm) dominating chlorophyll *a* biomass. The ICB phytoplankton composition appeared primarily driven by the physicochemical environment, with periodic events of increased mixing restricting further increases in biomass. In contrast, the NWB phytoplankton community was potentially limited by physicochemical and/or biological factors such as grazing.

Diatoms dominated the ICB, with the genus *Chaetoceros* (1-166 cells mL^{-1}) being succeeded by *Pseudo-nitzschia* (0.2-210 cells mL^{-1}). However, large diatoms (> 10 μm) were virtually absent (< 0.5 cells mL^{-1}) from the NWB, with only small nanno-sized (< 5 μm) diatoms (i.e. Minidiscus spp.) present (101-600 cells mL^{-1}). I suggest micro-zooplankton grazing, potentially coupled with the lack of a seed population of bloom forming diatoms, was restricting diatom growth in the NWB, and that large diatoms may be absent in NWB spring blooms.

Emiliania huxleyi was generally numerically dominant within the coccolithophore community, which formed 0.1 – 4.4 % of the total phytoplankton Chl *a* biomass. However, *C. pelagicus* and *A. robusta* were significant components of the community, with *C. pelagicus* responsible for on average 53 % of the coccolithophore calcite. Coupled with the higher net growth rates of *C. pelagicus* (μ = 0.06 to 0.12 d^{-1}) than *E. huxleyi* (μ = 0.06 d^{-1}), this suggests that *C. pelagicus* is a major calcite producer during the early stages of the North Atlantic spring bloom.

Despite both phytoplankton communities being in the early stages of bloom formation, different physicochemical and biological factors controlled bloom formation at the two sites. If these differences in phytoplankton composition persist, the subsequent spring blooms are likely to be significantly different in terms of biogeochemistry and trophic interactions throughout the growth season, with important implications for carbon cycling and organic matter export.

3.1 Introduction

3.1.1 Mechanisms of spring bloom formation

The spring bloom is a key annual event in the phenology of pelagic ecosystems, where a rapid increase in phytoplankton biomass has a significant influence on upper ocean biogeochemistry and food-availability for higher trophic levels (Townsend et al., 1994; Behrenfeld and Boss, 2014). Spring blooms are particularly prevalent in coastal and high latitude waters. The high levels of phytoplankton biomass and primary production that occur during these blooms, and its subsequent export out of the surface ocean, result in a significant contribution to the biological carbon pump (Townsend et al., 1994; Sanders et al., 2014). The North Atlantic spring bloom is one of the largest blooms on Earth, making a major contribution to the annual export of ~ 1.3 Gt C yr^{-1} from the North Atlantic (Sanders et al., 2014). The timing and magnitude of the spring bloom can have a significant biogeochemical impact (Henson et al., 2009); hence it is important to understand both the controls on, and the variability in, bloom timing, magnitude and community structure. Despite its importance there remains little consensus as to the environmental and ecological conditions required to initiate high latitude spring blooms (Townsend et al., 1994; Behrenfeld, 2010; Taylor and Ferrari, 2011a).

Phytoplankton blooms occur when growth rates exceed loss rates (i.e. a sustained period of net growth); phytoplankton growth rate constraints include irradiance, nutrient supply, and temperature, while losses can occur through predation, advection, mixing out of the euphotic zone, sinking and viral attack (Miller, 2003). Therefore, the rapid increase in (net) growth rates during the spring bloom must be due to either an alleviation of those factors constraining growth, a reduction in factors determining losses, or (more likely) some combination of both.

The critical depth hypothesis (Sverdrup, 1953), the seminal theory of spring bloom initiation, proposes that there exists a critical depth such that when stratification shoals above this depth, phytoplankton growth will exceed mortality and a bloom will

occur. However, this hypothesis has been more recently brought into question as bloom formation has been observed to start earlier than expected (Mahadevan et al., 2012), and in the absence of stratification (Townsend et al., 1992; Eilertsen, 1993). Several new theories have now been developed to explain these occurrences (reviewed in Behrenfeld and Boss, 2014; Fischer et al., 2014; Lindemann and St. John, 2014).

Eddies and oceanic fronts have both been identified as sources of stratification prior to the wider onset of seasonal stratification (Taylor and Ferrari, 2011b; Mahadevan et al., 2012). However, they do not explain blooms in the complete absence of stratification, which can instead be explained by the critical turbulence hypothesis (Huisman et al., 1999; Taylor and Ferrari, 2011a; Brody and Lozier, 2014). Both of these theories distinguish between a convectively driven actively mixed layer and a density-defined mixed layer such that if convective mixing reduces sufficiently, blooms can occur in the actively mixing layer although the density-defined mixing layer remains deep. Therefore, blooms are able to form in the apparent absence of stratification, as defined by the presence of a thermocline. An alternative to the hypotheses concerning physical controls on bloom formation is the disturbance-recovery hypothesis proposed by Behrenfeld (2010), who suggests that the decoupling of phytoplankton and microzooplankton contact rates in deep winter mixed layers results in phytoplankton net growth from winter onwards due to reduced mortality (via grazing). It is also possible that there are multiple biological and physical controls, acting on different spatial and temporal scales, that drive the heterogeneous bloom distributions observed via remote sensing (e.g. Lindemann and St. John, 2014).

Significant interannual and decadal variability in the structure and timing of spring blooms in the North Atlantic has been documented (Henson et al., 2009). Such variability in bloom timing has been attributed to the variation in the winter mixed layer depth (WMLD). A deeper WMLD results in a delayed bloom in the subarctic North Atlantic (Henson et al., 2009). A strong latitudinal trend exists in the North Atlantic where the spring bloom propagates north due to seasonal relief from light limitation at high latitudes (Siegel et al., 2002; Henson et al., 2009). Both the role of the WMLD in

interannual variability in bloom timing and the northwards progression of bloom start dates highlight how physical processes have a clear and significant impact on bloom formation. The controls on the variability in bloom magnitude are less certain, although it appears to be a combination of WMLD variability influencing the start date as well as biological factors such as phytoplankton composition and grazing (Henson et al., 2009).

Despite considerable discussion on the various factors that may or may not influence bloom initiation, timing, magnitude and phenology, few studies have actually examined the in situ phytoplankton community. Instead, because of the need for temporally resolved data, satellite-derived products and models have been used in much of the previous work on spring blooms. However, such methods cannot address the potential influence of the complex plankton community structure on the development of a spring bloom.

3.1.2 Phytoplankton communities in spring blooms

The traditional text book view of a phytoplankton spring bloom is that the pre-bloom pico-phytoplankton (cells < 2 μm) dominated community is directly succeeded by a diatom dominated community (Margalef, 1978; Barber and Hiscock, 2006); as conditions become more favourable for growth, a diatom bloom develops, 'suppressing' growth of other phytoplankton groups. Through either increased predation, nutrient stress or a changing physical environment (Margalef, 1978), diatoms decline and are then replaced by other phytoplankton such as dinoflagellates and coccolithophores (Lochte et al., 1993; Leblanc et al., 2009). In this way, a series of phytoplankton functional type successions occur as the spring bloom develops. That diatoms often dominate intense spring blooms is well accepted (Lochte et al., 1993; Rees et al., 1999), however the dynamics of the interplay between diatoms and the rest of the community have been questioned (Barber and Hiscock, 2006).

The rapid proliferation of diatoms in a spring bloom does not necessarily suppress other phytoplankton (Lochte et al., 1993; Barber and Hiscock, 2006), and the “rising tide” hypothesis states that instead of succession, the favourable conditions for

diatoms also favour other phytoplankton groups and therefore all phytoplankton will respond positively and grow (Barber and Hiscock, 2006). The apparent suppression of the phytoplankton community by diatoms is due to the relatively high intrinsic growth rates of diatoms resulting in concentrations far exceeding the rest of the community. The "rising tide" hypothesis is a contrasting theory to succession, however it may be that the phytoplankton community response will not be universal, with some taxa-specific succession due to competition or increased grazing (Brown et al., 2008). Furthermore, succession may appear to occur if phytoplankton loss rates are taxonomically specific, such that while many phytoplankton groups concurrently grow, successive loss of specific groups occurs.

3.1.3 Coccolithophores in spring blooms

Through the production and subsequent export of their calcium carbonate coccoliths, coccolithophores comprise a key component of the global carbon cycle (De Vargas et al., 2007). In the seasonal cycle of phytoplankton, coccolithophores are generally thought to succeed diatom spring blooms (Margalef, 1978), forming "blooms" in the late spring/summer (Holligan et al., 1993). As such, studies of coccolithophores tend to focus on this period of the seasonal cycle, attempting to elucidate the conditions required for these "blooms" to occur (Tyrrell and Merico, 2004; Raitsos et al., 2006).

However, the seasonal cycle of coccolithophores has recently been questioned, with a satellite based study suggesting potential co-existence of both diatoms and coccolithophores (Hopkins et al., 2015). The community structure and dynamics of coccolithophores in non-"bloom" periods is relatively poorly understood, yet this period encompasses most of their seasonal cycle and thus could be biogeochemically important. Coccolithophores formed a significant component (10 – 20 %) of the phytoplankton community in the Iceland Basin in late summer (Poulton et al., 2010), and have been observed in spring in the North Atlantic (Savidge et al., 1995; Silva et al., 2008; Schiebel et al., 2011) and Norwegian Sea (Dale et al., 1999). However few studies have examined coccolithophore dynamics and their biogeochemical importance in the context of spring blooms.

3.1.4 Chapter outline

The goal of this chapter was to determine the overall phytoplankton community structure, and its evolution during the onset of the spring bloom in the North Atlantic; linking the community structure to the physical environment and examining whether succession to a diatom dominated environment would occur early in the growth season (March-April). Within the context of the dynamics of the overall phytoplankton community, the structure, dynamics and biogeochemical role of the coccolithophore community can then be examined. Sampling for this study was carried out as part of the multidisciplinary EuroBASIN "Deep Convection Cruise". The timing and location of this cruise (19th March – 2nd May 2012) was chosen to try and observe the transition from deep winter convection to spring stratification, and examine the physical controls on the dynamics of phytoplankton, carbon export and trophic interactions. A recent study has previously suggested that winter convection in the North Atlantic and Norwegian Sea sustains an overwintering phytoplankton population, thus providing an inoculum for the spring bloom (Backhaus et al., 2003), although this transition has not been explicitly examined before.

3.2 Methods

3.2.1 Sampling

The Deep Convection cruise repeatedly sampled two pelagic locations in the North Atlantic (Fig. 3.1), sited in the Iceland (ICB, 61.50 °N, 11.00 °W) and Norwegian (NWB, 62.83 °N, 2.50 °W) Basins, onboard the R/V *Meteor*. The ICB was visited four times, and the NWB visited three times during the course of the cruise. Samples were collected from multiple casts of a conductivity-temperature-depth (CTD) - Niskin rosette, equipped with a fluorometer, at each station. Water samples for rates of primary production (PP), community structure and ancillary parameters (chlorophyll *a* [Chl *a*], calcite [PIC], particulate silicate [$bSiO_2$] and macronutrient concentrations) were collected from predawn (02:30-05:00 GMT) casts from six light depths (55 %, 20 %,

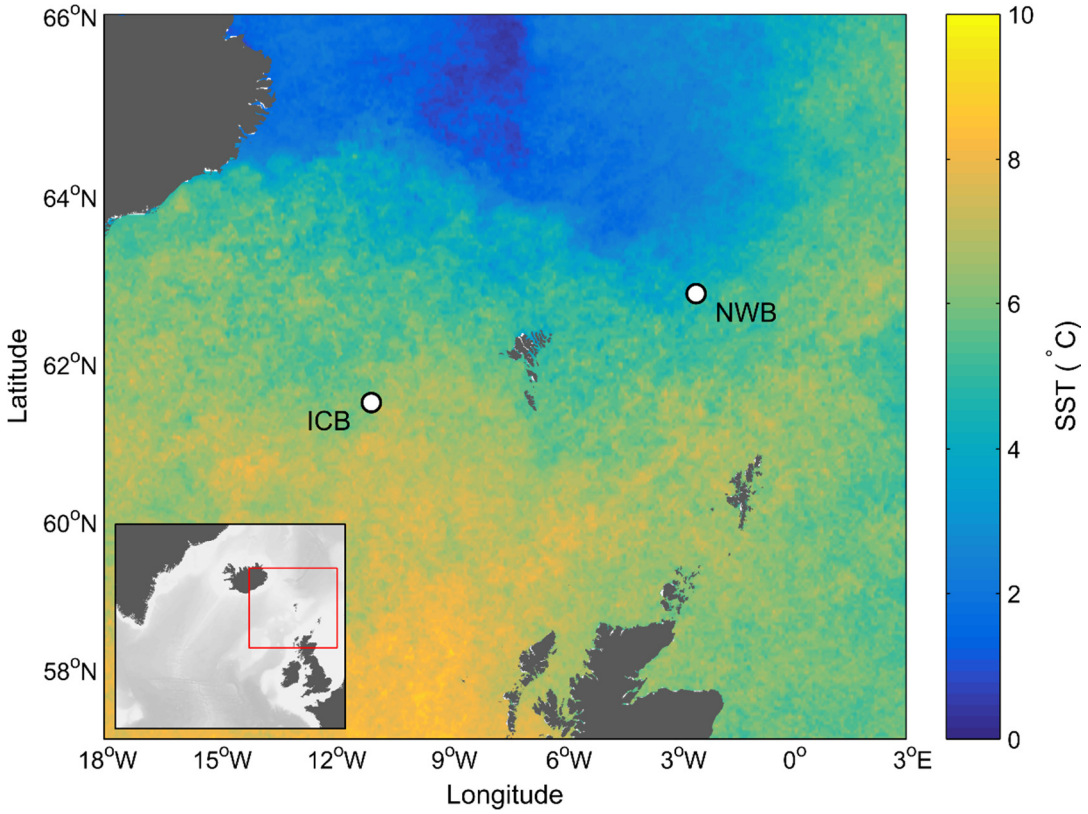

Fig. 3.1: Sampling locations in the Iceland Basin (ICB) and the Norwegian Basin (NWB), superimposed on a composite of MODIS sea surface temperature for 25 March – 29 April 2012.

14 %, 7 %, 5 % and 1 % of incidental PAR). The depth of 1 % incident irradiance was assumed to equate to the depth of the euphotic zone (e.g. Poulton et al., 2010). Optical depths were determined from a daytime CTD cast on preceding days at each site. Additional samples for coccolithophore community structure and ancillary parameters were collected from a second CTD cast, while samples for detailed size fractionated Chl *a* were collected from a third cast.

3.2.2 Primary production

Carbon fixation rates were determined using the ^{13}C stable isotope method (Legendre and Gosseline, 1996). Water samples (1.2 L) collected from the six irradiance depths were inoculated with 45 – 46 µmol L^{-1} ^{13}C labelled sodium bicarbonate, representing 1.7 – 1.8 % of the ambient dissolved inorganic carbon pool. Samples were incubated in

an on-deck incubator, chilled with sea surface water, and light depths were replicated using optical filters (Misty-blue and Grey, LEE™). Incubations were terminated after 24 hours by filtration onto pre-ashed (> 400 °C, > 4 hours) Whatman GF/F filters. Acid-labile carbon (PIC) was removed by adding 1 – 2 drops of 1 % HCl to the filter followed by extensive rinsing with freshly filtered (Fisherbrand MF300, ~ 0.7 µm pore size) unlabelled seawater. Filters were oven dried (40°C, 8 – 12 hours) and stored in Millipore PetriSlides™. A parallel 55 % bottle for size fractionated primary production (< 10 µm) was incubated alongside the other samples, with the incubation terminated by pre-filtration through 10-µm polycarbonate (Nuclepore™) filters and the filtrate was filtered and processed as above.

The isotopic analysis was performed on an Automated Nitrogen and Carbon Analysis prep system with a 20-20 Stable Isotope Analyser (PDZ Europa Scientific Instruments). The ^{13}C-carbon fixation rate was calculated using the equations described in Legendre and Gosseline (1996). The > 10-µm PP fraction was calculated as the difference between total PP and < 10-µm PP.

3.2.3 Community structure

Water samples for diatom and micro zooplankton counts, collected from the predawn cast surface samples (5 – 15 m), were preserved with acidic Lugol's solution (2 % final solution) in 100-mL amber glass bottles. Cells were counted in 50 mL Hydro-Bios chambers using a Brunel SP-95-I inverted microscope (X200; Brunel Microscopes Ltd). Samples for flow cytometry, collected by Maria Paulsen, were fixed with glutaraldehyde (0.5 % final solution) and stored at -80°C before being analysed using a FACS Calibur (Beckton Dickinson) flow cytometer (Zubkov et al., 2007).

Water samples (0.5 – 1 L) for coccolithophore cell numbers and species identification were collected from surface samples (5 – 15 m) onto cellulose nitrate filters (0.8-µm pore size, Whatman), oven dried and stored in Millipore PetriSlides™. Permanent slides of filter halves were prepared and analysed using polarizing light microscopy following Poulton et al. (2010). Coccolithophores were analysed to species level following Frada et al. (2010). For confirmation of species identification, a subset of

Table 3.1: Coccolith shape factors, coccolith calcite, coccoliths per cell and cellular calcite for the individual coccolithophore species.

Species	Coccolith Shape Factor (k_s)	Coccolith Calcite (pmol C coccolith $^{-1}$)	Coccoliths per Cell	Cellular Calcite (pmol C cell^{-1})
E. huxleyi (A)	0.020	0.023	16	0.37
E. huxleyi (B)	0.020	0.024	32	1.12
E. huxleyi (A over-calcified)	0.040	0.024	16	0.74
G. muellerae	0.050	0.08	16	1.28
C. pelagicus	0.060	1.61	13	20.8
A. robusta	0.045	0.010	43	0.42
Syracosphaera spp.	0.015	0.012	35	0.40
C. caudatus	0.013	0.002	54	0.09
C. leptoporus	0.080	0.74	20	14.8
C. mediterranea	0.070	0.12	40	4.84
S. pulchra	0.030	0.14	-	-

filter halves were analysed by scanning electron microscope (SEM) following Daniels et al. (2012). Coccolithophore species were identified according to Young et al. (2003).

Coccolithophore cell (coccosphere) and coccolith derived calcite was estimated following the method outlined in Daniels et al. (2012); coccolith calcite was estimated following Young and Ziveri (2000), Poulton et al. (2010) and Probert et al. (2007), and the number of coccoliths per cell were estimated from SEM images (Table 3.1). As in Daniels et al. (2012), for those species with an undefined calcite content, estimates were calculated from species with a similar shape coccolith.

3.2.4 Chlorophyll a

Water samples (250 mL) for total Chl *a* analysis were filtered onto Fisherbrand MF300 filters. Parallel samples were filtered onto polycarbonate filters (10-µm) for > 10 µm Chl *a*. Samples for detailed size fractionated Chl *a*, collected in duplicate from a single

depth in the upper water column (12 – 35 m), were filtered in parallel onto polycarbonate filters of various pore size (2, 10, 20-µm) and MF300 filters (effective pore size 0.7 µm). Filters were extracted in 8 mL of 90 % acetone (Sigma) for 20-24 hours (dark, 4°C). Measurements of Chl *a* fluorescence were analysed on a Turner Designs Trilogy Fluorometer, calibrated using a solid standard and a chlorophyll *a* extract.

3.2.5 Ancillary parameters

Particulate inorganic carbon (PIC) measurements were made on water samples (500 mL) filtered onto polycarbonate filters (0.8 µm pore-size, Whatman), rinsed with trace ammonium solution (pH ~ 10) and oven-dried (6 – 8 hours, 30 – 40 °C). The analysis was carried out following Daniels et al. (2012) except that extractions were carried out in 5.0 mL of 0.4 mol L^{-1} nitric acid, erroneously reported as 0.5 mL in Daniels et al. (2012). Particulate silicate ($bSiO_2$) samples were collected onto polycarbonate filters (0.8 µm pore-size, Whatman), rinsed with trace ammonium solution (pH ~ 10) and oven-dried (6 – 8 hours, 30 – 40 °C). Digestion of $bSiO_2$ was carried out in polypropylene tubes using 0.2 mol L^{-1} sodium hydroxide, before being neutralised with 0.2 mol L^{-1} hydrochloric acid (Ragueneau and Tréguer, 1994; Brown et al., 2003). The solutions were analysed by Mark Stinchcombe using a SEAL QuAAtro autoanalyser and no corrections were made for lithogenic silica. Macronutrient (nitrate, phosphate, silicic acid) concentrations were determined following Sanders et al. (2007) on a Skalar autoanalyser by Mario Esposito.

Samples for total dissolved inorganic carbon (C_T) were drawn into 500 mL borosilicate bottles. No filtering of samples occurred prior to analysis. Samples were stored in the dark and analysed within 12 hours of sampling, thus no poisoning was required. C_T was determined by Richard Bellerby using coulometric titration (Johnson et al., 1987) with a precision of ≤ 2 µmol kg^{-1}. Measurements were calibrated against certified reference material (CRM, Dickson, 2010). Seawater pH_T was measured by Richard Bellerby using the automated marine pH sensor (AMpS) system as described in Bellerby et al. (2002) modified for discrete mode. This system is an automated spectrophotometric pH

sensor that makes dual measurements of thymol blue. The pH_T data used in this study were computed using the total hydrogen ion concentration scale and has a precision of 0.0002 pH_T and an estimated accuracy of better than 0.0025 pH_T units against CRM standards. The measured C_T and pH_T, with associated temperatures and salinity, were input to CO2SYS (Lewis and Wallace, 1998) to calculate saturation state of calcite using the dissociation constants for carbonic acid of Dickson and Millero (1987), boric acid from Dickson (1990a), sulphuric acid following Dickson (1990b) and the CO_2 solubility coefficients from Weiss (1974).

Satellite data on Chl *a*, photosynthetically available radiation (PAR) and sea surface temperature (SST) were obtained from the Aqua Moderate Resolution Image Spectroradiometer (MODIS) as 4 km resolution, 8 day composites. Data were extracted as averaged 3 x 3 pixel grids, centred on the sampling locations. Day length was calculated according to Kirk (1994). The R/V *Meteor* was not fitted with a PAR sensor, thus satellite measurements were the only available source of PAR data.

3.2.6 Data availability

Data included in the chapter are available from the data repository PANGAEA via Daniels and Poulton (2013) for the measurements of primary production, chlorophyll *a*, particulate inorganic carbon and particulate silicate, cell counts of coccolithophores, diatoms and microzooplankton; Esposito and Martin (2013) for measurements of nutrients; Paulsen et al. (2014) for measurements of picoplankton and nanoplankton; and Bellerby (2014) for measurements of the carbonate chemistry.

3.3 Results

3.3.1 General oceanography

The two sites were characterised by very different water column profiles throughout the study period. In the NWB, a pycnocline persisted over the upper 400 m with a variable mixed layer (20 – 100 m, Fig. 3.2D). In contrast, the ICB appeared well mixed

over the upper 400 m when considered over the equivalent density range (Fig. 3.2A). However, weak unstable stratification was observed in the upper 100 m when examined over a much narrower range in density (Fig. 3.2A inset).

Sea surface temperature (SST) showed little variation at both sites (Table 3.1), while the ICB (8.6 – 8.9 °C) was consistently warmer than the NWB (6.5 – 7.2 °C). Satellite estimates of SST were colder than in situ measurements and exhibited greater variability (Fig. 3.3A). However, the general pattern of the ICB being warmer than the NWB was observed from both in situ measurements and satellite derived ones. Sea - surface salinity (SSS), pH_T and Ω_{Ca} were relatively stable throughout the study with total ranges of 35.1 – 35.3, 8.0 – 8.1 and 3.0 – 3.2, respectively (Table 3.1).

Initial surface water concentrations of nitrate (NO_3) and phosphate (PO_4) were ~ 12 mmol N m^{-3} and ~ 0.7 – 0.8 mmol P m^{-3} at both sites (Table 3.1). Silicic acid (dSi) was high throughout the study period (mostly > 4 mmol Si m^{-3}), with slightly higher concentrations in the NWB (5.3 – 5.7 mmol Si m^{-3}) than the ICB (< 5 mmol Si m^{-3}). Drawdown of 1 mmol m^{-3} of NO_3 and dSi occurred in the ICB between the 19th and April, but then returned to previous levels by the 29th April. Nutrient drawdown did not occur in the NWB during the cruise period.

Both sites showed a similar trend of increasing daily PAR during the study (Fig. 3.3B); a twofold increase in the NWB (from 12.3 to 28.4 mol quanta m^{-2} d^{-1}) and a slightly smaller increase in the ICB (from 13.5 to 24.3 mol quanta m^{-2} d^{-1}). Daily irradiance continued to increase after the cruise finished, peaking around 40 – 45 days later at values in excess of 40 mol quanta m^{-2} d^{-1} (Fig. 3.3B). The general trend of increasing PAR was also reflected in the day length (Fig. 3.3B). At both sites, the euphotic depth shoaled as the study progressed, from 115 m to 50 m in the ICB and from 80 m to 56 m in the NWB (Table 3.2). However, the euphotic depth again deepened by 36 m between the 3rd and 4th visits to the ICB.

For the duration of the cruise until the 27th April (Day 118), surface and euphotic zone integrated particulate silicate ($bSiO_2$) increased in the ICB, peaking at 0.66 mmol Si m^{-3}

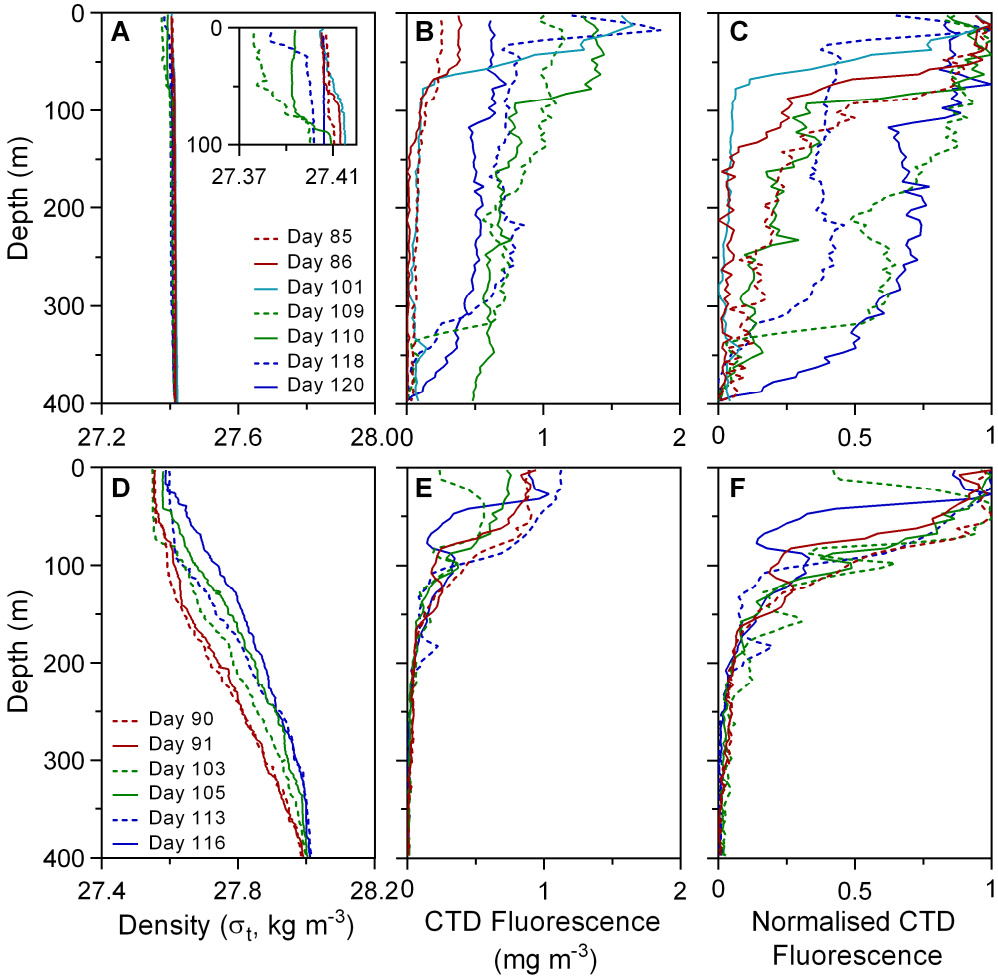

Fig. 3.2: Upper water column profiles for the ICB (A, B, C) and the NWB (D, E, F), of A,D) density, B,E) CTD fluorescence and C,F) CTD fluorescence normalised to peak CTD fluorescence for each profile.

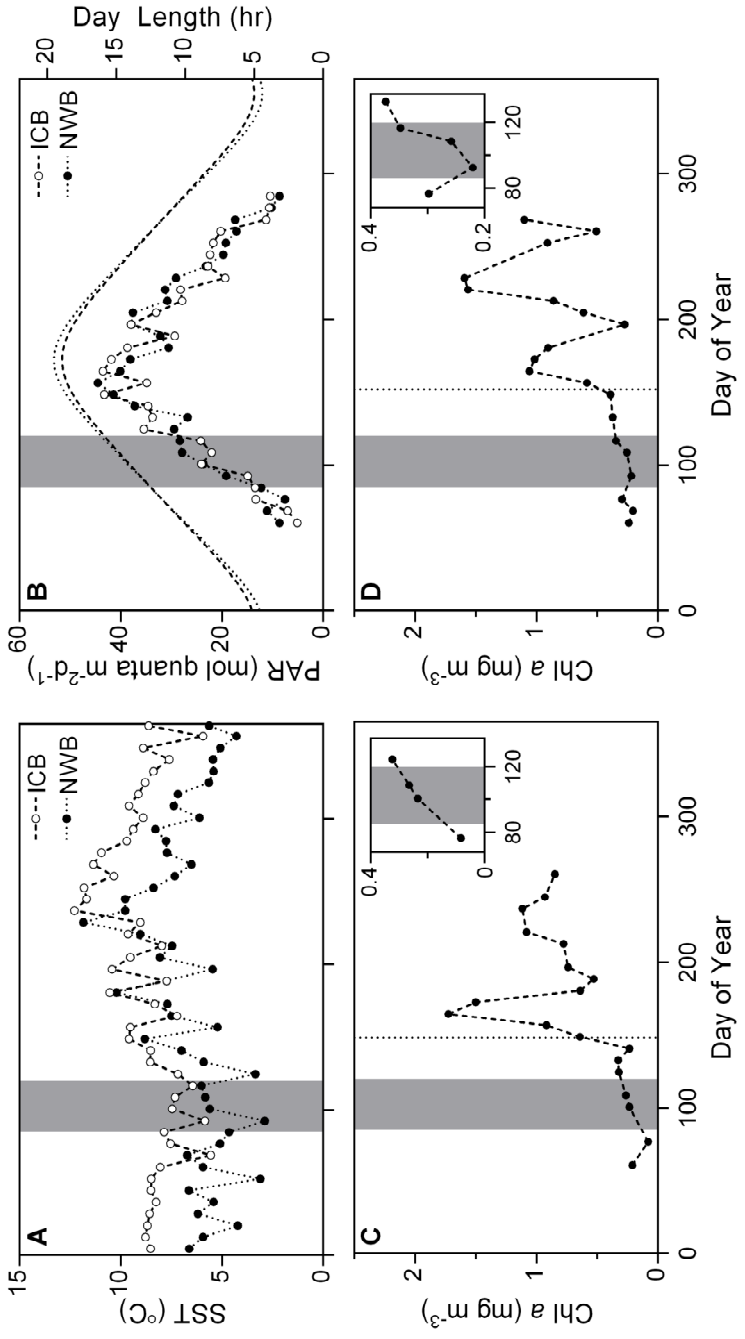

Fig. 3.3: Seasonal variation in A) satellite sea surface temperature (SST), B) satellite daily incidental PAR and day length and C,D) satellite chlorophyll *a* (Chl *a*) for C) the Iceland Basin (ICB) and D) the Norwegian Basin (NWB) for 2012. The grey region indicates the period of the cruise. The vertical dotted lines in plots C and D indicate bloom initiation, calculated following Henson et al. (2009). The insets in C & D show the variation in satellite chlorophyll during the period of the cruise.

and 37.1 mmol Si m^{-2}, respectively (Fig. 3.4A, Table 3.2), with a significant decline in $bSiO_2$ after this date. Lower values of $bSiO_2$, with little temporal variation, were found in the NWB, although a small increase in surface $bSiO_2$ was observed between the 14th and 22nd April (from 0.05 to 0.08 mmol Si m^{-3}, Fig. 3.4A). Standing stocks of PIC were less variable than $bSiO_2$ (Figs. 3.5A & 3.5B). Highest surface values were observed during the last visit to the NWB (0.20 mmol C m^{-3}), while integrated calcite peaked at 11 mmol C m^{-2} on the 27th April in the ICB (Table 3.2).

3.3.2 Chlorophyll a

Profiles of CTD fluorescence in the NWB had a relatively consistent structure with high fluorescence in the stratified upper water column (Figs. 3.2E & 3.2F). Intra-site variation can be seen in the relative fluorescence values in surface waters, but a consistent increase over time was not observed. Fluorescence profiles in the ICB were more variable (Figs. 3.2B & 3.2C), ranging from profiles with high surface fluorescence (e.g. 10th April, Day 101) to profiles with elevated fluorescence throughout the upper 300 m (e.g. 29th April, Day 120).

Acetone extracted measurements of chlorophyll *a* (Chl *a*) ranged from 0.1 to 2.3 mg m^{-3} with highest values generally in surface waters (5 – 15 m). Surface Chl *a* was variable in the ICB, with the lowest surface values (0.27 – 0.31 mg m^{-3}) measured during the first visit (Table 3.2). Peak Chl *a* values in the ICB occurred on the 10th April (2.2 mg m^{-3}), after which Chl *a* declined reaching a low of 0.62 mg m^{-3} by the end of the study (but remaining above initial Chl *a* values). Initial surface Chl *a* values were higher in the NWB (0.58 mg m^{-3}) than the ICB, and generally increased throughout the cruise. However, the magnitude of this increase was significantly smaller than in the ICB, peaking at only 0.93 mg m^{-3}. Euphotic zone integrated Chl *a* showed a similar pattern to surface Chl *a* across both stations, with highest values on the 10th April (ICB, 146.4 mg m^{-2}).

Satellite estimates of Chl *a* also showed an increase in Chl *a* at both sites during the cruise (Figs. 3.3C & 3.3D), although these values (< 0.4 mg m^{-3}) were much lower than measured in situ Chl *a* (Table 3.2). The large increase in Chl *a* associated with North

Table 3.2: Physicochemical features of the Iceland Basin and Norwegian Basin stations: SST, sea surface temperature; SSS, sea surface salinity; CT, dissolved inorganic carbon; ΩC, calcite saturation state; NO3, nitrate; PO4, phosphate; dSi, silicic acid.

						Carbonate Chemistry			Surface Macronutrients (mmol m^{-3})		
Location	Sta.	Date	Day of Year	SST (°C)	SSS	C_T (µmol m^{-3})	pH_T	Ω_C	NO_3	PO_4	dSi
Iceland Basin	1	25 Mar	85	8.7	35.3	2149	8.0	3.1	12.3	0.79	4.7
	1	26 Mar	86	8.7	35.3	2148	8.0	3.1	12.6	0.81	4.7
	2	7 Apr	98	8.7	35.3	2140	8.0	3.1	12.4	0.81	4.5
	2	10 Apr	101	8.7	35.3	2139	8.1	3.2	11.5	0.75	4.3
	3	18 Apr	109	8.8	35.3	2144	8.1	3.2	11.6	0.79	4.3
	3	19 Apr	110	8.7	35.3	2150	8.1	3.2	11.9	0.76	4.1
	4	27 Apr	118	8.9	35.3	2135	8.1	3.2	10.7	0.70	3.1
	4	29 Apr	120	8.6	35.3	2148	-	-	12.0	0.80	4.2
Norwegian Basin	1	30 Mar	90	7.0	35.2	2142	8.1	3.0	12.1	0.67	5.3
	1	31 Mar	91	7.1	35.2	2161	8.1	3.0	12.5	0.81	5.4
	2	12 Apr	103	7.2	35.2	2153	8.1	3.0	13.4	0.84	5.6
	2	14 Apr	105	6.9	35.2	2152	8.1	3.0	13.5	0.82	5.6
	3	22 Apr	113	6.5	35.1	2150	8.1	3.0	12.2	0.79	5.7
	3	25 Apr	116	6.8	35.2	2143	8.1	3.0	12.5	0.82	5.7

Table 3.3: Biological features of the Iceland Basin and Norwegian Basin stations: Chl *a*, chlorophyll *a*; PP, primary production; $bSiO_2$, particulate silicate; PIC, particulate inorganic carbon.

						Surface size fractions			Euphotic zone integrals			
Location	Sta.	Date	Day of Year	Surface Chl *a* (mg m^{-3})	Surface PP (mmol C m^{-3} d^{-1})	>10 µm Chl *a* (%)	>10 µm PP (%)	Euphotic zone depth (m)	Chl *a* (mg m^{-2})	$bSiO_2$ (mmol Si m^{-2})	PIC (mmol C m^{-2})	PP (mmol C m^{-2} d^{-1})
Iceland Basin	1	25 Mar	85	0.27		28		115	22.3	8.3	7.7	
	1	26 Mar	86	0.31	0.41	24	35	115	26.5	2.5	4.5	2.2
	2	7 Apr	98	1.13		80		72	61.4	8.7	8.7	
	2	10 Apr	101	2.18	4.89	84	61	72	146.4	19.6	6.9	221.9
	3	18 Apr	109	1.01		56		50	49.2	13.4	6.5	
	3	19 Apr	110	1.15	2.11	67	40	50	55.6	15.4	5.8	58.0
	4	27 Apr	118	1.18		-		86	75.7	37.1	11.0	
	4	29 Apr	120	0.62	1.19	94	61	86	55.3	27.6	8.1	61.5
Norwegian Basin	1	30 Mar	90	0.58		6		80	34.6	5.5	7.7	
	1	31 Mar	91	0.59	0.67	7	5	80	39.2	7.0	7.1	27.3
	2	12 Apr	103	0.54		9		65	32.3	4.4	5.9	
	2	14 Apr	105	0.69	0.90	13	5	65	37.2	4.4	6.4	38.2
	3	22 Apr	113	0.93		10		56	46.7	5.0	9.7	
	3	25 Apr	116	0.84	1.11	21	20	56	40.5	6.4	10.5	39.8

Atlantic spring blooms occurred between 20 and 30 days after the cruise (Figs. 3.3C & 3.3D). Both sites were characterised by two peaks in Chl *a* throughout the year, one in late spring (mid-June) and another in late summer (mid-August). The largest satellite-derived Chl *a* values occurred in the ICB in late spring (1.7 mg m^{-3}, Fig. 3.3C), while in the NWB, peak Chl *a* occurred during the late summer bloom (1.6 mg m^{-3}, Fig. 3.3D).

Size fractionated Chl *a* revealed very different communities at the two sites (Table 3.2 and Fig. 3.6). Initially in the ICB, approximately a quarter of the Chl *a* biomass was derived from the > 10 µm fraction (24 – 28 %; Table 3.2, Fig. 3.6A). On subsequent visits this increased significantly to 56 – 94 % (Table 3.2, Fig. 3.6A). A general trend of an increasing contribution from the > 10 µm fraction was also observed in those samples collected for more detailed size fractionation (Fig. 3.6C). The detailed size fractionation showed that excluding the first ICB visit where samples were not collected, the > 10 µm fraction was completely dominated by the > 20 µm fraction in the ICB (Fig. 3.6C). Conversely, the > 10 µm fraction formed only a minor component (< 21 %) of the Chl *a* biomass in the NWB, although the > 10 µm contribution did increase throughout the cruise (Table 3.2, Fig. 3.6B). Detailed size fractionation in the NWB showed that the biggest increase in contribution came from the 2-10 µm fraction, increasing from 14 % to 32 % (Fig. 3.6D), which was due to an increase in the absolute value of 2 – 10 µm Chl *a* (from 0.09 to 0.31 mg m^{-3}).

3.3.3 Primary production

Primary production (PP) in surface waters (5 – 15m) ranged from 0.41 to 4.89 mmol C m^{-3} d^{-1} in this study (Table 3.2), with PP generally decreasing with depth. Surface PP correlated well with euphotic zone integrated PP ($r = 0.98$, $p < 0.001$, $n = 7$). The largest change in PP occurred in the ICB, between the 26th March and the 10th April, when peak PP rates were observed in both the surface waters (4.89 mmol C m^{-3} d^{-1}) and integrated over the euphotic zone (221.9 mmol C m^{-2} d^{-1}, Table 3.2). Following this peak, PP in the ICB declined, although it generally remained higher than pre-peak PP rates. The > 10 µm PP fraction contributed between 35 – 61 % of the total PP in the ICB. In contrast, the range and maximum rate of PP in the NWB was much lower than

the ICB (0.67 – 1.11 mmol C m^{-3} d^{-1}, Table 3.2) with the > 10 µm PP making up a much smaller fraction (< 20 %). However, a clear increase in the > 10 µm PP fraction was observed between the 14th April (5 %) and the 25th April (20 %). The general trend in total and size-fractionated PP at both sites reflected that observed in the Chl *a* measurements.

3.3.4 Community structure

3.3.4.1 Community structure – picoplankton and nanoplankton

Flow cytometry identified *Synechococcus*, autotrophic picoeukaryotes and autotrophic nanoplankton (< 10 µm) in relatively high abundance in all samples (Table 3.3). In general, *Synechococcus* and picoeukaryotes were more abundant in the NWB than the ICB. In the NWB, a contrasting pattern between *Synechococcus,* nanoplankton and picoeukaryotes was observed; while *Synechococcus* and the nanoplankton increased significantly from 2,617 to 5,483 cells mL^{-1} and 484 to 1,384 cells mL^{-1} respectively, a large decrease in picoeukaryotes was also observed, from 18,016 to 8,456 cells mL^{-1}. A less coherent pattern was observed in the ICB, where peak concentrations of both *Synechococcus* (2,112 cells mL^{-1}) and picoeukaryotes (6,982 cells mL^{-1}) occurred on the 19th April, with a general decline after this date.

3.3.4.2 Community structure – coccolithophores

The coccolithophore species identified by polarised light microscopy were: *Emiliania huxleyi*, *Coccolithus pelagicus*, *Calcidiscus leptoporus*, *Coronosphaera mediterranea* and *Syracosphaera pulchra*. More detailed SEM observations found a number of other species at low cell densities not clearly identified by the light microscope: *Algirosphaera robusta*, *Acanthoica quattrospina*, *Calciopappus caudatus*, *Gephyrocapsa muellerae*, *Syracosphaera corolla*, *S. marginaporata, S. molischii, S. nodosa*, *S. ossa* and unidentified *Syracosphaera* spp. Many of these coccolithophore species have cell diameters between 10 and 20 µm, with the notable exceptions of *E. huxleyi*, *G. muellerae* and the smaller *Syracosphaera* spp. (Young et al., 2003).

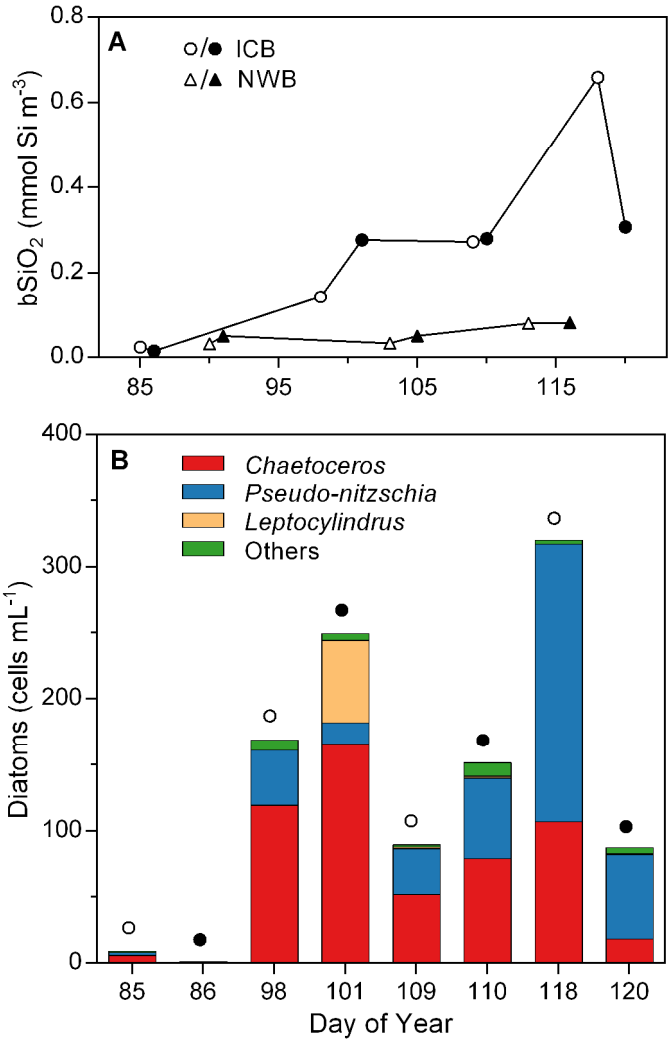

Fig. 3.4: Surface (5 – 15 m) measurements of A) Particulate silicate ($bSiO_2$) and B) diatom species abundance in the Iceland Basin. Black symbols indicate where diatoms were counted from Lugol's samples, while open symbols indicate SEM counts.

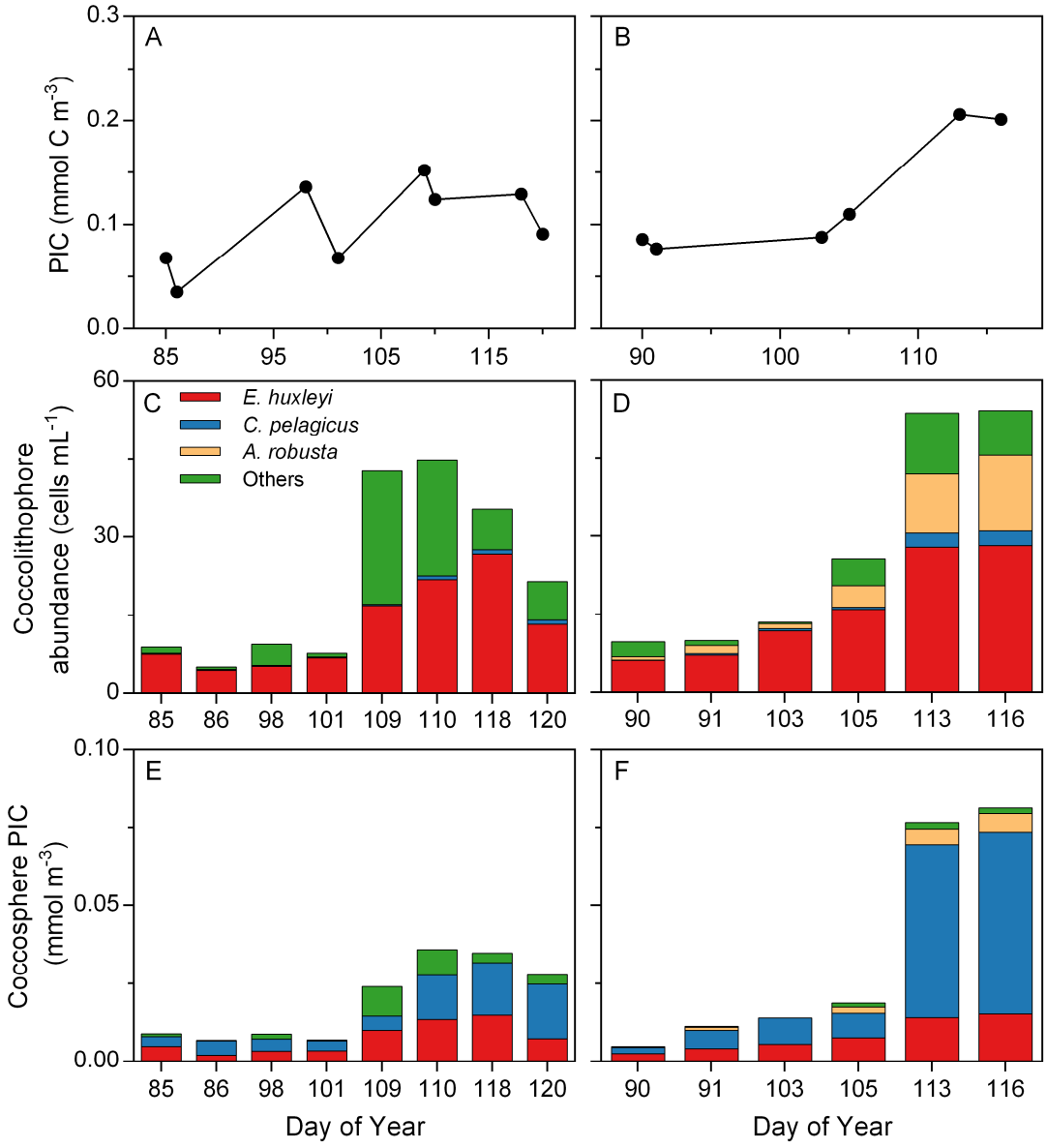

Fig. 3.5: Surface (5 – 15 m) measurements for the ICB (A, C, E) and the NWB (B, D, F) of A,B) particulate inorganic carbon (PIC), C,D) coccolithophore species abundance and E,F) Coccosphere derived PIC

Two morphotypes of *E. huxleyi* were observed in all samples (A and B) with morphotype A consistently dominant (71 – 100 % of total *E. huxleyi* numbers). The coccolithophore composition at both sites were similar, with *E. huxleyi* generally the most abundant species (4.4 – 28.1 cells mL^{-1}, Table 3.3) at both sites, while *Coccolithus pelagicus* was present in all samples at relatively low cell densities (0.15 – 2.79 cells mL^{-1}). The NWB was also characterised by the presence of *A. robusta* (2.7 – 12.7 cells mL^{-1}), while *S. marginaporata* (0 – 21.3 cells mL^{-1}) was only present in the ICB.

A general increase in coccolithophore abundance was observed in the ICB (Fig. 3.5C), with a large increase between the 10th and 18th April (Days 101 and 109, 7.7 – 42.8 cells mL^{-1}). *Emiliania huxleyi* abundance decreased between the 27th and 29th April (Days 118 and 120, 26.7 – 13.2 cells mL^{-1}), but *C. pelagicus* remained relatively constant (0.81 – 0.84 cells mL^{-1}). In the NWB, coccolithophores generally followed the trend of increasing Chl *a* (Fig. 3.5D), with increases in abundance over time (Table 3.3). Within the coccolithophore communities, the largest relative increase in species abundance was by *C. pelagicus* with a sevenfold increase (0.38 to 2.66 cells mL^{-1}) between the 14th and 22nd of April (Days 105 and 133) in the NWB.

Coccosphere derived calcite was dominated by *E. huxleyi* (18 – 54 %) and *C. pelagicus* (19 – 72 %), but represented on average only 20 % (6 – 41 %) of the total PIC pool (Figs. 3.6E & 3.6F). Loose coccoliths of both species formed a significant component of the calcite pool (7 – 30 %); total coccolithophore derived calcite comprised on average 34 % (13 – 54 %) of the total PIC pool.

3.3.4.3 Community structure – diatoms and microzooplankton

The diatom taxa identified by light microscopy were: *Chaetoceros*, *Cylindrotheca*, *Dactyliosolen*, *Guinardia*, *Leptocylindrus*, *Navicula*, *Pseudo-nitzschia*, *Rhizosolenia*, *Thalassionema*, and *Thalassiosira.* Whilst samples for diatom counts were collected only once per visit to each station, particulate silicate ($bSiO_2$) samples were collected from two CTD casts per visit. As the major source of $bSiO_2$, the significant variability observed in $bSiO_2$ between the two CTD casts at each visit (Fig. 3.4A) suggested a temporal variability in the diatom cell abundance not captured in the Lugol's counts.

Table 3.4: Surface Phytoplankton abundance at the Iceland Basin and Norwegian Basin stations, measured by flow cytometry (*Synechococcus*, pico-eukaryotes and nanoplankton), inverted microscopy (diatoms and microzooplankton) and polarizing light microscopy (coccolithophores).

					Phytoplankton abundance (cells mL^{-1})								
										Coccolithophores			
Location	Sta.	Date	Day of Year	Depth (m)	*Synechococcus*	Pico-eukaryote	Nanoplankton (<10 µm)	Diatoms (>10 µm)	Micro-zooplankton	*E. huxleyi*	*C. pelagicus*	*A. robusta*	Others
Iceland Basin	1	25 Mar	85	5	-	-	-	-	-	7.5	0.15		1.2
	1	26 Mar	86	15	675	2347	1116	1.3	2.5	4.4	0.22		0.5
	2	7 Apr	98	5	400	3375	215	-	-	5.2	0.19		4.1
	2	10 Apr	101	10	180	64715	813	249.2	4.0	6.8	0.15		0.7
	3	18 Apr	109	5	-	-	-	-	-	16.9	0.22		25.6
	3	19 Apr	110	7	2112	6962	712	151.3	2.8	21.9	0.69		22.3
	4	27 Apr	118	8	1299	1486	298	-	-	26.7	0.81		7.9
	4	29 Apr	120	11	782	1215	313	87.8	4.7	13.2	0.84		7.5
Norwegian Basin	1	30 Mar	90	8	-	-	-	-	-	6.1	0.09	4.8	2.9
	1	31 Mar	91	10	2617	18016	484	0.2	10.8	7.2	0.28	3.8	1.0
	2	12 Apr	103	8	-	-	-	-	-	11.8	0.41	2.7	0.3
	2	14 Apr	105	10	3372	10433	858	0.1	17.6	16.0	0.38	3.7	5.1
	3	22 Apr	113	7	-	-	-	-	-	27.9	2.66	12.7	11.7
	3	25 Apr	116	7	5483	8456	1384	0.5	14.0	28.1	2.79	7.8	8.6

Therefore, diatom abundance counts were supplemented using SEM image based diatom counts from samples collected from those CTDs where Lugol's were not collected (Fig. 3.4B). However, due to the relatively smaller volumes examined by SEM (~ 4.2 mL versus 50 mL), there is a greater inherent error in the counts and as such Lugol's counts were used wherever possible.

The diatom community was highly variable in the ICB (Fig. 3.4). Initially present only in very low abundances (1.3 cells mL^{-1}, Table 3.3), a peak concentration of 249 cells mL^{-1} was reached 15 days later on the 10th April. The population then decreased over the rest of the study, down to 88 cells mL^{-1}, but remained above initial levels. A shift in composition was observed after the population peaked, from a *Chaetoceros* dominated community on the 7th to 10th April (67 – 71 %) to one dominated by *Pseudo-nitzschia* (65 – 73 %, Fig. 3.4B) on the 27th to 29th April. Diatoms were virtually absent from light microscope measurements of the NWB, reaching a maximum of only 0.5 cells mL^{-1} (Table 3.3). The main microzooplankton groups present were planktonic ciliates and small (~ 5 – 10 µm) naked dinoflagellates (e.g. *Gyrodinium* and *Gymnodinium*). Microzooplankton concentrations were ~ 4 times higher in the NWB (10.8 – 17.6 cells mL^{-1}, Table 3.3) than in the ICB (2.5 – 4.7 cells ml^{-1}, Table 3.3). Dinoflagellates initially dominated in the NWB (8.5 cells mL^{-1}), but were succeeded by ciliates (11.9 – 12.9 cells mL^{-1}). Both dinoflagellates and ciliates were present in similar concentrations in the ICB, except for the final visit, when dinoflagellates dominated (4.2 cells mL^{-1}).

3.4 Discussion

3.4.1 Time series or mixing?

The dynamic nature of the ocean causes inherent difficulties in interpreting data collected from fixed-point, Eulerian time-series, such as those in this study. The distribution of phytoplankton in the ocean exhibits significant heterogeneity, which can be driven by mesoscale physical processes (Martin, 2005). Therefore, Eulerian

time-series are vulnerable to advection such that instead of repeatedly sampling the same phytoplankton community, each sample is potentially from a different population, possibly with a different composition. Before examining the development of the phytoplankton community, it is therefore necessary to consider the physicochemical environment. Eddies and other mesoscale features would potentially cause significant variations in measured SST, SSS, nutrients and carbonate chemistry. With the possible exception of the nutrient concentrations, which will also be affected by the biology present, the measured physicochemical parameters were stable throughout the study period (Table 3.1). Therefore, although I cannot rule out the influence of mesoscale features and advection during the study, the relative consistency of the sampled physicochemical environment suggests that the community structure is representative of the location, rather than from multiple eddies, and thus I can examine how the community developed during the cruise and compare between two geographically separated sites.

3.4.2 Drivers of the phytoplankton bloom

Density profiles in the Iceland Basin (ICB) were seemingly indicative of a well-mixed water column (Fig. 3.2A), yet elevated fluorescence in the upper 100 m of the water column suggests that phytoplankton cells were not being evenly mixed throughout the water column (Fig. 3.2B). A detailed examination of the upper 100 m found small changes in the density profiles (Fig. 3.2A inset), corresponding to the elevated fluorescence, however the change in density with respective to depth was smaller ($\Delta\sigma_t$ < 0.025 over 1 m) than most metrics used to identify mixed layers (e.g. Kara et al., 2000). Elevated fluorescence with only minimal stratification is consistent with the critical turbulence hypothesis (Huisman et al., 1999); here it is likely that active mixing had ceased, allowing phytoplankton net growth, while the response of the physical environment was slower than the biological response, and stratification was only just beginning to develop.

Although ICB upper water column fluorescence was elevated throughout the study, there was significant variation in the magnitude and structure of the fluorescence

profiles (Figs. 3.3B & 3.3C), as well as a peak and decline in surface chlorophyll *a* (Chl *a*) and primary production (PP). The general theory of bloom formation is that once conditions are favourable for bloom formation, the pre-bloom winter ecosystem will transition into a blooming ecosystem, identifiable by increasing Chl *a* biomass and PP. However, I did not observe this smooth transition; periods of stability, characterised by increased stratification, Chl *a* and PP, were followed by periods of instability where increased mixing weakened the developing stratification. Increased mixing detrains phytoplankton out of the surface waters, reducing both Chl *a* biomass and PP, and exporting them to depth (Giering et al., *in review*). One such mixing event occurred between the 27th and 29th April (Days 118 and 120), where minor stratification ($\Delta\sigma t$ = 0.019) disappeared ($\Delta\sigma t < 0.001$) over the upper 25 m, surface Chl *a* halved from 1.18 mg m^{-3} to 0.62 mg m^{-3}, and the fluorescence profile became well-mixed (Fig. 3.2C). Furthermore, surface nutrients were replenished (Table 3.1); all of which are indicative of a mixing event.

The transition period from winter to spring was also observed in satellite data from the ICB. Bloom metrics (Siegel et al., 2002; Henson et al., 2009) of satellite Chl *a* estimate that the main spring bloom did not begin until ~ 20 days after our study period (dashed line in Fig. 3.3C). However, there was a significant increase (r = 0.99, $p < 0.015$, n = 4) in Chl *a* during the study period (Fig. 3.3C inset), consistent with our in situ observations, that suggests that while the environment was not yet stable enough for sustained and rapid phytoplankton growth, intermittent net phytoplankton growth did occur. Therefore, I suggest that the early stages of a spring bloom are characterised by periods of instability and net growth, and that rather than a single smooth transition into a bloom, for a period of weeks prior to the main spring bloom event, phytoplankton form temporary mini-blooms during transient periods of stability. The export flux from these pre-bloom communities is a potentially significant food source to the mesopelagic (Giering et al., *in review*).

In contrast to the instability of the ICB, the Norwegian Basin (NWB) was relatively stable with a strong and persistent pycnocline (Fig. 3.2D), as well as elevated fluorescence in the upper mixed layer (Fig. 3.2E). However, a variable mixed layer that

did not consistently shallow in the NWB (Fig. 3.2D) suggests variability in the strength of the physical forcing, that may explain why although Chl *a* and PP increased throughout the cruise, they remained below that observed in the ICB during the study period (Table 3.2). Furthermore, the net community growth rate (Chl *a* derived, μ_{Chl}), was relatively low (0.02 d^{-1}), suggesting that as was the case for the ICB, the main spring bloom was yet to start. This was also confirmed from the satellite Chl *a,* which showed a very similar pattern to the ICB: although Chl *a* increased during our study period (Fig. 3.3D inset), the main bloom did not start until ~ 20 days later (Fig. 3.3D). Therefore despite very different physical environments, the two sites both represented early stages in the development of spring blooms.

Unlike the ICB, the factors limiting bloom formation in the NWB cannot easily be attributed to the physicochemical environment. A switch from negative to positive net heat flux has been linked to spring bloom formation (Smyth et al., 2014), but here the net heat flux was negative for the majority of the study at both sites (C. Lindemann, pers. comm., Giering et al., *in review*). Irradiance is a key driver of phytoplankton growth and bloom formation; the main spring bloom did not occur until daily PAR reached its seasonal maximum of 45 mol photons m^{-2} d^{-1} (Figs. 3.3B, 3.3C & 3.3D). The general increase in daily PAR over our study period was coupled with an increase in Chl *a* and PP in the NWB, suggesting that despite a stratified environment, irradiance was an important driving factor. Although the magnitude of the daily flux of PAR at both sites was similar, Chl *a* and PP were higher in the less stable ICB than the NWB, suggesting that irradiance was not the only driver of the NWB phytoplankton community. Irradiance levels can also have a secondary influence on the requirements for phytoplankton growth. While macronutrients were replete at both sites, I did not measure micronutrients such as iron (Fe). The cellular Fe demand increases in low light conditions (Moore et al., 2006), and as such Fe may be limiting at this early stage of bloom formation in the Norwegian Basin. However, without measurements of Fe (or phytoplankton photophysiology), I cannot directly test this hypothesis. Although temperature limits phytoplankton gross growth rates (Eppley, 1972), the relatively small difference in temperature between the NWB and the ICB (~ 1.5 – 2.5 °C) is unlikely to have a significant impact on gross growth rates (Eppley, 1972).

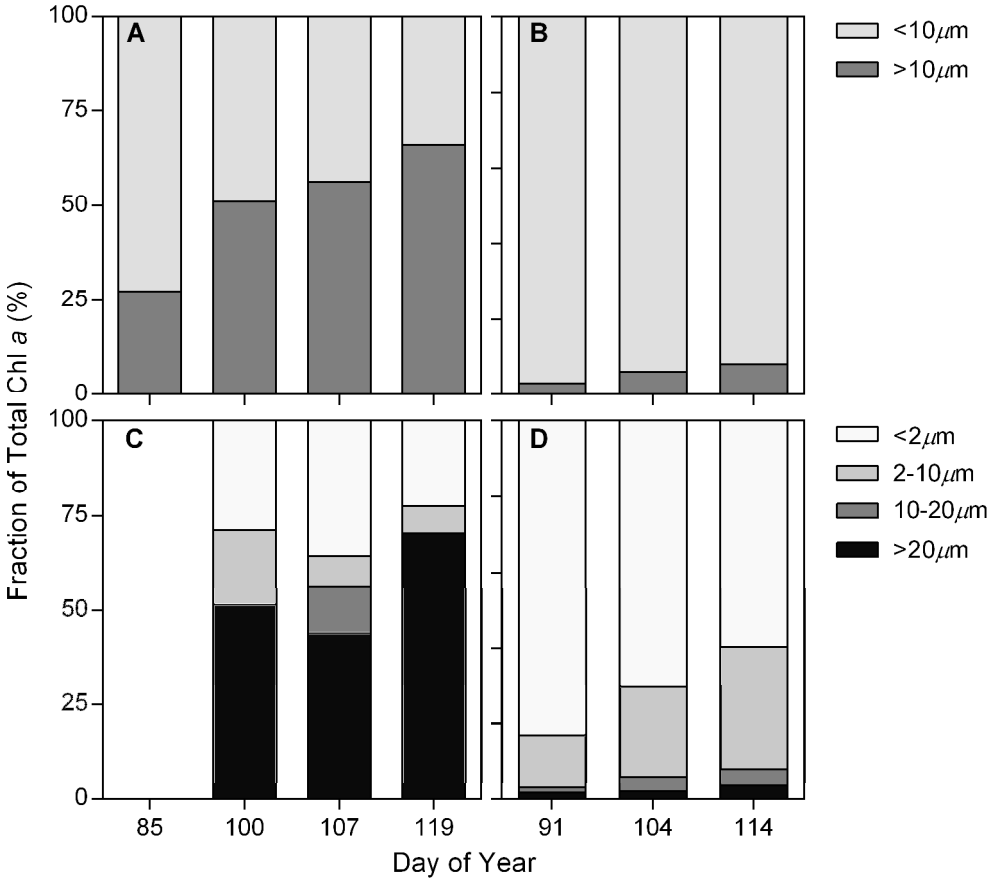

Fig. 3.6: Size fractionated chlorophyll *a* (Chl *a*) for A, C) the Iceland Basin, and B, D) the Norwegian Basin. Plots A and B show the < 10 µm and > 10 µm fractions, C and D show the < 2µm, 2 – 10 µm, 10 – 20 µm, and > 20 µm fractions.

Besides physicochemical drivers of bloom formation, the plankton community itself can play a large role in the development and formation of a bloom. Physiological parameters such as net growth rates (μ_{Chl}) and 'assimilation efficiency' (i.e. PP normalised to biomass, in this case Chl *a*) can provide an insight into the state of the phytoplankton community. The NWB community had a noticeably lower assimilation efficiency (13.5 – 15.8 g C [g Chl *a*]$^{-1}$ d^{-1}) than that in the ICB (15.7 – 27.0 g C [g Chl *a*]$^{-1}$ d^{-1}), thus the relative increase in biomass in the NWB was slower, as reflected in the growth rates where the maximum estimated (net) growth rate in the NWB (μ_{Chl} = 0.05 d^{-1}) was much lower than in the ICB (μ_{Chl} = 0.22 d^{-1}). Assimilation efficiency varies with both environmental conditions and species composition, and therefore the composition of the phytoplankton community is likely to be another key driver behind the contrasting phytoplankton dynamics observed in the ICB and NWB.

3.4.3 Overall community composition

The contrasting structures of Chl *a* and PP size fractions observed at the two sites (Fig. 3.6, Table 3.2), were reflected in the contrasting composition of the phytoplankton communities (Table 3.3). In the ICB, a change in dominance in both Chl *a* and PP, from < 10 µm to the > 10 µm fraction, occurred as the diatom abundance increased between the 26th March and the 7th April. An increase in the abundance of the < 10 µm community was also observed during this period, composed mainly of < 2 µm *Synechococcus* and pico-eukaryotes (Table 3.3, Fig. 3.6C). However, with most of the diatom population having cells > 20 µm (Fig. 3.6C), their relatively large size allowed the diatoms to dominate both the Chl *a* and PP while remaining numerically inferior. The decline in total Chl *a* and PP later in our study was reflected by a decreasing abundance of most of the phytoplankton community (Table 3.3). However, the relative decrease of pico-phytoplankton (*Synechococcus* and picoeukaryotes) was greater than that of the diatoms, such that the > 10 µm fraction increased its dominance for both Chl *a* (94 %) and PP (61 %). Therefore, although surface Chl *a* and PP declined after the 'mini-bloom event' which peaked around the 10th April, the community structure did not return to a pre-bloom composition, but instead remained dominated by diatoms.

Interestingly, the phytoplankton response to the increased diatom abundance was not uniform, with the nanoplankton abundance decreasing and *Synechococcus* increasing only after the peak in diatom abundance. Thus, I observed that the phytoplankton community response during the spring bloom was not universal across functional types as has been previously observed elsewhere (Brown et al., 2008).

In contrast to the ICB, a large shift in the NWB community was not observed. Pico-eukaryotes dominated both in terms of abundance (Table 3.3) and Chl *a*, through the < 2 µm fraction (Fig. 3.6D). This is consistent with previous observations of early stage spring blooms (Joint et al., 1993). Although the < 2 µm Chl *a* fraction showed little variation throughout the study (0.45 – 0.58 mg m^{-3}), variation in the < 2 µm phytoplankton composition did occur, with an apparent succession from pico-eukaryotes to *Synechococcus* and nanoplankton. This may represent a community shift

early in development of the spring bloom or may demonstrate the inherent variability within pre-bloom communities.

The increase in total Chl *a* in the NWB was driven primarily by the 2 to 10 µm fraction, which was likely composed of the nanoplankton, which itself had a threefold increase in population size (from 484 to 1384 cells mL^{-1}, Table 3.3). The phytoplankton responsible for the observed increase in the >10 µm Chl *a* and PP fraction cannot be confidently determined; large diatoms were absent and thus could not contribute. The microzooplankton population consisted of ciliates and dinoflagellates (*Gyrodinium* and *Gymnodinium*), both of which have been reported to be mixotrophic (Putt, 1990; Stoecker, 1999), and thus could potentially have contributed to the Chl *a* measurements. Furthermore, it is possible that part of the nanoplankton community, as measured by flow cytometry, was > 10 µm and thus the increasing concentration of nanoplankton could also contribute to the increase in the > 10 µm fraction.

3.4.4 Contrasting patterns of diatoms

The diatom bloom in the ICB, which began between the 26th March (Day 86) and the 7th April (Day 98), was initially dominated by *Chaetoceros* (71 – 67 % of total cell numbers, Fig. 3.4B). As the community developed however, *Pseudo-nitzschia* succeeded as the dominant diatom genera (65 – 73 % of total). Both *Chaetoceros* and *Pseudo-nitzschia* are common spring bloom diatoms (Sieracki et al., 1993; Rees et al., 1999; Brown et al., 2003), with *Chaetoceros* often dominant in the earlier stages of North Atlantic spring blooms (Sieracki et al., 1993; Rees et al., 1999). Resting spores of *Chaetoceros* have also been observed to dominate the export flux out of the Iceland Basin during the North Atlantic spring bloom in May 2008 (Rynearson et al., 2013), suggesting dominance of the spring bloom prior to this period, consistent with the early community observed in our study.

Pseudo-nitzschia (previously identified as *Nitzschia* in other studies), tends to dominate later in the spring bloom (Sieracki et al., 1993; Moore et al., 2005), also consistent with this study. This suggests that as a genera, *Chaetoceros* are either able to adapt more quickly than *Pseudo-nitzschia*, or that they have a wider niche of

growing conditions through a large diversity of species. However, once established, *Pseudo-nitzschia* are able to outcompete *Chaetoceros*, resulting in a community shift. That the succession of the diatom community observed in the ICB is consistent with that expected in the main diatom spring bloom, suggests that a mini-diatom bloom occurred prior to the formation of the main spring bloom.

The observed variability in the relationship between diatoms (the main source of $bSiO_2$) and $bSiO_2$ was likely due to the species-specific variability in the cellular $bSiO_2$ content of diatoms (Baines et al., 2010). The abundance of *Pseudo-nitzschia*, rather than *Chaetoceros*, best explained the trend in $bSiO_2$ ($r = 0.92$, $p < 0.001$, $n = 8$), suggesting that *Pseudo-nitzschia* was the major producer of $bSiO_2$. Previously *Chaetoceros* has been observed as the major exporter of $bSiO_2$ in the Iceland Basin (Rynearson et al., 2013). Here as the major producer of $bSiO_2$, *Pseudo-nitzschia* has the potential to be the major exporter.

In contrast to the ICB, diatoms appeared to be virtually absent (< 0.5 cells mL^{-1}) in the NWB. While the $dSi:NO_3$ ratio was below the 1:1 requirement for diatoms, consistent with previous studies of North Atlantic blooms (Leblanc et al., 2009), dSi did not become depleted (always above 5 mmol Si m^{-3}, Table 3.1) and thus was not limiting. Furthermore, significant and increasing concentrations of particulate silicate ($bSiO_2$) were measured throughout the cruise (Fig. 3.4A). As the main source of $bSiO_2$, diatoms would therefore be expected to be present. Although absent in the Lugol's counts, examination of SEM images found significant numbers (101 – 600 cells mL^{-1}) of small (< 5 µm) diatoms (predominantly Minidiscus spp.) that were too small to be identified by light microscopy. However, they may still constitute an important component of the nanoplankton, as measured by flow cytometry. As a result of their small cell size, nanno-sized diatoms, such as *Minidiscus*, are easily missed when identifying and enumerating the phytoplankton community, and as such their potential biogeochemical importance may be greatly underestimated (Hinz et al., 2012). Other nanno-sized diatom species have been observed as major components of the phytoplankton community on the Patagonian Shelf (Poulton et al., 2013), in the Scotia

Sea (Hinz et al., 2012), the northeast Atlantic (Boyd and Newton, 1995; Savidge et al., 1995) and in the Norwegian Sea (Dale et al., 1999).

The *Minidiscus* spp. observed in this study exhibited a significant increase in population size during the study, from initial concentrations of 100 to 200 cells mL^{-1}, then up to 600 cells mL^{-1} by the end of the study, and correlating well with both $bSiO_2$ ($r = 0.93$, $p < 0.01$, $n = 6$), and Chl *a* ($r = 0.93$, $p < 0.01$, $n = 6$). Furthermore, the increasing concentration of *Minidiscus* corresponded to the increase in the 2 to 10 µm Chl *a* size fraction (Fig. 3.6D). The maximum net growth rate of *Minidiscus*, estimated from changes in cell abundances ($\mu = 0.13\ d^{-1}$), was significantly higher than that calculated for the total community using Chl *a* ($\mu_{Chl} = 0.05\ d^{-1}$). While different methods were used to determine these growth rates, it does suggest that conditions were favourable for the small nanno-sized diatoms to grow more rapidly than the bulk community.

The question therefore remains as to why the larger (> 10 µm) diatoms were virtually absent in an environment that is physically stable and nutrient replete, while small diatoms were able to thrive? The fate and ecology of overwintering oceanic diatoms is poorly understood. Many diatom species, both neritic and pelagic, are capable of forming resting stages that sink post bloom (Smetacek, 1985; Rynearson et al., 2013), yet diatoms must be present in spring when the diatom bloom begins. Therefore, either a diatom population is sustained in the upper water column over winter (Backhaus et al., 2003), or the spring diatom community is sourced from elsewhere (horizontally or vertically). In relatively shallow coastal environments, benthic resting stages overwinter until spring when they are remixed up into the water column, providing the seed population for the spring bloom (Mcquoid and Godhe, 2004). It is unlikely that oceanic diatom blooms are seeded from the sediment, as the depths are far too great for remixing. However, viable diatom cells have been observed suspended at depth (> 1000 m) in the ocean (Smetacek, 1985), and it is possible that these suspended deep populations are remixed to seed the spring bloom. An alternative hypothesis is based on the observation that diatom blooms generally occur first in coastal waters before progressing to the open ocean (Smetacek, 1985), suggesting that coastal diatom populations are horizontally advected into pelagic

waters, thus seeding the spring bloom in the open ocean from shelf waters. The location of the source coastal populations, and their transit time to the open ocean location, would then affect the timing of the diatom blooms

With such low concentrations of > 10 µm diatoms (< 0.5 cells mL^{-1}) in the NWB, it is possible that the overwintering diatom population was too small to seed the spring bloom. Grazing pressure by microzooplankton and mesozooplankton may influence the composition and timing of the onset of the spring bloom (Behrenfeld and Boss, 2014). The potential grazing pressure from the significant microzooplankton population (10.8 – 17.6 cells mL^{-1}) in the NWB may have exerted such a control on the observed diatom population that it could not develop into a diatom bloom. Instead an alternative seed population of diatoms may be required for the diatom bloom to initiate in the NWB. Whether the absence of large diatoms is a regular occurrence in the NWB, or whether inter-annual shifts between small and large diatoms occur, as observed in the northeast Atlantic (Boyd and Newton, 1995), will have significant implications for export and the functioning of the biological carbon pump. The absence of larger diatoms in pelagic spring blooms in the Norwegian Sea has also been observed by Dale et al. (1999), and it may be that large diatoms are completely absent from the pelagic south east Norwegian Sea. The lack of large diatoms in the NWB could explain the seasonal profile of satellite Chl *a* (Fig. 3.3D); with no large diatoms present, the spring bloom is less intense, peaking at only ~ 60 % of the Chl *a* concentration found in the ICB. Clearly, further work is required to examine why large diatoms are absent from the initial stages of the spring bloom in the NWB, and whether they ever become abundant in this region.

3.4.5 Biogeochemistry and dynamics of the coccolithophore community

Despite the contrasting environments and overall community structures of the two sites, the coccolithophore community structures were generally similar, with *E. huxleyi* numerically dominant (4 – 28 cells mL^{-1}) in nearly all samples and *C. pelagicus* present but in relatively low concentrations (0.2 – 2.8 cells mL^{-1}). The traditional view on the

seasonality of coccolithophores is that they succeed the diatom spring bloom, forming coccolithophore blooms in late summer. However, a typical North Atlantic community of coccolithophores (Savidge et al., 1995; Dale et al., 1999; Poulton et al., 2010), was growing alongside the ICB diatom bloom, rather than just succeeding the diatoms. This is consistent with the "rising tide" hypothesis of Barber and Hiscock (2006), as well as observations from both in situ (Leblanc et al., 2009) and satellite measurements (Hopkins et al., in review) suggesting that coccolithophores are present in North Atlantic spring blooms.

Although the coccolithophore community in the Iceland Basin has been well studied (Savidge et al., 1995; Leblanc et al., 2009; Poulton et al., 2010), this study observed coccolithophores earlier in the season than previously thought. That the ICB coccolithophore community, dominated by *E. huxleyi* with *C. pelagicus* and *Syracosphaera* sp. also present, is structurally similar to communities observed during the late spring bloom (Savidge et al., 1995; Leblanc et al., 2009) and later summer (Poulton et al., 2010) periods in the Iceland Basin, would suggests a relatively stable community structure of coccolithophores persists in the Iceland Basin. The NWB coccolithophore community, characterised by *E. huxleyi*, *A. robusta* and *C. pelagicus* is similar to that observed previously at Ocean Weather Station Mike (OWSM) (Dale et al., 1999). However *C. pelagicus* was only rarely observed and generally later in the season by Dale et al. (1999). In comparison to OWSM, the coccolithophores were more numerically abundant and were present earlier in the season at the NWB site. This is likely due to OWSM being located approximately 3 °N of the study site.

The relatively high frequency that the two sites were sampled for coccolithophores allows species-specific growth rates to be determined. With the assumption made that the two sites represent evolving community structures, using the changes in cell concentration I have calculated species-specific net growth rates for the coccolithophore community. Despite the contrasting environment and overall community structure of the two sites, the coccolithophore dynamics were similar, appearing independent of the overall community dynamics. The net growth rates of *E. huxleyi* in the ICB and NWB were very similar (μ = 0.059 d^{-1} and 0.060 d^{-1} respectively),

while the net growth rate of *C. pelagicus* was slightly higher than *E. huxleyi* in the ICB (μ = 0.068 d^{-1}). In the NWB, both *C. pelagicus* and *A. robusta* had higher net growth rates than *E. huxleyi* (μ = 0.130 d^{-1} and μ = 0.129 d^{-1} respectively). From the culture study performed in chapter 2, I observed comparable gross growth rates of *E. huxleyi* and *C. pelagicus* in temperatures below 10 °C, such as those observed here (7 – 9 °C). That the in situ growth rates measured here are smaller than the growth rates observed in culture (*E. huxleyi*: μ = 0.2 – 0.6 d^{-1}, *C. pelagicus*: μ = 0.2 – 0.5) is likely due to the fact that growth rates measured in culture are gross growth rates, while those measured in situ are net gross growth rates; cultures will experience reduced mortality rates, as they are not subject to predation, viral attack or mixing out of the sampled environment. Therefore although I cannot directly compare the values of gross growth rates with net growth rates, they both provide us with insight into species-specific coccolithophore dynamics.

In order to examine the relative contribution of coccolithophores to biomass and calcite production, I combined cell counts with cellular calcite estimates to derive the individual species contributions to Chl *a* biomass and the calcite pool (PIC). Few species of coccolithophore have known values of cellular Chl *a*, and thus I was not able to account for all species, and concentrated on the largest and most abundant species when considering biomass: *E. huxleyi*, *C. pelagicus* and *A. robusta*. The cellular Chl *a* values of *E. huxleyi* (0.3 pg Chl $cell^{-1}$) and *C. pelagicus* (5 pg Chl $cell^{-1}$) as determined in Chapter 2 were assumed. For *A. robusta*, the cellular POC content was determined using an average cell diameter of 6.7 µm applied to Menden-Deuer and Lessard (2000). Assuming the same ratio of Carbon:Chl as measured for *E. huxleyi* in Chapter 2 (26), the cellular Chl *a* content *A. robusta* was estimated to be 1 pg Chl $cell^{-1}$.

These estimates suggest that coccolithophores formed 0.1 – 4.4% of the total Chl *a* biomass during the early stages of the spring bloom, with a greater contribution in the NWB (0.5 – 4.4%) than in the ICB (0.1 – 1.3%). This represents a lower fraction than estimated in late summer non-bloom Iceland Basin communities (10 – 20 %, Poulton et al., 2010) but similar to that observed in the subtropics (Poulton et al., 2006). While coccolithophores formed only a minor component of the community biomass, their

contribution generally increased as the bloom progressed. In particular the increasing abundance of *C. pelagicus* and *A. robusta* in the NWB drove a large increase in the coccolithophore Chl *a* contribution (from 1.6 % to 4.4 %). The trend of an increasing fraction of biomass suggests that as the bloom progresses, coccolithophores may become a greater component of the phytoplankton community, until they potentially dominate in the late spring and early summer.

As the two main sources of coccolithophore calcite during the onset of the spring bloom (Figs. 3.6E & 3.6F), *E. huxleyi* and *C. pelagicus* are likely to be biogeochemically important during this period. The relatively high abundance of *E. huxleyi* and the relatively high cellular calcite content of *C. pelagicus* resulted in both species being major sources of calcite. In the NWB, *C. pelagicus* dominates the coccosphere associated PIC concentrations in the latter stage of the time series (72 %), suggesting that *C. pelagicus* may be a key calcifier during the spring bloom itself.

Coccosphere associated PIC accounted for only a minor fraction (6 – 40 %) of the total PIC pool. Although loose coccoliths provided a further source of quantifiable PIC, a discrepancy of between 46 and 87 % of the total PIC remained unaccounted for. While there are inherent errors in the method for calculating coccolith PIC (Young and Ziveri, 2000; Daniels et al., 2012), this method has previously been used successfully in the Iceland Basin (Poulton et al., 2010). Examination of SEM images suggest that unquantifiable detrital coccoliths bound into faecal matter may be partly responsible for this discrepancy, rather than the presence of other calcifiers or lithogenic material (Daniels et al., 2012). The ratio of detached *E. huxleyi* coccoliths to cells (9 – 40) is similar to those reported in coccolithophore blooms, and lower than reported in late summer (Poulton et al., 2010). This ratio, along with the fraction of calcite derived from coccoliths, decreased as the bloom progressed, suggesting that excess coccolith production was not the reason for relatively high concentration of coccoliths. Instead it is likely that winter mixing keeps coccoliths suspended in the water column resulting in an accumulation of coccoliths.

3.5 Conclusions

During March-May 2012, satellite and in situ data from study sites in the Iceland Basin (ICB) and the Norwegian Basin (NWB) suggested that despite very different physical environments, the two sites both represented early stages in the development of the North Atlantic spring bloom. Spring bloom initiation in the ICB was limited by the physical environment, with periods of increased mixing inhibiting bloom formation. The physicochemical environment alone was not limiting bloom formation in the NWB as, in spite of a stable stratified water column and ample nutrients, Chl *a* biomass and primary production were relatively low. Phytoplankton efficiency (Chl *a* -normalised primary production) was also lower in the NWB, suggesting that the phytoplankton community composition and/or physiology was also a limiting factor in bloom formation.

The phytoplankton community in the NWB was dominated by the < 2 µm Chl *a* fraction, with high concentrations of pico-eukaryotes (~ 18,000 cells mL^{-1}) succeeded by *Synechococcus* and nanoplankton. In contrast, although the initial dominance of the < 10 µm Chl *a* fraction (pico-eukaryotes and nanoplankton) was succeeded by diatoms dominating in the > 10 µm Chl *a* fraction, the ICB phytoplankton community generally followed the "rising tide" hypothesis, with most of the community positively responding to the onset of the diatom bloom. Species-succession occurred within the ICB diatom community, with *Chaetoceros* replaced by *Pseudo-nitzschia*; *Chaetoceros* was a key species in bloom formation, while *Pseudo-nitzschia* was the major source of particulate silicate ($bSiO_2$). High numbers (101 – 600 cells mL^{-1}) of only small (< 5 µm) diatoms suggests that micro-zooplankton grazing, coupled with a potential lack of a seed population, was restricting diatom growth in the NWB, or that large diatoms are absent in NWB spring blooms.

These results suggest that despite both phytoplankton communities being in the early stage of bloom formation and exhibiting positive net growth rates, different physicochemical and biological factors control bloom formation with the resulting blooms likely to be significantly different in terms of biogeochemistry and trophic

interactions throughout the growth season. Clearly, more in situ studies are needed in the transitional period between winter and the peak productivity of the spring bloom to examine compositional differences, growth and mortality factors, and how regional variability impacts on upper ocean biogeochemistry and deep-sea fluxes of organic material. Coupled studies of satellite derived products, including bloom phenology and phytoplankton physiology, and in situ processes are needed to examine the full spectrum of factors forming the spring bloom.

Coccolithophore community dynamics were similar at both sites, relatively independent of the overall phytoplankton community. While *E. huxleyi* was generally the most abundant coccolithophorid, *C. pelagicus* was generally both a greater contributor to phytoplankton biomass (0 – 1.7 %) and a greater source of calcite (53 %). Species-specific net growth rates showed that although *E. huxleyi* and *C. pelagicus* grew at comparable rates in the ICB (μ = 0.06 d^{-1}), *C. pelagicus* grew faster (μ = 0.13 d^{-1}) than *E. huxleyi* (μ = 0.06 d^{-1}) in the NWB, in contrast to the generally higher relative growth rates of *E. huxleyi* observed in the culture experiments of Chapter 2. Relatively higher net growth rates, coupled with a large calcite contribution, suggests that *C. pelagicus* may be a major source of calcite during the early stages of the North Atlantic spring bloom. The contribution of *C. pelagicus* to calcite production within a mixed coccolithophore community will be investigated in Chapter 4.

Chapter 4: Species-specific calcite production reveals *Coccolithus pelagicus* as the key calcifier in the Arctic Ocean

Abstract

Through the production and export of their calcite coccoliths, coccolithophores are a key component of the global carbon cycle. Despite this, very little is known about the biogeochemical role of different coccolithophore species in terms of calcite production, and how these species will respond to future climate change and ocean acidification. Here we present the first study to determine species-specific calcite production, from samples collected in the Arctic Ocean and subarctic Iceland Basin in June 2012. We show that although *Coccolithus pelagicus* comprised only a small fraction of the total community abundance (2 %), it was the major calcifier in the Arctic Ocean and Iceland Basin (57 % of total calcite production). In contrast, *Emiliania huxleyi* formed 27 % of the total abundance and was responsible for only 20 % of the calcite production. *Coccolithus pelagicus* was able to dominate because of its relatively high cellular calcite content compared with many other species. Our results demonstrate the importance of considering the complete coccolithophore community when considering pelagic calcite production, as both abundant weakly calcified species (e.g. *Calciopappus caudatus*) and relatively rare heavily calcified species (e.g. *C. pelagicus*) both have the potential to be key calcite producers rather than species that are neither highly abundant or heavily calcified (e.g. *E. huxleyi*).

4.1 Introduction

Coccolithophores are a major group of phytoplankton, comprising up to 10% of primary production (Poulton et al., 2007), dominating pelagic calcite production and export with their calcite coccoliths (Broecker and Clark, 2009), thus forming a key component of the global carbon cycle (De Vargas et al., 2007; Ziveri et al., 2007). Marine calcifiers, including coccolithophores, face an uncertain future, as they have to contend with the effects of both global warming and ocean acidification (Society, 2005; Winter et al., 2013). Culture experiments considering the response of coccolithophores to ocean acidification have produced conflicting results (Iglesias-Rodriguez et al., 2008; Langer et al., 2009; Hoppe et al., 2011) with long term studies suggesting adaptive evolution could partly compensate for the effect of global warming and ocean acidification (Lohbeck et al., 2012; Schluter et al., 2014). However, these studies, along with the majority of the current literature, consider only a single species of coccolithophore: *Emiliania huxleyi*. Although *E. huxleyi* is considered the keystone coccolithophore species due to its global dominance and ability to form large-scale highly visible blooms (Paasche, 2002), there are ~ 200 extant species of coccolithophore which vary in size, shape and cellular calcite quota (Young et al., 2003). In this context, *E*. *huxleyi* is a relatively small species of coccolithophore (~ 5 μm) with a relatively low cellular calcite content and low calcification rates; other larger and more heavily calcified species, such as *Coccolithus pelagicus* which has ~ 30 times more calcite per cell compared to *E. huxleyi*, as determined in Chapter 2, therefore have the potential to be key species in terms of calcite production and export (Chapter 2 and Ziveri et al., 2000).

The response of coccolithophores to ocean acidification in culture experiments appears to differ between species and strains (Langer et al., 2006; Langer et al., 2009), and culture experiments do not necessarily reflect the response of natural populations

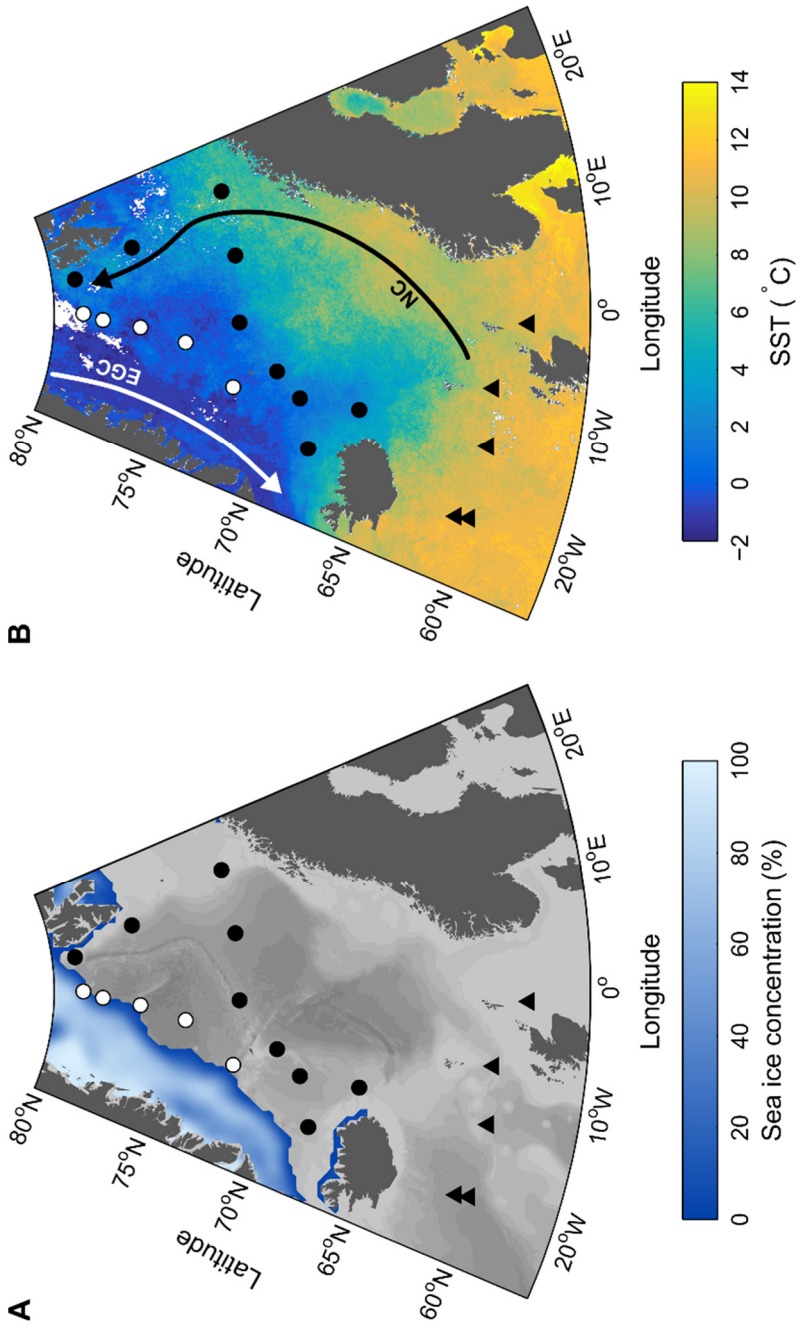

Fig. 4.1: Sampling locations in the Iceland Basin (triangles), the Norwegian Sea (filled circles) and the Greenland Sea (open circles). A) Sea ice concentration (%) in June 2012, taken from www.nsidc.org. B) MODIS sea surface temperature for June 2012, overlaid with the East Greenland Current (EGC) and the Norwegian Current (NC).

of coccolithophores (Smith et al., 2012). Therefore it is unlikely that *E. huxleyi*'s response to ocean acidification in culture can be applied to multi-species populations of coccolithophores. In natural communities the response to variability in pH is often mediated by light, nutrient availability and growth rate (Zondervan, 2007; Charalampopoulou et al., 2011; Poulton et al., 2014). As discussed in Chapter 2, to examine how a diverse coccolithophore community will respond to environmental changes, and to assess the relative biogeochemical importance of different coccolithophore species, field studies considering the whole coccolithophore community are required.

The effect of anthropogenic CO_2 emissions on the Arctic Ocean is expected to be among the largest and most rapid of any region on the globe (Acia, 2004). The Arctic is already experiencing rapid warming (Acia, 2004). Ocean acidification is also expected to be particularly enhanced at high latitudes because of the increased solubility of CO_2 at low temperatures. Within the Nordic Seas (Greenland Sea and Norwegian Sea) of the Arctic Ocean large natural gradients of environmental variables such as temperature and carbonate chemistry parameters already exist. In the west, the East Greenland Current transports cold (< 0 °C) Polar Water southwards through the Greenland Sea (Fig. 4.1), while in the east the Norwegian Current carries relatively warm (6 – 10 °C) Atlantic water northwards into the Norwegian Sea (Johannessen, 1986). Contrasting communities of coccolithophores inhabit the Greenland and Norwegian Seas; *C. pelagicus* is thought to be numerically dominant in the Greenland Sea, while *E. huxleyi* dominates abundance in the Norwegian Sea (Andruleit, 1997; Baumann et al., 2000a). This diversity, coupled with the strong natural environmental gradients, means that this region is an ideal location to examine the influence of both the environment and the coccolithophore community structure on calcite production.

My results from Chapter 2 demonstrated the potential for *C. pelagicus* to be a larger calcite producer than *E. huxleyi* if in a high enough abundance, and showed that these relative abundances were achieved in samples collected from the Iceland Basin and Irminger Basin. However, they did not take into account the potential variability in total calcite production rates between samples and thus it is not directly possible to

estimate over the study area which species is a greater calcite producer. In order to derive this, measured total calcite production must be incorporated into the method. The aim of this study therefore was to measure total calcite production from samples collected from the Arctic Ocean and Iceland Basin, and combine this with a development of the novel method established in Chapter 2, incorporating species–specific cellular calcite, growth rates and abundance, to partition CP and determine species-specific calcite production (CP_{sp}) for each individual coccolithophore species. The working hypothesis for this chapter is that *E. huxleyi* is not the major calcite producer, whereas *C. pelagicus*, with its relatively large cellular calcite content, will be a significant calcite producer in this region.

This is the first study to determine both the abundance and calcite production rates of individual coccolithophore species within a natural multi-species community. Here I present the results from 19 stations within the Arctic Ocean and the subarctic Iceland Basin (Fig. 4.1); calcite production (CP), coccolithophore abundances, carbonate chemistry parameters and other environmental variables were measured and CP_{sp} derived for each station.

4.2 Methods

4.2.1 Sampling

Sampling was carried out aboard the RRS James Clark Ross in the summer (4^{th} – 30^{th} June) of 2012, with samples collected from the subarctic Iceland Basin and the Greenland and Norwegian Seas within the Arctic Ocean (Fig. 4.1). Water sampling was carried out at 45 conductivity-temperature-depth (CTD) stations, of which 19 CTD stations were sampled for rate measurements (primary production, calcite production), coccolithophore community structure, macronutrients and carbonate chemistry. Temperature and salinity were obtained from the CTD. Incidental photosynthetically active radiation (PAR), measured with ship-mounted scalar irradiance sensors (Kipp & Zonen ParLite 0348900, Skye Instruments SK3), was

integrated over the incubation periods to calculate daily irradiance (mol photons m^{-2} d^{-1}). The vertical diffuse attenuation coefficient of PAR (K_d) in the water column was calculated from the CTD casts, with the depth of the euphotic zone (Z_{eup}) calculated as the depth of 1 % incident irradiance.

4.2.2 Calcite Production

Daily rates (dawn-dawn, 24 h) of calcite production (CP) were measured following Poulton et al. (2014). Water samples (70 mL, 3 light, 1 formalin-killed), collected from one depth within the middle of the mixed layer, and were inoculated with 25 – 50 µCi ^{14}C labelled sodium bicarbonate. Samples were incubated for 24 hours in an on-deck incubator, chilled with surface seawater and a 55% incidental irradiance light depth was replicated using Misty-blue optical filters (LEE™). When the surface seawater supply was unavailable, samples were incubated in a refrigeration container (Richier et al., 2014) with the temperature and photoperiod set to replicate the in situ environment. Formalin-killed blanks were prepared by addition of 1 mL of 0.2 µm filtered and sodium-borate buffered formalin solution.

Incubations were terminated by filtration through 25 mm 0.45 µm polycarbonate filters (Nuclepore™). The micro-diffusion technique (MDT, Paasche and Brubak, 1994; Balch et al., 2000) was used to determine both organic (PP) and inorganic (CP) carbon fixation; filters were secured in glass scintillation vials with a gas-tight septum and a bucket containing a CO_2 trap (Whatman GFA filter soaked with 200 µl β-phenylethylamine), acidified with a weak acid (1 ml, 1% phosphoric acid), thus releasing the acid-labile CP as $^{14}CO_2$ to be absorbed by the CO_2 trap. After 24 hours, the GFA filters were removed to separate scintillation vials, and the activity of the filters was determined in Ultima Gold (Perkin-Elmer, UK) using a Tri-Carb 2100 Low Level Liquid Scintillation Counter. Spike activity was checked by the removal of triplicate 100 µL subsamples immediately after inoculation; 200 µL of β-phenylethylamine and Ultima Gold were added and activity determined. Average coefficient of variation of the triplicate (light) CP measurements was 27 % (3 – 113 %), and the formalin-killed blank represented on average 26 % (7 – 60 %) of the CP signal,

with generally higher contributions in lower CP signals. These are comparable to other studies using the same method (e.g. Poulton et al., 2010; Poulton et al., 2014).

4.2.3 Coccolithophore community structure

Samples for the determination and enumeration of the coccolithophore community were collected from the same depths from which CP was measured. Water samples (100 – 250 mL) were filtered under gentle pressure through 25 mm 0.8 µm polycarbonate and cellulose nitrate filters, rinsed with trace ammonium solution (pH ~ 10), oven dried (40°C, 2-4 hours) and stored in Millipore PetriSlides (Daniels et al., 2012). Permanent slides were prepared immediately on board by mounting the cellulose nitrate filters using a low viscosity Norland Optical Adhesive (NOA 74) (Poulton et al., 2014). Coccolithophore cell counts and species identification were performed by Jeremy Young using a Leitz Ortholux polarizing microscope (x1000, oil immersion). A minimum of 54 fields of view were counted per filter for abundant species, with additional fields of view analysed for rarer species. The light microscopy species identification and enumeration were verified and supplemented using scanning electron microscopy (SEM) following Daniels et al. (2012).

4.2.4 Species-specific calcite production

As discussed in Chapter 2, species-specific calcite production (CP_{sp}) can be considered as a product of the growth rate (µ), cellular calcite (C) and abundance (N) of a species. Species-specific cellular calcite was estimated from SEM images by combining derived estimates of coccolith calcite (Young and Ziveri, 2000) with the number of coccoliths per cell (Table 4.1). The method of Young and Ziveri (2000) incorporates a species-specific coccolith shape factor (k_s) to estimate coccolith calcite. Of the species observed here, only 4 (*E. huxleyi*, *C. pelagicus*, *A. quattrospina*, *Syracosphaera* spp.) had a defined k_s. For those species with an undefined shape factor, shape factors were calculated from SEM images for *C. pelagicus* HOL and *C. caudatus* (Table 4.1), the k_s for *A. robusta* was adapted from *E. huxleyi* (Probert et al., 2007), and a "typical coccolith" k_s was used for *Ophiaster* sp. (Young and Ziveri, 2000).

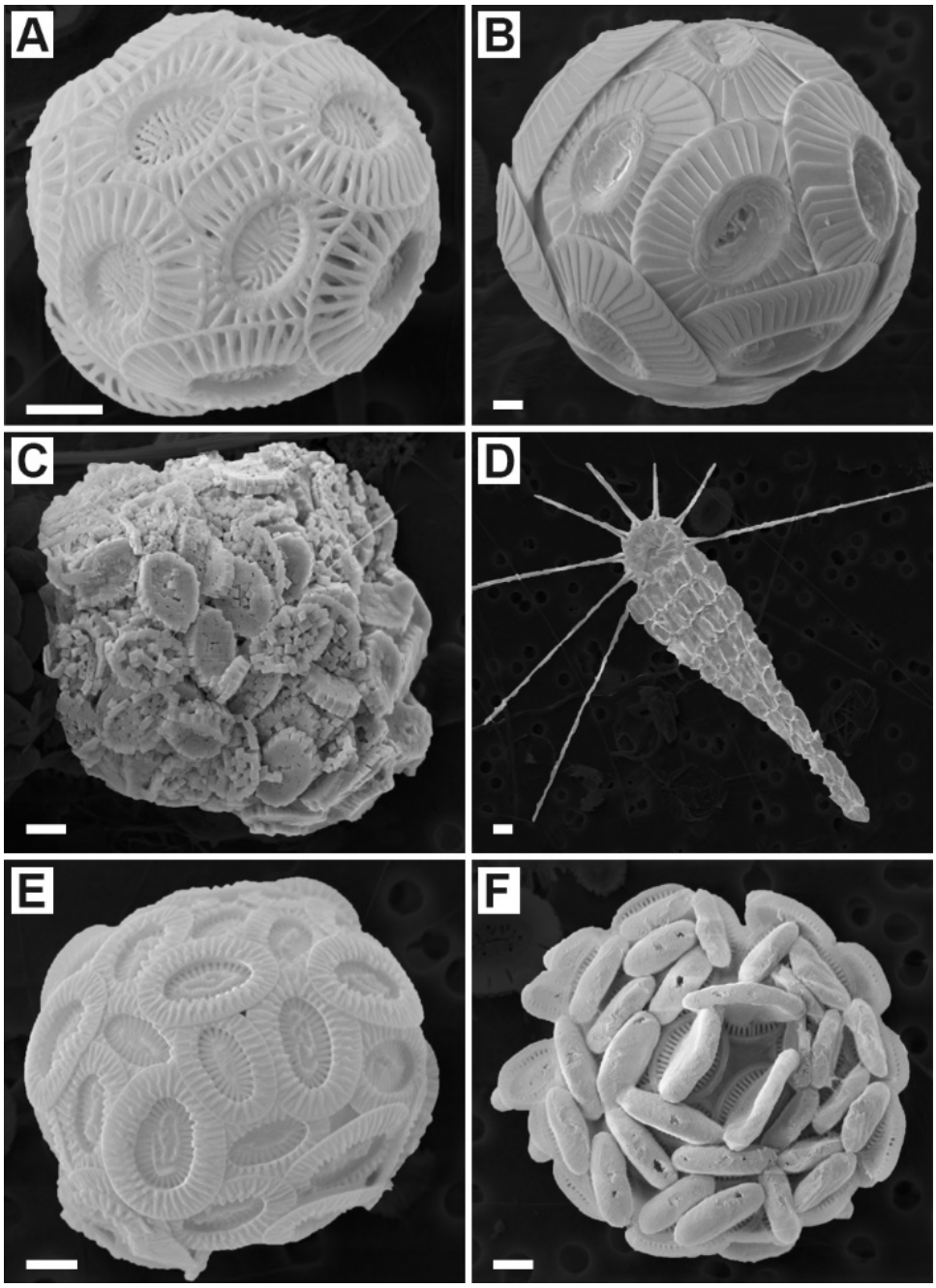

Fig. 4.2: SEM images. A) *Emiliania huxleyi*. B) *Coccolithus pelagicus*. C) *Coccolithus pelagicus* HOL. D) *Calciopappus caudatus*. E) *Syracosphaera molischii*. F) *Algirosphaera robusta.* Scale bars represent 1 µm.

Table 4.1: Coccolith shape factors, coccolith calcite, coccoliths per cell and cellular calcite for the individual coccolithophore species.

Species	Coccolith Shape Factor, k_s	Coccolith Calcite (pmol C coccolith^{-1})	Coccoliths per Cell	Cellular Calcite (pmol C cell^{-1})
E. huxleyi	0.020	0.024	22	0.52
C. pelagicus	0.060	1.218	13	15.2
Syracosphaera spp.	0.015	0.012	35	0.40
A. quattrospina	0.030	0.008	36	0.27
C. caudatus	0.013	0.002	54	0.09
Ophiaster sp.	0.035*	0.001	70	0.09
A. robusta	0.045	0.010	43	0.42
C. pelagicus HOL	0.036	0.008	100	0.78

* the "typical coccolith" k_s of Young and Ziveri (2000) was used

$$CP_{sp} = \frac{\mu_{sp} C_{sp} N_{sp}}{\sum_{i=1}^{n} \mu_i C_i N_i} \times CP_{bulk} \quad (4.1)$$

Species-specific growth rates cannot be directly determined from our measurements. However, I can assume a relative growth rate to determine the fraction of the calcite production per species, and multiply this by the measured total CP (Eq. 4.1) to obtain CP_{sp}. This method is an adaptation of that used in Chapter 2, however here I have a more diverse community than previously considered. For the initial analysis, I have made the simplifying assumption that all coccolithophores have the same growth rate. Although I found in Chapter 2 that *E. huxleyi* generally grew faster than *C. pelagicus*, I observed *C. pelagicus* growing faster than *E. huxleyi* in the coldest experimental temperature (6 °C), and in Chapter 3 I observed *C. pelagicus* growing at a rate similar to, or faster than, *E. huxleyi* in both the Norwegian Sea and the Iceland Basin. Therefore, although the relative growth rates of coccolithophores are likely to be more complex than assuming they all have the same growth rate, there is not enough field validated data to determine the relative growth rates, and as such this assumption is

justified for this analysis. The impacts of this assumption will be tested and discussed later in this chapter.

4.2.5 Macronutrients and carbonate chemistry

Macronutrients (nitrate + nitrite, NO_x; phosphate, PO_4; silicic acid, dSi) were determined following Sanders et al. (2007) on a Skalar autoanalyser by Mario Esposito. Samples for total dissolved inorganic carbon (C_T) and total alkalinity (A_T) were collected into 250 mL borosilicate glass bottles and poisoned with 50 µL of saturated mercuric chloride solution following (Dickson et al., 2007). Using a VINDTA 3C instrument (Marianda, Germany), C_T was measured by coulometric titration, and A_T by potentiometric titration and calculated using a modified Gran technique (Bradshaw et al., 1981). Collection and analysis was performed by Matthew Humphreys, Marianna Ribas-Ribas and Eithne Tynan. The results were calibrated using certified reference material (Batch 117) obtained from A.G. Dickson (Scripps Institution of Oceanography, USA). The measurement precision was ± 3.8 and ± 1.7 µmol kg^{-1} for C_T and A_T respectively. Calcite saturation state (Ω_C), pH on the Total scale (pH_T) and seawater partial pressure of CO_2 (pCO_2^{sw}) were calculated using version 1.1 of the CO_2SYS program for MATLAB (Van Heuven et al., 2011) using the carbonic acid dissociation constants of Lueker et al. (2000), the boric acid dissociation constant of Dickson (1990a), the bisulfate ion acidity constant of Dickson (1990b), and the boron:chlorinity of Lee et al. (2010).

4.2.6 Statistical analysis

Multivariate statistics were used to assess spatial changes in coccolithophore community composition and CP_{sp} (biotic data) and environmental variables (abiotic data). The coccolithophore abundance data were square-root transformed and standardised before analysis to reduce the influence of the dominant coccolithophore species. As CP_{sp} is a percentage, it was already standardised and suitable for analysis. Bray-Curtis similarity resemblance matrices were calculated from the transformed

biotic data to determine changes in species abundance and CP_{sp}. The abiotic data (temperature, salinity, Ω_C, pH, N*, Si*, daily PAR and Z_{eup}) were normalised to bring all variables to a comparable scale, and a resemblance matrix was calculated using Euclidean distance to determine changes in the environmental variables.

Spearman's rank correlation (BEST routine) were performed in E-PRIMER (Clarke, 1993) between the biotic and the abiotic resemblance matrices to identify which environmental variables explained most of the variation in the coccolithophore community and their CP_{sp}. Principal component analysis (PCA) was carried out using MATLAB on the normalised environmental data to reduce the 8 dimensional environmental space to a lower dimensional representation on the environment. Pearson product-moment correlations were carried out between the calculated principal components (PC) and coccolithophore community abundance, composition, and CP_{sp} to further examine the relationship between the biotic and abiotic data.

4.3 Results

4.3.1 General Oceanography

A wide variety of hydrographic environments were sampled during the cruise, throughout the Iceland Basin and the Nordic Seas (Greenland Sea and Norwegian Sea) of the Arctic Ocean (Fig. 4.1, Table 4.2), with two major fronts dividing the regions; the Norwegian Sea was separated from the Iceland Basin by the Iceland-Faroes Front, while the East Greenland Front separated the Greenland Sea from the Norwegian Sea (Cottier et al., 2014). The Iceland Basin was characterised by the warmest (10 – 10.6 °C) and most saline (35.2 – 35.3) waters of the study. The Greenland Sea, with the influence of the East Greenland Current, had the coldest (1 – 3.5 °C) and freshest (34.7 – 35.0) waters sampled. The Norwegian Sea lay between the two extremes of the Iceland Basin and the Greenland Sea, in terms of both temperature (3.1 – 7.8 °C) and salinity (34.8 – 35.2).

Table 4.2: Physicochemical features: Z_{eup}, euphotic depth; $\Omega_{C,}$ calcite saturation state; NO_x, nitrate + nitrite; $PO_{4,}$ phosphate; dSi, silicic acid; N*, excess NO_x relative to PO_4; Si*, excess dSi to NO_x.

Sta.	Location	Lat (°N)	Lon (°E)	Date	Depth (m)	Temp (°C)	Salinity	Daily PAR (mol photons m^{-2} d^{-1})	Zeup (m)	Carbonate Chemistry			Surface Macronutrients (mmol m^{-3})				
										pCO_2 (µatm)	pH_T	Ω_C	NO_x	PO_4	dSi	N*	Si*
6	ICB	58.74	-0.86	04 Jun	9	10.0	35.3	45	40	277	8.18	4.23	0.5	0.11	1.7	-1.3	-1.2
8	ICB	60.13	-6.71	05 Jun	10	10.4	35.4	33	48	326	8.12	3.84	6.5	0.45	4.3	-0.7	2.3
10	ICB	59.97	-11.98	06 Jun	20	10.6	35.3	51	28	310	8.14	3.98	2.9	0.21	1.4	-0.4	1.5
12	ICB	60	-18.67	07 Jun	10	10.2	35.2	41	37	340	8.11	3.66	6.1	0.40	1.7	-0.3	4.4
17	ICB	60.59	-18.86	08 Jun	20	10.4	35.2	10	40	310	8.14	3.94	5.2	0.35	1.3	-0.4	3.9
19	NWS	65.98	-10.72	09 Jun	24	3.6	34.8	34	23	240	8.23	3.68	0.6	0.22	2.5	-3	-1.9
20	NWS	69.9	-7.58	10 Jun	15	3.1	35	53	36	363	8.07	2.65	9.1	0.64	6.1	-1.2	3.0
21	GS	74.12	-4.69	11 Jun	15	1.0	34.9	40	48	308	8.13	2.76	9.8	0.70	5.7	-1.4	4.0
27	GS	76.18	-2.55	12 Jun	20	1.5	34.9	42	50	319	8.12	2.75	9.3	0.67	4.7	-1.4	4.6
29	GS	78.72	0.00	13 Jun	10	3.5	35	51	15	209	8.28	4.07	2.6	0.31	5.5	-2.4	-2.9
40	GS	78.25	-5.55	14 Jun	15	3.1	34.9	20	25	309	8.14	3.01	8.7	0.62	5.6	-1.2	3.1
42	NWS	78.22	-6.00	15 Jun	15	6.0	35.1	28	22	208	8.29	4.46	4.0	0.38	4.3	-2.1	-0.4
45	NWS	77.82	-4.97	16 Jun	20	5.7	35.2	19	41	309	8.14	3.34	9.8	0.72	5.8	-1.8	4.0
54	NWS	77.85	-1.29	17 Jun	13	7.8	35	24	41	320	8.13	3.50	6.0	0.49	3.8	-1.8	2.2
56	NWS	78.99	7.98	18 Jun	15	6.7	35.2	33	31	305	8.15	3.50	6.8	0.50	5.2	-1.2	1.6
58	NWS	76.26	12.54	19 Jun	20	5.4	35.1	35	38	316	8.13	3.20	10.6	0.77	5.7	-1.7	4.9
60	GS	76.16	23.07	20 Jun	26	1.4	34.7	49	45	328	8.11	2.60	8.6	0.64	2.2	-1.6	6.5
63	NWS	72.89	26.00	22 Jun	20	3.8	34.8	40	32	318	8.12	3.00	8.9	0.65	2.6	-1.5	6.3
65	NWS	71.75	17.90	23 Jun	20	5.1	34.9	33	48	246	8.22	3.80	4.0	0.43	4.1	-2.8	0.0

Table 4.3: Coccolithophore abundances (cells mL^{-1})

Sta.	Location	Coccolithophore abundance (cells mL^{-1})						
		E. huxleyi	*C. pelagicus*	*C. pelagicus* HOL	*Syracosphaera* spp.	*A. quattrospina*	*C. caudatus*	*Ophiaster* sp.	*A. robusta*
6	ICB	31.7	-	-	-	1.5	-	-	-
8	ICB	21.2	3	1.5	3	-	24.2	-	2.6
10	ICB	64.1	-	2.4	0.6	2.4	7.9	3	2.3
12	ICB	76.2	-	27.2	348.3	10.9	179.6	-	7.7
17	ICB	91.2	-	50.3	179.6	12.2	84.4	5.4	4.2
19	NWS	1.9	-	-	-	-	-	-	2.8
20	NWS	-	5.4	-	359.2	-	-	59.9	0.6
21	GS	-	-	-	-	-	-	3.8	0.4
27	GS	-	-	-	-	-	-	6	-
29	GS	17	0.9	-	-	-	-	0.9	0.4
40	GS	1.9	-	-	-	-	-	11.3	-
42	NWS	25.2	-	-	-	-	-	-	-
45	NWS	69.5	4.5	-	1.5	-	-	1.5	0.1
54	NWS	19.7	4.5	-	-	-	-	-	-
56	NWS	424.5	119.7	-	157.8	-	-	223.1	7.1
58	NWS	33.1	47.4	-	72.8	-	-	2.2	15.4
60	GS	-	-	-	-	-	-	54.8	2.8
63	NWS	20.8	-	-	274	-	-	-	32.7
65	NWS	2.8	-	-	-	-	-	-	2.9

Macronutrient concentrations of NO_x (0.5 – 10.6 mmol N m^{-3}), PO_4 (0.11 – 0.77 mmol P m^{-3}) and dSi (1.3 – 6.1 mmol Si m^{-3}) were highly variable and no spatial patterns were observed (Table 4.2). The values of N* (NO_x – 16 × PO_4 (Moore et al., 2009)) were negative at all sites (-3.0 – -0.3) indicating that, assuming Redfield stoichiometry (Redfield, 1958), NO_x was low relative to PO_4. The values of Si* (dSi - NO_x (Bibby and Moore, 2011)) ranged from -2.9 to 6.5. While generally positive, indicating high residual dSi concentrations, four stations exhibited a negative Si*, indicating depleted dSi relative to NO_x. No spatial patterns in the N* or Si* were identified.

Euphotic zone depth (Z_{eup}) ranged from 15 – 50 m, and daily PAR varied from 10 – 53 mol photons m^{-2} d^{-1}, with both showing variability within and between regions. As the cruise occurred in mid-summer, the stations in the Nordic Seas experienced a 24 hour photoperiod, while the Iceland Basin stations experienced a shorter photoperiod (~ 18 hours). The effect of this on daily PAR is not clear, suggesting a stronger influence through varying cloud cover. Values of pH_T varied from 8.07 – 8.29 and Ω_C varied from 2.65 – 4.46, with the low Ω_C particularly in the Greenland Sea.

4.3.2 Coccolithophore community structure

Coccolithophore abundance was highly variable, ranging from 5 – 932 cells mL^{-1} (Table 4.3). The most commonly observed coccolithophore species were *Emiliania huxleyi* (0 – 425 cells mL^{-1}), *Coccolithus pelagicus* (0 – 33 cells mL^{-1}) and the holococcolithophorid (HOL) life stage of Coccolithus *pelagicus* (0 – 223 cells mL^{-1}, Fig. 4.2). Other species present included *Acanthoica quattrospina, Algirosphaera robusta*, *Calciopappus caudatus*, *Ophiaster* sp. and *Syracosphaera* spp. (Fig. 4.2). While each species has been considered individually in determining CP_{sp} and in the environmental analysis, for the purpose of graphical representation, species other than *E. huxleyi*, *C. pelagicus* and *C. pelagicus* HOL were grouped into one category (termed 'others', Fig. 4.3) as they were minor contributors to regional calcite production. Scanning electron microscopy identified *Syracosphaera* spp. as including: *S. borealis*, *S. corolla*, *S. dilata*, *S. marginaporata* and *S. molischii*. The cellular calcite content of the *Syracosphaera* genus however are not well constrained (Young and Ziveri, 2000), thus I have not

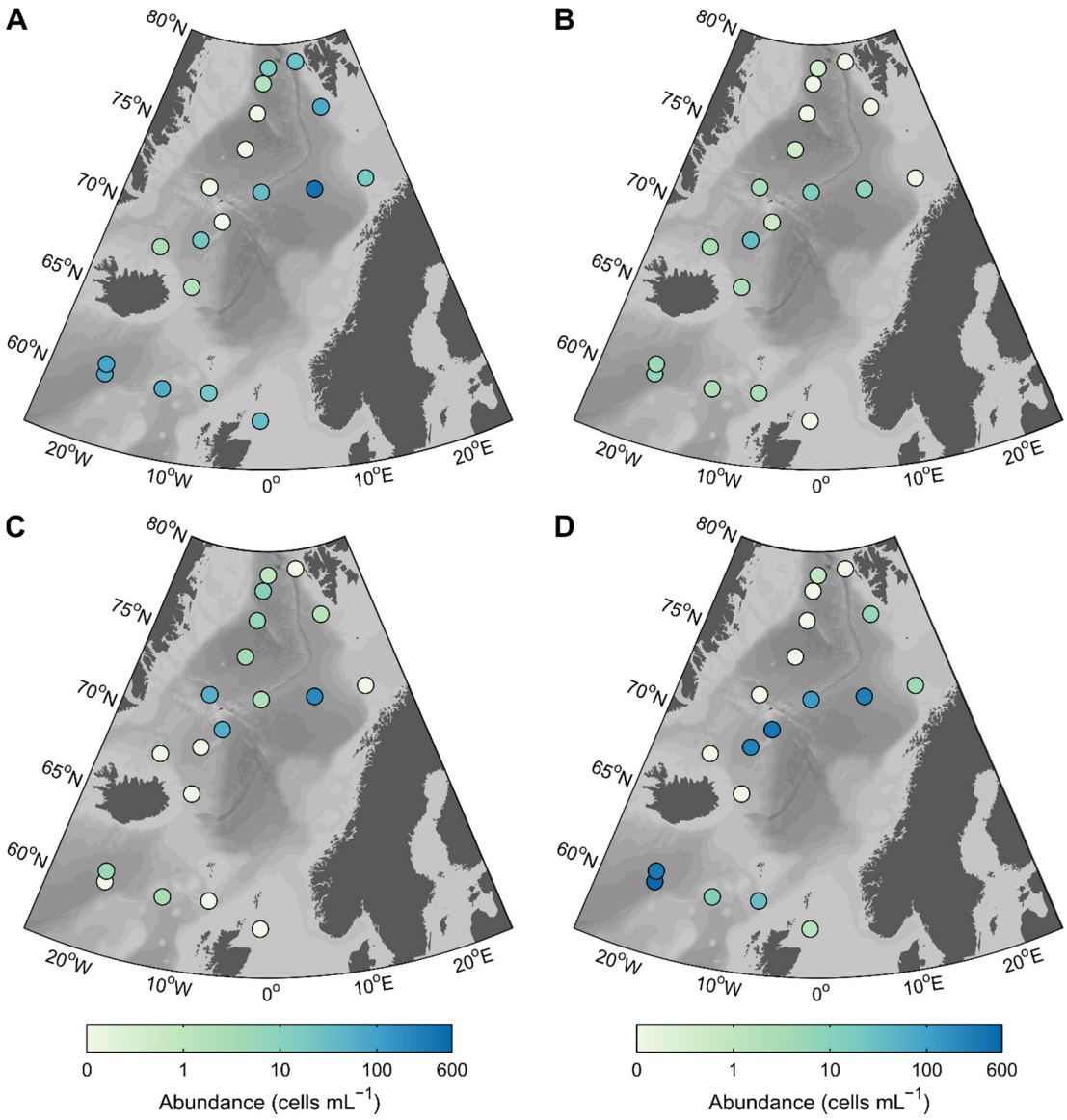

Fig. 4.3: The distribution of coccolithophore abundances (cells mL^{-1}). A) *Emiliania huxleyi*, B) *Coccolithus pelagicus,* C) *Coccolithus pelagicus* HOL, D) Other coccolithophore species.

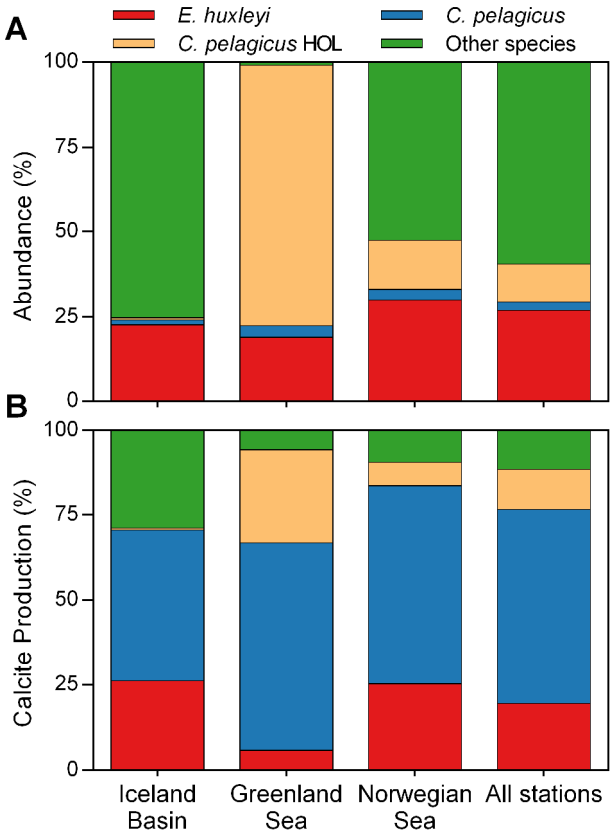

Fig. 4.4: The percentage contribution of coccolithophore species to A) abundance and B) calcite production, aggregated over each hydrographic region and the entire study area.

considered these species individually and have used a "small Syracosphaera" (Young and Ziveri, 2000) estimate for calculating cellular calcite. The different coccolithophore species had varying spatial distributions (Fig. 4.3, Table 4.3). *Emiliania huxleyi* was most abundant in the Iceland Basin and Norwegian Sea (Fig. 4.3A), *C. pelagicus* HOL was present in the highest latitude stations (Fig. 4.3C), while *Syracosphaera* spp. was restricted to the Iceland Basin.

To account for the large variability in coccolithophore abundances between stations, the stations were grouped into the three regions (Iceland Basin, Greenland Sea and Norwegian Sea) as defined from the characteristic hydrography of each station (Fig. 4.1, Table 4.2).Coccolithophore abundances, aggregated over these regions, and the entire study (Fig. 4.4A) showed that *E. huxleyi* represented 27 % of the total coccolithophore abundance, with a relatively consistent contribution across all regions

(19 – 30 %, Fig. 4.4A). In contrast, *Coccolithus pelagicus* formed only a small component of the coccolithophore community in all regions in terms of abundance (1 – 4 %, Fig. 4.4A). The Iceland Basin community was dominated by *C. caudatus* (43 %) and *Syracosphaera* spp (24 %), the Norwegian Sea by *C. caudatus* (43 %), and the Greenland Sea by *C. pelagicus* HOL (77 %, Fig. 4.4A).

4.3.3 Species-specific calcite production

The total community calcite production was highly variable throughout the study (2 – 202 µmol C m^{-3} d^{-1}, Table 4.4), with rates similar to those measured in the subtropics (Poulton et al., 2006), and generally lower than those previously measured on the north-west European shelf (Poulton et al., 2014) and in the Iceland Basin in late summer (Poulton et al., 2010). There were no clear spatial patterns in the distribution of calcite production (Appendix Fig. B.1). The largest calcite production (202 µmol C m^{-3} d^{-1}) was measured in the central Norwegian Sea, with the lowest rates in the Greenland Sea (<10 µmol C m^{-3} d^{-1}).

Derived species-specific calcite production (CP_{sp}) showed significant variability for the individual species (Table 4.4, Fig. 4.5). *Emiliania huxleyi* populations produced between 0.3 and 24.9 µmol C m^{-3} d^{-1} with the highest rates occurring in the Norwegian Sea, and the lowest rates occurring in the central Greenland Sea (Fig. 4.5A). Calcite production rates of *C. pelagicus* were significantly higher (1.2 – 168.6 µmol C m^{-3} d^{-1}, Fig. 4.5B); the highest rates occurred in the central Norwegian Sea (168.6 µmol C m^{-3} d^{-1}) and in the southern Greenland Sea (28.6 – 52 µmol C m^{-3} d^{-1}). Species-specific calcite production rates of *C. pelagicus* HOL (0.2 – 26.7 µmol C m^{-3} d^{-1}) were similar to *E. huxleyi* but were distributed differently with highest rates in the northern Nordic Seas (Fig. 4.5C). Of the other species, *Syracosphaera* spp. produced 0.3 – 11.5 µmol C m^{-3} d^{-1} of calcite in the Iceland Basin, while *A. robusta* (0.2 – 14.4 µmol C m^{-3} d^{-1}) and *C. caudatus* (0.1 – 6.4 µmol C m^{-3} d^{-1}) were responsible for the remaining calcite production, particularly in the Norwegian Sea (Fig. 4.5D).

At each individual station, the major calcite producers were *E. huxleyi* (0 – 100 %), *C. pelagicus* (0 – 98 %) and *C. pelagicus* HOL (0 – 100 %). However, there was significant

Table 4.4: Total calcite production (µmol C m^{-3} d^{-1}) and species-specific calcite production (%)

Sta.	Location	Total Calcite Production (µmol C m^{-3} d^{-1})	Calcite production (%)							
			E. huxleyi	*C. pelagicus*	*C. pelagicus* HOL	*Syracosphaera* spp.	*A. quattrospina*	*C. caudatus*	*Ophiaster* sp.	*A. robusta*
6	ICB*	7.25	97.6	-	-	-	2.4	-	-	-
8	ICB	21.65	17.7	64.1	-	15.5	-	0.5	0.2	2
10	ICB	7.06	44.4	47.1	3.1	4.2	0.9	0.1	0.3	-
12	ICB	42.51	14.9	43.9	-	27	1.1	12.3	0.9	-
17	ICB	13.56	27.2	37	2.4	19.3	1.9	9.7	2.5	-
19	NWS	11.31	2.3	97.7	-	-	-	-	-	-
20	NWS	17.45	-	9.8	50.8	-	-	36.8	-	2.5
21	GS	1.65	-	70	30	-	-	-	-	-
27	GS	3.54	-	-	100	-	-	-	-	-
29	GS	9.04	54.8	38.2	4.5	-	-	-	-	2.5
40	GS	29.64	10	-	90	-	-	-	-	-
42	NWS	18.96	100	-	-	-	-	-	-	-
45	NWS	16.69	88.6	3.5	2.9	-	-	0.3	-	4.7
54	NWS	8.61	84.2	-	-	-	-	-	-	15.8
56	NWS	63.93	38.9	19	30.5	-	-	2.6	-	8.9
58	NWS	201.55	6.2	83.6	0.6	-	-	2.4	-	7.1
60	GS	16.21	-	50.3	49.7	-	-	-	-	-
63	NWS	55.87	2	93.2	-	-	-	4.8	-	-
65	NWS	29.58	3.2	96.8	-	-	-	-	-	-

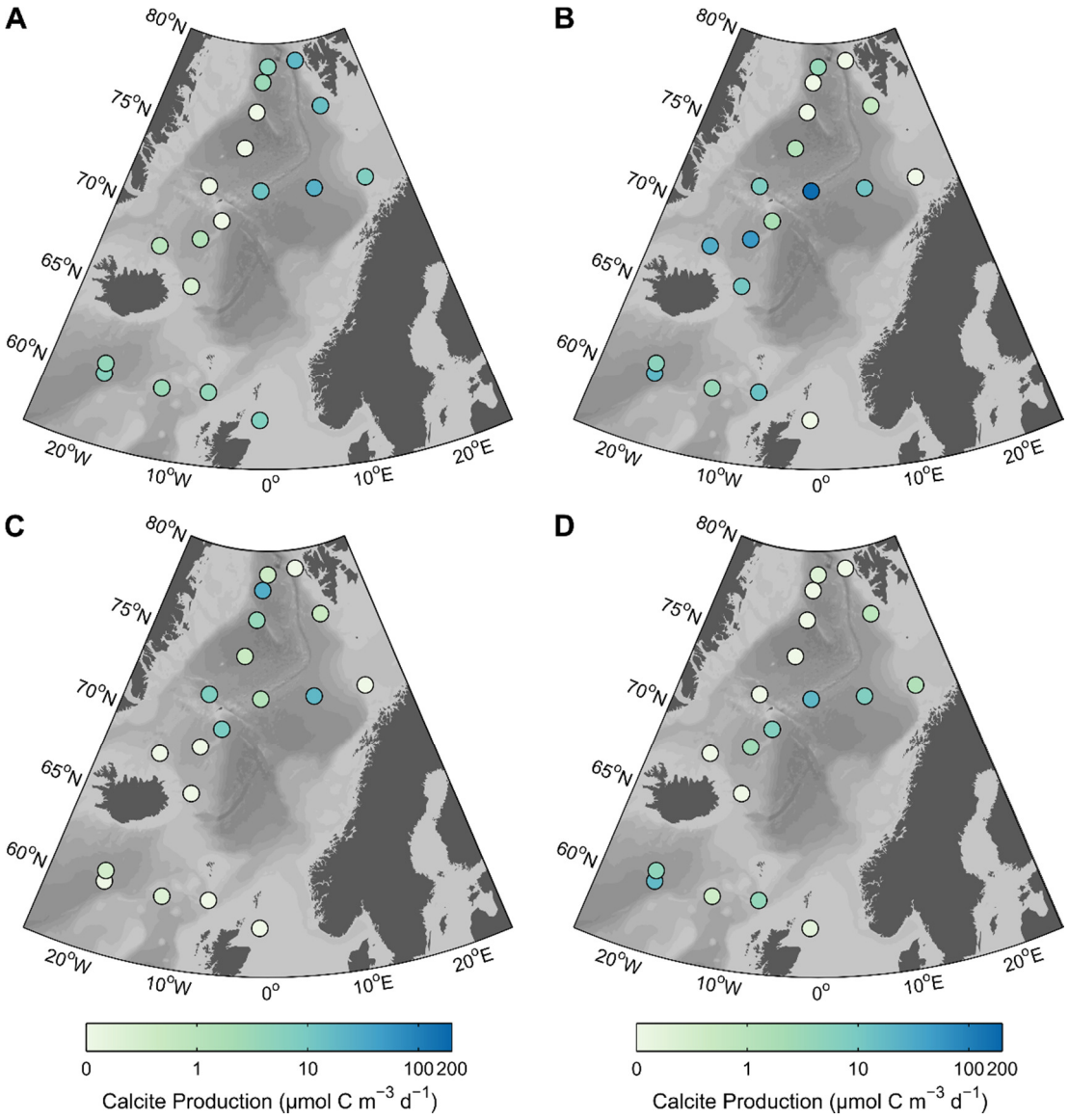

Fig. 4.5: The distribution of species-specific calcite production (µmol C m^{-3} d^{-1}). A) *Emiliania huxleyi*. B) *Coccolithus pelagicus* C) *Coccolithus pelagicus* HOL D) Other coccolithophore species.

variability between the stations (Table 4.4, Fig. 4.5), and when considering each station individually, *E. huxleyi* was the largest contributor at 6 stations, *C. pelagicus* at 10 stations and *C. pelagicus* HOL at 3 stations. Of the other species, *Syracosphaera* spp. were also a significant source in the Iceland Basin (0 – 27 %), and *C. caudatus* was generally a small source (0 – 12 %) except at station 20 in the Norwegian Sea where it contributed 37 % of the calcite production. When present, *A. robusta* was a minor contributor to calcite production in the Norwegian Sea (3 – 16 %).

Considering the percentage calcite production of each species on a per station basis however does not account for the high variability in the measured total calcite production. Incorporating total calcite production and aggregating over the three regions and the entire cruise reveals that *C. pelagicus* was the major calcifier, responsible for 57 % of the total calcite production (Fig. 4.4B), with a higher contribution in the Greenland Sea (61 %) and the Norwegian Sea (59 %) than in the Iceland Basin (44 %). In contrast, *E. huxleyi* represented only 20 % of the total calcite production (Fig. 4.4B), with a much smaller contribution in the Greenland Sea (6 %) than in the Norwegian Sea (26 %) and Iceland Basin (25 %). *Coccolithus pelagicus* HOL was a significant calcite producer in the Greenland Sea (28 %), but less so in the other regions, resulting in a total contribution of only 12 % (Fig. 4.4B). The contribution of the other observed species to calcite production was greatest in the Iceland Basin (29 %), of which *Syracosphaera* spp (19 %) and *C. caudatus* (7 %) were the major calcifiers. In the Greenland and Norwegian Seas, *C. caudatus* (2 – 5 %) and *A. robusta* (0 – 7 %) were the largest calcite producers in terms of the other species present.

4.4 Discussion

4.4.1 *Coccolithus pelagicus* as a key calcifier

Calculating CP_{sp} reveals that *C. pelagicus* is the major calcifier in this Arctic study, responsible for 57 % of the calcite production in the Arctic Ocean and Iceland Basin, despite forming only 2 % of the total coccolithophore community abundance (Fig. 4.4).

The influence of *C. pelagicus* on calcite production is further confirmed by a significant correlation between *C. pelagicus* abundance and total calcite production ($r = 0.55$, $p < 0.02$, $n = 19$); no other species correlated significantly with total calcite production. That *C. pelagicus* is able to dominate calcite production at such low relative abundances is due to its significantly higher cellular calcite quota than compared to the rest of the coccolithophore species present in the community (Table 4.1). This potential to dominate community calcite production has been demonstrated in Chapter 2 using a simplified two species model of *C. pelagicus* and *E. huxleyi*. Although the natural communities in our samples are more complex and diverse, *C. pelagicus* still has at least a 20 fold greater cellular calcite quota than the rest of the community (Table 4.1). Thus, when present *C. pelagicus* is able to dominate coccolithophore calcite production, confirming the conclusions reached in Chapter 2.

The dominance of *C. pelagicus* is not dependent on any single station. Removing the station which has the highest rate of calcite production (202 µmol C m^{-3} d^{-1}), and therefore the largest influence over CP_{sp}, does not change the overall result. Although removing this station from the analysis results in a reduction of *C. pelagicus*-derived calcite production from 57 % to 43 %, *C. pelagicus* remained the single largest source of calcite in the mixed communities of the Arctic Ocean and Iceland Basin. The effect of removing any other station from the analysis was minimal with *C. pelagicus* remaining the dominant calcifier.

Although *E. huxleyi* is often perceived to be the most abundant and keystone coccolithophore species (Paasche, 2002), I found that it was neither the most abundant (27 % total abundance, Fig. 4.4A), or the major calcifier (20 % of total calcite production, Fig. 4.4B). This suggests that it may not be the keystone species of coccolithophore in this region of the North Atlantic and Arctic, as hypothesised in Chapter 2 (Fig. 2.4). However, previous studies have identified *E. huxleyi* as the most abundant coccolithophore in the Norwegian Sea (Baumann et al., 2000a; Charalampopoulou et al., 2011). The change in dominance between studies is possibly due to significant seasonal variability occurring within the coccolithophore community (Baumann et al., 2000a). However, an increase in the abundance of *E. huxleyi*, coupled

with a reduction in the abundance of other species such as *C. caudatus* and *A. robusta*, resulting in the numerical dominance of *E. huxleyi*, would be unlikely to affect the overall result as *C. pelagicus* was the key calcifier (57 %) despite forming a small fraction (2 %) of the coccolithophore community.

Despite dominating calcite production in the Arctic and subarctic Iceland Basin, *C. pelagicus* is unlikely to be a globally dominant calcite producer, as its distribution is constrained to the Arctic and subarctic (Mcintyre and Bé, 1967). Other heavily calcified species, relative to *E. huxleyi*, such as *Calcidiscus leptoporus*, *Helicosphaera carteri* and *Gephyrocapsa oceanica* are more widely distributed than *C. pelagicus* (Mcintyre and Bé, 1967; Ziveri et al., 2004) and can dominate calcite export (Ziveri et al., 2007), such that they have the potential to dominate calcite production in other regions. Whilst the importance of such heavily calcified species has been demonstrated both here and in Chapter 2, there has been little consideration of the role of holococcolith bearing coccolithophores, such as *C. pelagicus* HOL (which I estimate to have a greater cellular calcite than *E. huxleyi*, Table 4.1), and relatively weakly calcified but potentially highly abundant coccolithophores such as *C. caudatus*. Estimated to be responsible for 12 % of the calcite production in this study (Fig. 4.4B), and with a potentially wider distribution than its heterococcolith bearing life-cycle phase (Kleijne, 1991), *C. pelagicus* HOL has the potential to be a globally significant calcifier. In contrast to *C. pelagicus* and even *C. pelagicus* HOL, *C. caudatus* is relatively weakly calcified; while abundant it formed a relatively small component of the calcite production (5 %). However, this is still a significant contribution to total calcite production and demonstrates the potential for it and other similarly weakly calcified species to be important calcifiers. Further research into these lesser-studied species is required in order to improve our understanding of the role of different species in calcite production.

4.4.2 A robust measure of CP_{sp}?

As CP_{sp} cannot be directly measured, its calculation requires assumptions, which may have errors, as discussed in Chapter 2. The two main potential errors are associated

with the estimates of cellular calcite and the assumption that all coccolithophore species have the same relative growth rate to each other.

With the natural variability in coccolith size and shape, determining cellular calcite following Young and Ziveri (2000) has an associated error estimated to be ~30 – 50 % (Young and Ziveri, 2000; Daniels et al., 2012), which can be minimised by using species-specific shape factors and sample measurements of coccolith length, as done here (Daniels et al., 2012). The cellular calcite estimates for *C. pelagicus* (15.2 pmol C cell^{-1}) and *E. huxleyi* (0.52 pmol C cell^{-1}) are consistent with both the cultures estimates in Chapter 2 (16.6 pmol C cell^{-1} and 0.43 – 0.52 pmol C cell^{-1}) and literature values of *E. huxleyi* (0.22 – 1.1 pmol C cell^{-1}, see Chapter 2 and Paasche, 2002). However, the cellular calcite content of the other species present are generally poorly constrained (Young and Ziveri, 2000). While generally thought to be relatively lightly calcified (Young and Ziveri, 2000; Young et al., 2003), their relatively high abundance coupled with the uncertainty in cellular calcite may cause a significant error.

That all coccolithophores have the same growth rate is an assumption with a potentially large associated error. Although *E. huxleyi* is perceived to be a fast growing coccolithophore species relative to other species (Paasche, 2002; Tyrrell and Merico, 2004), little data exists concerning relative in situ growth rates of coccolithophores in mixed communities. The results of Chapter 2 and Chapter 3 suggest that *E. huxleyi* may not be a faster growing species, particularly in the relatively cold environment (1.0 – 10.6 °C) encountered in this study. In particular, that net growth rates of *C. pelagicus* were similar or higher than *E. huxleyi* in the early spring North Atlantic communities considered in Chapter 3 suggest that in situ relative growth rates of coccolithophores are more complex than previously thought, and that the assumption of the same growth rate may introduce significant error.

To test the influence of these potential errors on species-specific calcite production, the relative growth rates of the three main calcifiers, *E. huxleyi* (Fig. 4.6A, *C. pelagicus* (Fig. 4.6B), and *C. pelagicus* HOL (Fig 4.7C) were independently varied from between 10 – 200 % of the coccolithophore community growth rate (Fig. 4.6). Using a similar modelling framework to that used in Chapter 2, increasing the relative growth rate of a

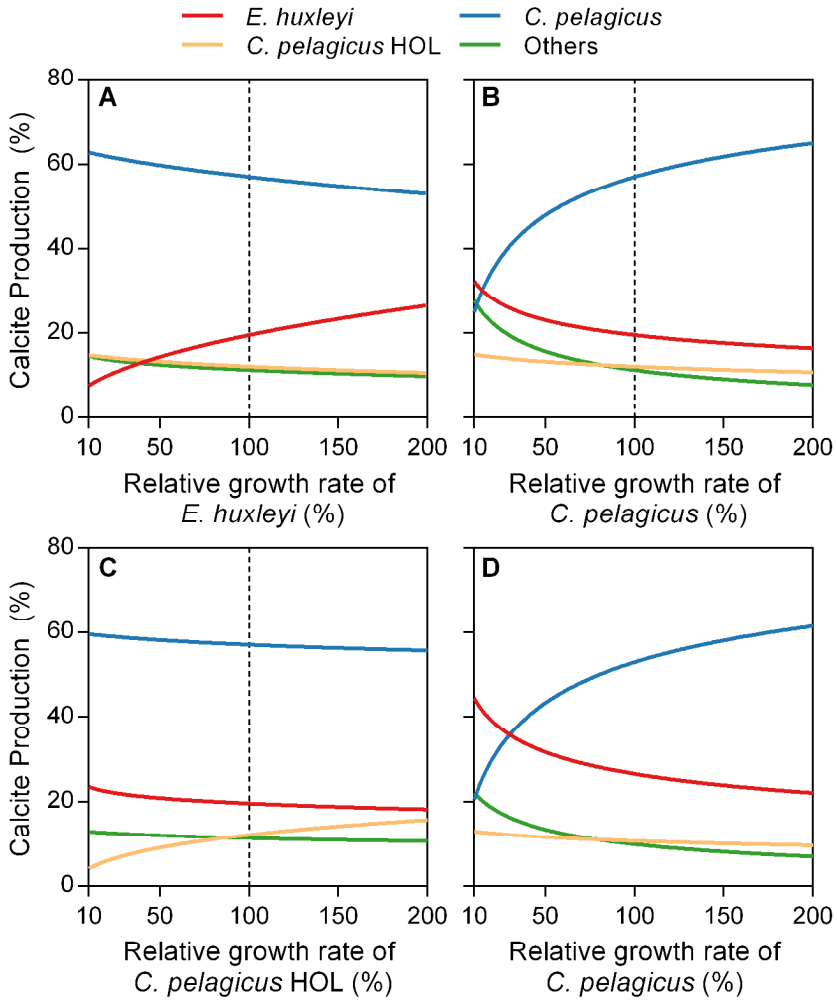

Fig. 4.6: The effect of varying the relative growth rate of one species on the species contribution to calcite production. The growth rates of A) *Emiliania huxleyi*, B) *Coccolithus pelagicus*, and C) *Coccolithus pelagicus* HOL were singly varied whilst all other species had a relative growth rate of 100%. D) The relative growth rate of *Coccolithus pelagicus* was varied, whilst *Emiliania huxleyi* had a relative growth rate of 200 % and other species 100 %. The dashed line indicates the original scenario.

species can represent either an increase in the growth rate or cellular calcite content of that species (Eq. 4.1). Of the three scenarios (Fig 4.7 A-C), *C. pelagicus* remained the major calcifier except when the relative growth rate of *C. pelagicus* was less than 15 % of the rest of the community (Fig. 4.6B); *E. huxleyi* became the major calcifier but *C. pelagicus* still contributed > 25 % of the calcite production. To further perturb the community, a fourth scenario was examined (Fig. 4.6D), where the relative growth rate of *E. huxleyi* was increased to 200 % of the other species, and then the relative growth rate of *C. pelagicus* varied as in Fig 4.6B. In this scenario, with a growth rate less than 30 % of the total community growth rate, *C. pelagicus* would not dominate calcite production. However, despite this extreme and potentially unrealistic scenario, *C. pelagicus* remained a significant calcifier (> 20 %).

These scenarios demonstrate the potential influence of variable growth rates on CP_{sp}. Further research is required to constrain both cellular calcite quotas and coccolithophore growth rates from natural communities, which will both reduce the potential error and allow for a greater understanding of relative roles in calcite production and be highly informative in terms of coccolithophore ecology. However, that *C. pelagicus* remained the dominant calcifier in all but the most extreme scenarios suggests that the result that *C. pelagicus* is a key calcifier in the Arctic is robust.

4.4.3 Environmental influences

The relationship between coccolithophore abundance, calcite production, and environmental variables is complex and difficult to elucidate (Poulton et al., 2014), with carbonate chemistry (Charalampopoulou et al., 2011; Smith et al., 2012), irradiance (Poulton et al., 2010; Charalampopoulou et al., 2011; Poulton et al., 2014), and nutrients (Poulton et al., 2011; Poulton et al., 2014) all shown to affect coccolithophore community composition and calcite production. Charalampopoulou et al. (2011) used Spearman's rank correlations of biotic and abiotic data to show that pH and irradiance affected coccolithophore community structure. Employing the same multivariate approach here finds that temperature and Ω_C were the combination of 2 variables best correlated with the composition of the coccolithophore community (r_s =

0.55, $p < 0.01$). It should be noted that the species richness was 8 in this study, but 40 in the study by Charalampopoulou et al. (2011), which may affect the analyses. The variability in CP_{sp} was best correlated with Ω_C alone ($r_s = 0.42$, $p < 0.01$).

Correlations do not necessarily imply causality and therefore it should not be directly inferred that CP_{sp} in controlled by Ω_C. A principal component analysis (PCA) of normalised environmental variables (temperature, salinity, Ω_C, pH, N*, Si*, daily PAR and Z_{eup}) correlated with community abundances, CP_{sp} and total calcite production allows for the relationship between abiotic and biotic data to be examined in more detail. The first principal component (PC-1) explained 40 % of the variance and was strongly related to Ω_C, pH and Si*. The second principal component (PC-2) explained 33 % of the variance and was related to temperature, salinity and N*. Essentially, PC-2 described the north-south environmental gradient, being well correlated with latitude ($r = 0.68$, $p < 0.002$, $n = 19$), and thus correlated well with both the abundance ($r = 0.63 – 0.67$, $p < 0.04$) and CP_{sp} ($r = 0.65 – 0.67$, $p < 0.01$) of those species found only in the warmer Iceland Basin (*Syracosphaera* spp, *A. quattrospina* and *Ophiaster* sp.). Although the abundance of *E. huxleyi* was correlated with PC-2 ($r = 0.53$, $p < 0.03$, $n = 19$), CP_{sp} of *E. huxleyi* was correlated with PC-1 ($r = 0.49$, $p < 0.04$, $n = 19$). This pattern is likely due to the absence of *E. huxleyi* in the southern Greenland Sea (Fig. 4.5B), which was characterised by the lowest values of Ω_C (< 3).

The multivariate analysis suggests that Ω_C significantly affects CP_{sp}, through its influence on *E. huxleyi* distribution and abundance. However, the relationship is likely to be more complex as there was no significant environmental influence on total calcite production ($p > 0.09$, or the abundance ($p > 0.19$) and CP_{sp} ($p > 0.10$) of *C. pelagicus* and *C. pelagicus* HOL. Furthermore, correlations of individual environmental variables with abundance and CP_{sp} did not produce any significant results, thus demonstrating the complexity of the interaction between coccolithophore abundance, calcite production, and environmental variables (Poulton et al., 2014).

4.4.4 Wider Implications

Research into the effect of ocean acidification and climate change on coccolithophores has been dominated by studies of *E. huxleyi*, which can be considered an atypical coccolithophore species in terms of its genetic lineage, physiology and ecology (De Vargas et al., 2007); hence the response of *E. huxleyi* may not be fully applicable to other coccolithophore species. Few studies have examined the impact of ocean acidification on other species of coccolithophore (Langer et al., 2006; Fiorini et al., 2011; Krug et al., 2011), and very little is known about the Arctic species *C. pelagicus*. As a key calcifier in a region considered particularly vulnerable to ocean acidification and warming, the response of *C. pelagicus* to climate change and ocean acidification could have a major effect on calcite production in the Arctic and Iceland Basin. Examination of the fossil record of *C. pelagicus* during the Palaeocene-Eocene Thermal Maximum (PETM), arguably the best geological equivalent of modern-day climate change (Gibbs et al., 2013), found that it was not able to maintain optimum growth during this period (Gibbs et al., 2013), and had reduced calcification rates (O'dea et al., 2014). If *C. pelagicus* exhibits a similar response in the modern ocean to current perturbations, this could result in a significant reduction in calcite production within the Arctic Ocean and Iceland Basin, with a significant impact on carbon cycling in the North Atlantic.

4.5 Conclusions

In this study I have used a novel method to determine for the first time, species-specific calcite production (CP_{sp}) within a natural multi-species community of coccolithophores. In deriving CP_{sp} I have found that *C. pelagicus* was the major calcifier in the Arctic Ocean and Iceland Basin, responsible for 57 % of the total calcite production. This dominance was despite *C. pelagicus* forming only a small fraction (2 %) of the total coccolithophore community abundance, and occurred because *C. pelagicus* has a much larger (x 20) cellular calcite content relative to the other coccolithophore species present. In contrast, *E. huxleyi*, generally perceived to be the

keystone coccolithophore species, was responsible for only 20 % of the total calcite production.

The robustness of this method to variability in growth rates was demonstrated by manipulating relative growth rates of the three main species, *E. huxleyi*, *C. pelagicus* and *C. pelagicus* HOL. *C. pelagicus* remained the major calcifier in all scenarios except when the relative growth rate was reduced to 15 % of the overall community, a potentially unrealistic scenario.

Temperature and calcite saturation state (Ω_C) could best explain the coccolithophore community composition, while Ω_C alone best explained the variability in CP_{sp}. This effect was primarily due to the distribution and abundance of *E. huxleyi* in relation to Ω_C. The relationship between CP_{sp} is likely to be more complex as CP_{sp} by *C. pelagicus* and *C. pelagicus* HOL were not influenced by environmental factors.

This study demonstrates the importance of *C. pelagicus* as a key calcifier in the Arctic and subarctic Iceland Basin, suggesting that it is the biogeochemically key coccolithophore in this region. With a restricted distribution, *C. pelagicus* is unlikely to be a globally dominant calcite producer. However, this study demonstrates the potential for both relatively rare but heavily calcified species (such as *C. pelagicus*), and highly abundant but relatively weakly calcified species (such as *C. caudatus*) to be key calcite producing species. The approach of CP_{sp} needs to be applied to other coccolithophore communities in order to further our understanding of calcite production by coccolithophore species.

Chapter 5: Synthesis

5.1 Chapter aim

The work presented in this thesis aimed to test the hypothesis that ***Coccolithus pelagicus*** **has a significant biogeochemical role, dominating calcite production within a mixed community in the North Atlantic**. The individual aims of the chapters were:

1. To experimentally determine the relative growth rates and cellular calcite contents of *Emiliania huxleyi*, *Coccolithus pelagicus* and *Coccolithus braarudii* and assess their biogeochemical role with model and field data;

2. To determine the phytoplankton community structure during the onset of the North Atlantic spring bloom, examining the dynamics of the coccolithophore community and the contribution of *C. pelagicus* to coccolithophore calcite;

3. To determine species-specific calcite production in the Arctic and Iceland Basin and examine the role of *C. pelagicus* in calcite production from this region.

In this synthesis chapter, I will draw together the results of these three chapters, to examine the biogeochemical role of *C. pelagicus*, including considering the effect of seasonality on the coccolithophore community and calcite production. The wider implications of the main findings will be discussed, along with a consideration of the limitations and future directions.

5.2 Thesis Synopsis

Chapter 2 – Culture experiments found that over a range of experimental conditions the relative growth differences between *E. huxleyi* and *Coccolithus* were generally small (12 % and 28 % respectively for *C. pelagicus* and *C. braarudii*). Modelling relative calcite production found that assuming the measured relative growth rates and

estimates of cellular calcite, *C. pelagicus* would be a greater source of calcite than *E. huxleyi* if the relative abundance of *E. huxleyi* to *C. pelagicus* was less than 34:1. Using abundance data collected from 29 North Atlantic samples, the ratio of the abundance of *E. huxleyi* to *C. pelagicus* varied from 1:1 – 212:1 and *C. pelagicus* was found to be the major source (> 50 %) of calcite in 69 % of the samples

Chapter 3 – In the early stages of the North Atlantic spring bloom, contrasting phytoplankton community structures at two sites were observed, with different physiochemical and biological factors controlling bloom formation in the Iceland Basin and Norwegian Basin. The absence of diatoms in the Norwegian Basin may be due to micro-zooplankton grazing and a lack of a seed population of diatoms. Coccolithophores were present at both sites, forming a small fraction (< 5 % Chl *a* biomass) of the total phytoplankton community. *Emiliania huxleyi* was the most abundant coccolithophore species, but *C. pelagicus* was present and represented a significant source of calcite (53 % of total coccolithophore calcite). Net growth rates of *C. pelagicus* (μ = 0.12 d^{-1}) were higher than *E. huxleyi* (μ = 0.06 d^{-1}) in the Norwegian Basin, suggesting it may be a significant calcite producer in spring blooms.

Chapter 4 – Species-specific calcite production, estimated from measured total calcite production and estimates of species-specific cellular calcite, revealed *C. pelagicus* to be the major calcifier in the Arctic Ocean and Iceland Basin (57 % of total calcite production) despite forming only a small fraction (2 %) of the coccolithophore community. That *C. pelagicus* was able to dominate was due to its relatively high cellular calcite content. A robustness test was performed by varying the relative growth rate of the major calcifiers; *C. pelagicus* remained the major calcifier in all but the extreme scenarios (i.e. the growth rate of *C. pelagicus* was less than 15 % of the growth rate of the total community).

Chapter 5 aims to draw together the results and knowledge gained in Chapters 2, 3 and 4 to consider the seasonality of calcite production by *C. pelagicus* and other coccolithophores in the North Atlantic.

5.3 The seasonal biogeochemical role of *Coccolithus pelagicus* in the North Atlantic

Although a relatively common subarctic species of coccolithophore (Mcintyre and Bé, 1967; Okada and Mcintyre, 1979), *C. pelagicus* rarely numerically dominates the coccolithophore community, (Milliman, 1980; Tarran et al., 2001). Thus, if present at only low relative abundances (Poulton et al., 2010; Poulton et al., 2014), *C. pelagicus* must have both a high cellular calcite quota, and a high enough relative growth rate if it is to contribute significantly to calcite production.

Cellular calcite quotas of *C. pelagicus* and *E. huxleyi* were estimated from culture experiments (Chapter 2) and field studies (Chapter 3 and 4) to allow a relative comparison of cellular calcite. Estimates of *C. pelagicus* cellular calcite varied from 15.2 pmol C cell^{-1} (Chapter 4), to 16.6 pmol C cell^{-1} (Chapter 2) and 20.8 pmol C cell^{-1} (Chapter 3), while estimates of *E. huxleyi* ranged from 0.43 – 0.52 pmol C cell^{-1} in culture (Chapter 2), to 0.52 pmol C cell^{-1} (Chapter 4) and 0.37 – 0.74 pmol C cell^{-1} in field studies (Chapter 3). The variability between clonal cultures and field populations is to be expected, but the values are generally similar and comparable to the literature for *E. huxleyi* (0.22 – 1.1 pmol C cell^{-1}, Fritz and Balch, 1996; Paasche, 2002; Hoppe et al., 2011). There is a general lack of comparative literature for *C. pelagicus,* with only one reported value of cellular calcite (26 pmol C cell^{-1}, Gerecht et al., 2014). This value is higher than my estimates, however there are uncertainties (A. Gerecht, pers. comm.) about the value presented by Gerecht et al. (2014) as they reported *C. pelagicus* to have a higher cellular calcite content than *C. braarudii*, which is a larger species than *C. pelagicus* (Geisen et al., 2004). Estimates of cellular calcite of *C. pelagicus* and *E. huxleyi* result in *C. pelagicus* having a calcite content x28 – 56 greater than *E. huxleyi*.

Relative gross growth rates, measured from culture experiments in Chapter 2, found that *E. huxleyi* grew on average 12 % faster than *C. pelagicus*. However, this relatively small difference in growth rates resulted in *C. pelagicus* still being a greater source of calcite than *E. huxleyi* in 69 % of the field samples from the subarctic North Atlantic

considered in Chapter 2. Net growth rates of *E. huxleyi* and *C. pelagicus* were determined from the time series study in Chapter 3, where *C. pelagicus* grew up to 217 % faster than *E. huxleyi*. Applying this to the model considered in Chapter 2 would result in *C. pelagicus* being an even greater source of calcite than *E. huxleyi*, with one cell of *C. pelagicus* producing up to 84 times more calcite than a cell of *E. huxleyi*.

That the growth rates obtained from cultures and field samples are measurements of gross and net growth rates respectively is an important consideration. Growth rates measured in time series samples are net – the cells are subject to mortality factors including predation, viral attack and mixing out of the sampled environment. In contrast, cultures experience minimal loss and thus rates of growth in culture are considered to represent gross growth rates. That gross growth rates of *C. pelagicus* were slightly lower than *E. huxleyi* while net growth rates of *C. pelagicus* in spring in the North Atlantic were the same or higher than *E. huxleyi* is of significant interest. Despite the fact that *C. pelagicus* was both measured to be significantly larger (~1100 μm^3) than *E. huxleyi* (~50 μm^3) and (assuming Redfield stoichiometry (Redfield, 1958)) that *C. pelagicus* was calculated to have a higher cellular nutrient requirement than *E. huxleyi* (Chapter 2), gross growth rates were broadly comparable, and net growth rates of *C. pelagicus* in Chapter 3 were higher than *E. huxleyi*. As maximal (optimal) growth rates generally increase with decreasing size (Sarthou et al., 2005; Finkel et al., 2009), the results from Chapters 2 and 3 suggest perhaps that *C. pelagicus* has more efficient nutrient uptake pathways than *E. huxleyi* or that both the experimental and in situ conditions were less optimal for *E. huxleyi* than *C. pelagicus*. Significantly higher net growth rates could also suggest that *C. pelagicus* experiences lower mortality than *E. huxleyi*. That *C. pelagicus* is much more heavily calcified than *E. huxleyi* may afford it increased protection from zooplankton grazing (Young, 1994), thus resulting in an increased net growth rate. The cellular calcite and growth rate data of Chapters 2 and 3 both suggested *C. pelagicus* as a major source of calcite in the North Atlantic. The results of Chapter 4 confirmed this, with *C. pelagicus* estimated to be responsible for 57 % of the calcite production in the Iceland Basin and Arctic Ocean.

The calculation of species-specific calcite production in Chapter 4 demonstrated not only that *C. pelagicus* was the major calcifier, but that species other than *E. huxleyi* and *C. pelagicus* (e.g. *Algirosphaera robusta, Coccolithus pelagicus* HOL, and *Calciopappus caudatus*) were responsible for 23 % of the calcite production in the Arctic and Iceland Basin. While Chapter 2 only considered field data concerning *E. huxleyi* and *C. pelagicus*, other species were also present. Therefore it is possible to apply the methods used in Chapter 4 to this field data to estimate species-specific cellular calcite contributions for all species present. However, without calcite production measurements, it is not possible to determine species-specific calcite production rate estimates.

Calcite production is likely to vary seasonally; species succession occurs within coccolithophore communities (Okada and Mcintyre, 1979), thus the key calcifiers may change throughout the seasons. Incorporating the field data considered in Chapter 2 (the spring bloom [early May, D350], the late spring coccolithophore bloom [late May, D351] and the summer [July, D354]), Chapter 3 (early spring bloom [April, M87/1]) and Chapter 4 (summer [June, JR271]) allows for a seasonal analysis of coccolithophores and calcite production, summarised in Table 5.1.

5.3.1 Calcite production in early spring

During the early stages (April) of the onset of the 2012 North Atlantic spring bloom, I observed in Chapter 3 that coccolithophores represented only a small fraction of the total phytoplankton community (0.1 – 4.4 % Chl *a* biomass), and were relatively low in abundance (5 – 54 cells mL^{-1}) compared to both coccolithophore blooms (1000 - 15000 cells mL^{-1}, Fernandez et al., 1993) and late summer populations (100 – 870 cells mL^{-1}, Poulton et al., 2010). With low abundances, low calcite production rates would be expected. Calcite production was not measured on the cruise and thus was not discussed in Chapter 3. However, species-specific growth rates, cellular calcite and abundances were determined in Chapter 3. Using the equation defined in Chapter 2 (Eq. 2.1) it is possible to estimate species-specific calcite production (Appendix Table C.1). Of the species present, species-specific calcite production was estimated for

Table 5.1: Summary of seasonality in coccolithophore abundances, calcite production, and the significant (> 10 %) species in terms of abundance and calcite production

Cruise	Date	Coccolithophore Abundance (cells mL^{-1})	Most Abundant Species	Calcite Production ($\mu mol\ m^{-3}\ d^{-1}$)	Significant Calcifiers
M87/1	Early Spring 19th March – 2nd May 2012	5 – 54	*Algirosphaera robusta, Emiliania huxleyi*	0.4 – 10[a]	*Algirosphaera robusta, Coccolithus pelagicus, Emiliania huxleyi*
D350	Spring Bloom 29th April – 8th May 2010	195 – 1193	*Calciopappus caudatus, Coccolithus pelagicus, Coccolithus pelagicus* HOL, *Emiliania huxleyi*	-	*Coccolithus pelagicus, Coccolithus pelagicus* HOL, *Coronosphaera mediterranea, Emiliania huxleyi, Helicosphaera carteri*
D351	Late Spring 13th May – 21st May 2010	4 – 379	*Acanthoica quattrospina Calciopappus caudatus, Coccolithus pelagicus, Coccolithus pelagicus* HOL, *Syracosphaera dilatata,* small *Syracosphaera* spp.	-	*Coccolithus pelagicus, Coccolithus pelagicus* HOL, *Coronosphaera mediterranea, Emiliania huxleyi, Gephyrocapsa muellerae, Helicosphaera carteri*
JR271	Summer 4th June – 30th June 2012	33 – 650	*Calciopappus caudatus, Emiliania huxleyi, Syracosphaera* spp.	7 – 43[b]	*Coccolithus pelagicus, Emiliania huxleyi, Syracosphaera* spp.
D354	Late Summer 13th July – 30th July 2010	25 – 1029	*Acanthoica quattrospina, Calcidiscus leptoporus* HOL, *Calciopappus caudatus, Calyptrolithophora papillifera, Emiliania huxleyi, Ophiaster formosus,* small *Syracosphaera* spp.	-	*Calcidiscus leptoporus* HOL, *Calyptrolithophora papillifera*, *Coccolithus pelagicus, Coccolithus pelagicus* HOL, *Emiliania huxleyi*, small *Syracosphaera* spp.

[a] Estimated from measured growth rates and estimates of cellular calcite.
[b] Directly measured.

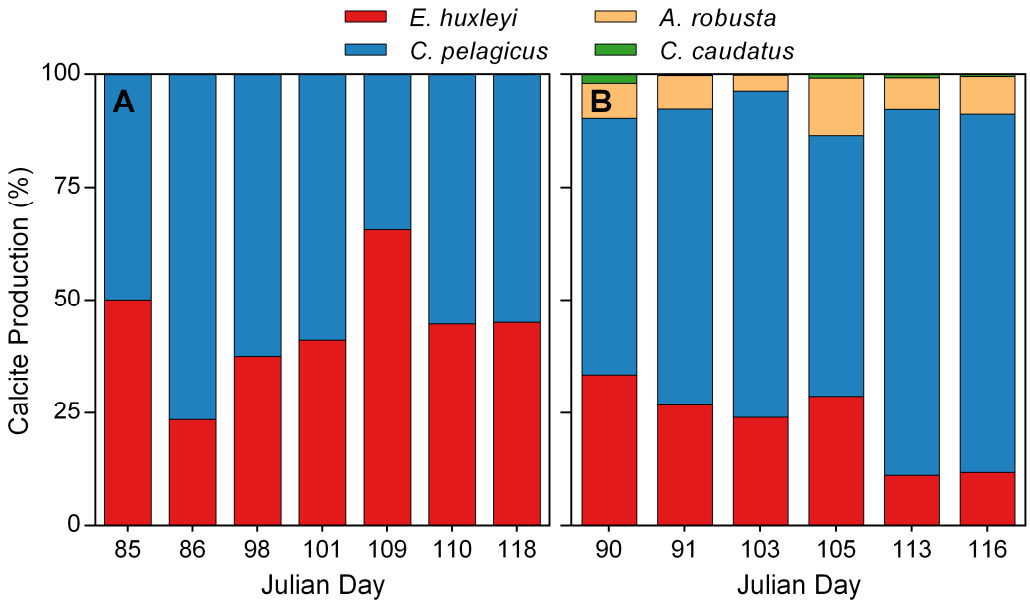

Fig 5.1: The percentage contribution of coccolithophore species to calcite production in A) the Iceland Basin and B) the Norwegian Basin in spring 2012.

E. huxleyi, *C. pelagicus*, *Algirosphaera robusta* and *Calciopappus caudatus* as they were consistently present. Multiple morphotypes of *E. huxleyi* were present (A, B, A over-calcified). As the relationship between morphotypes is not well understood (Smith et al., 2012), morphotype-specific calcite production was derived and combined to estimate *E. huxleyi* specific calcite production (Young and Ziveri, 2000).

As the calculated growth rates in the field are net, they are lower (0.06 – 0.13 d^{-1}) than gross growth rates (0.2 – 0.6 d^{-1}, Chapter 2) at similar temperatures. The species-specific calcite production determined in Chapter 4 used ^{14}C, which measures carbon uptake closer to gross than net (Pei and Laws, 2013). Thus we would expect the estimates of species-specific calcite production performed here to be lower than those in Chapter 4. This was the case for total calcite production, with rates (0.4 – 9.5 µmol C m^{-3} d^{-1}) generally lower than in the Iceland Basin in June of the same year (7.1 – 42.5 µmol C m^{-3} d^{-1}, Chapter 4), and in late summer (July – August) of a previous year (10 – 250 µmol C m^{-3} d^{-1}, Poulton et al., 2010).

Species-specific calcite production in early spring reveals that *C. pelagicus* was the major calcite producer during the early onset of the North Atlantic Spring bloom, in

both the Iceland Basin (34 – 76 % of total calcite production, Fig. 5.1A) and the Norwegian Basin (57 – 81 %, Fig. 5.1B). Aggregated over the time series, *C. pelagicus* was responsible for 58 % and 77 % of the calcite production in the Iceland Basin and Norwegian Basins respectively. With relatively high net growth rates, it is likely that *C. pelagicus* continued to be the major calcite producer during the bloom itself.

5.3.2 Calcite production in the spring bloom

In 2010, the spring bloom in the Iceland Basin peaked in early May during D350 (Ryan-Keogh et al., 2013). Coccolithophores were more abundant (200 – 1200 cells mL^{-1}) than in the early stages of the 2012 Iceland Basin spring bloom (7 – 27 cells mL^{-1}, Chapter 3). In addition to *E. huxleyi* and *C. pelagicus* there were 21 other species not considered in Chapter 2 (Appendix Table C.2). The species-specific contribution to calcite was estimated using the methods outlined in Chapter 4, with additional shape factors from (Young and Ziveri, 2000) for species not present in Chapter 4 (Table 5.2).

Despite accounting for the additional species, *E. huxleyi* and *C. pelagicus* were the major calcite contributors (Table 5.3); *C. pelagicus* was the largest single species source of calcite (41 – 81 %) at 6 stations, and a key contributor (> 30 %) in all but 1 station, where *C. pelagicus* HOL dominated abundance (138 cells mL^{-1}) and was the largest source of calcite (38 %). *Emiliania huxleyi* was a significant source (> 10 %) of calcite at all stations but was only the major source (> 50 %) at 2 stations. Despite achieving bloom level abundances (~ 1000 cells mL^{-1}, Tyrrell and Merico, 2004), *E. huxleyi* did not dominate calcite, as *C. pelagicus* was present in a high enough relative abundance (74 cells mL^{-1}) to remain the major calcifier (69 %). This demonstrates that even within *E. huxleyi* blooms, it is not necessarily the primary source of calcite if other species such as *C. pelagicus* are present.

In Chapter 4, I hypothesised that other heavily calcified species, such as *Calcidiscus leptoporus* and *Helicosphaera carteri* may also be significant sources (> 10 %) of calcite. Here I observed that *H. carteri* (20 pmol C $cell^{-1}$) and *C. mediterranea* (6.6 pmol C $cell^{-1}$) were present in the Iceland and Irminger Basins, and contributed up to 22 % and 18 %

Table 5.2: Cellular calcite of individual coccolithophore species

Species	Cellular Calcite (pmol)
Acanthoica sp. / *Anacanthoica* sp.	0.27
Algirosphaera robusta	0.42
Alisphaera unicornis	0.05
Calcidiscus leptoporus	8.15
Calcidiscus leptoporus HOL	0.78
Calciopappus caudatus	0.09
Calyptrolithina divergens	0.78
Calyptrolithophora papillifera	0.78
Coccolithus pelagicus	15.23
Coccolithus pelagicus HOL	0.78
Corisphaera gracilis	0.04
Coronosphaera mediterranea	6.61
Coronosphaera mediterranean HOL	0.78
Emiliania huxleyi	0.52
Gephyrocapsa muellerae	1.28
Helicosphaera carteri	20.25
Michaelsarsia elegans	0.09
Oolithus fragilis	48.40
Ophiaster formosus	0.09
Pappomonas	0.09
Pontosphaera syracusana	8.40
Rhabdosphaera clavigera	1.08
Rhabdosphaera xiphos	0.14
Syracosphaera anthos	0.44
Syracosphaera corolla	0.44
Syracosphaera dilatata	0.55
Syracosphaera pulchra	3.56
Syracosphaera pulchra HOL *oblonga*	0.78
Syracosphaera spp. (small)	0.40

Table 5.3 Species-specific contribution to coccolithophore calcite (%) for cruise D350

Station	Species-specific contribution to coccolithophore calcite (%)										
	Acanthoica quattrospina / *Anacanthoica acanthos*	*Algirosphaera robusta*	*Calcidiscus leptoporus*	*Calcidiscus leptoporus* HOL	*Calciopappus caudatus*	*Coccolithus pelagicus*	*Coccolithus pelagicus* HOL	*Coronosphaera mediterranea*	*Emiliania huxleyi*	*Gephyrocapsa muellerae*	*Helicosphaera carteri*	*Oolithus fragilis*	*Syracosphaera anthos* / *Syracosphaera corolla.*	*Syracosphaera* spp. (small)
1	0.2	0.1	3.9	0.1	0.4	2.4	38.4	17.8	12.7	0.2	22.4	-	0.3	1.1
3	0.1	-	-	-	-	81.2	2.0	-	16.5	-	-	-	-	0.2
5	0.2	-	-	-	1.0	62.1	7.6	-	26.9	0.3	-	-	-	1.9
6	0.1	-	1.3	-	0.3	40.9	16.2	2.1	36.2	-	1.0	-	-	1.8
8	0.1	-	0.2	-	-	64.3	4.1	1.5	29.2	0.1	-	-	-	0.5
11	0.1	-	-	-	-	30.1	10.4	8.2	46.3	-	5.0	-	-	0.1
13	-	-	-	-	0.1	60.0	-	-	39.3	-	-	-	-	0.5
15	0.1	-	-	-	-	40.0	7.8	5.0	40.0	0.9	-	4.6	0.1	1.5
17	0.1	0.1	-	-	0.1	68.6	1.5	-	27.5	1.2	-	-	-	1.1

of the coccolithophore calcite respectively, supporting the validity of the hypothesis. Besides heavily calcified species, I also discussed in Chapter 4 the potential importance of *C. pelagicus* HOL as a calcifier. Here I see further evidence that when present, *C. pelagicus* HOL can be a significant contributor (> 10%) to coccolith calcite.

5.3.3 Calcite production in late spring

Coccolithophores generally form seasonal "blooms" in late spring/summer in the North Atlantic (Holligan et al., 1993; Tyrrell and Merico, 2004; Raitsos et al., 2006). These blooms are typically dominated by *E. huxleyi* (Tyrrell and Merico, 2004), although other species are present (Holligan et al., 1993; Malin et al., 1993). During such blooms, *E. huxleyi* sheds coccoliths into the surrounding water column (Paasche, 2002), which can be detected by satellite (Holligan et al., 1983; Balch and Utgoff, 2009). In 2010, satellites identified the coccolithophore bloom (Fig 5.2) as occurring in late May (D351). Loose *E. huxleyi* coccoliths (upto 2500 mL^{-1}) were observed in the SEM images. These abundances are generally low for a coccolithophore bloom (Poulton et al., 2013), but may represent the outer regions of the bloom, as classified by Poulton et al. (2013). However, the abundance of coccolithophore cells was lower (4 – 400 cells mL^{-1}) than observed during the phytoplankton spring bloom (200 – 1200 cells mL^{-1}). The coccolithophore community was generally similar to early May; 27 species were observed other than *E. huxleyi* and *C. pelagicus* (Appendix Table C.3).

As observed for the spring bloom, the main sources of calcite were *E. huxleyi* (2 – 73 %, Table 5.4) and *C. pelagicus* (10 – 92 %), while *C. pelagicus* HOL, *C. mediterranea* and *H. carteri* all had significant calcite contributions (> 10 %). Some seasonal variability was observed with both *Gephyrocapsa muellerae* and *Syracosphaera dilatata* contributing > 10 % at certain stations. The contribution of *G. muellerae*, a close relative of *E. huxleyi* (Geisen et al., 2004) with 2-3 times more calcite per coccolith (0.08 pmol C $coccolith^{-1}$, Young and Ziveri, 2000) than *E. huxleyi*, is interesting because although it generally forms a minor component of the coccolithophore community abundance, (Young et al., 2014), it may be a significant calcifier.

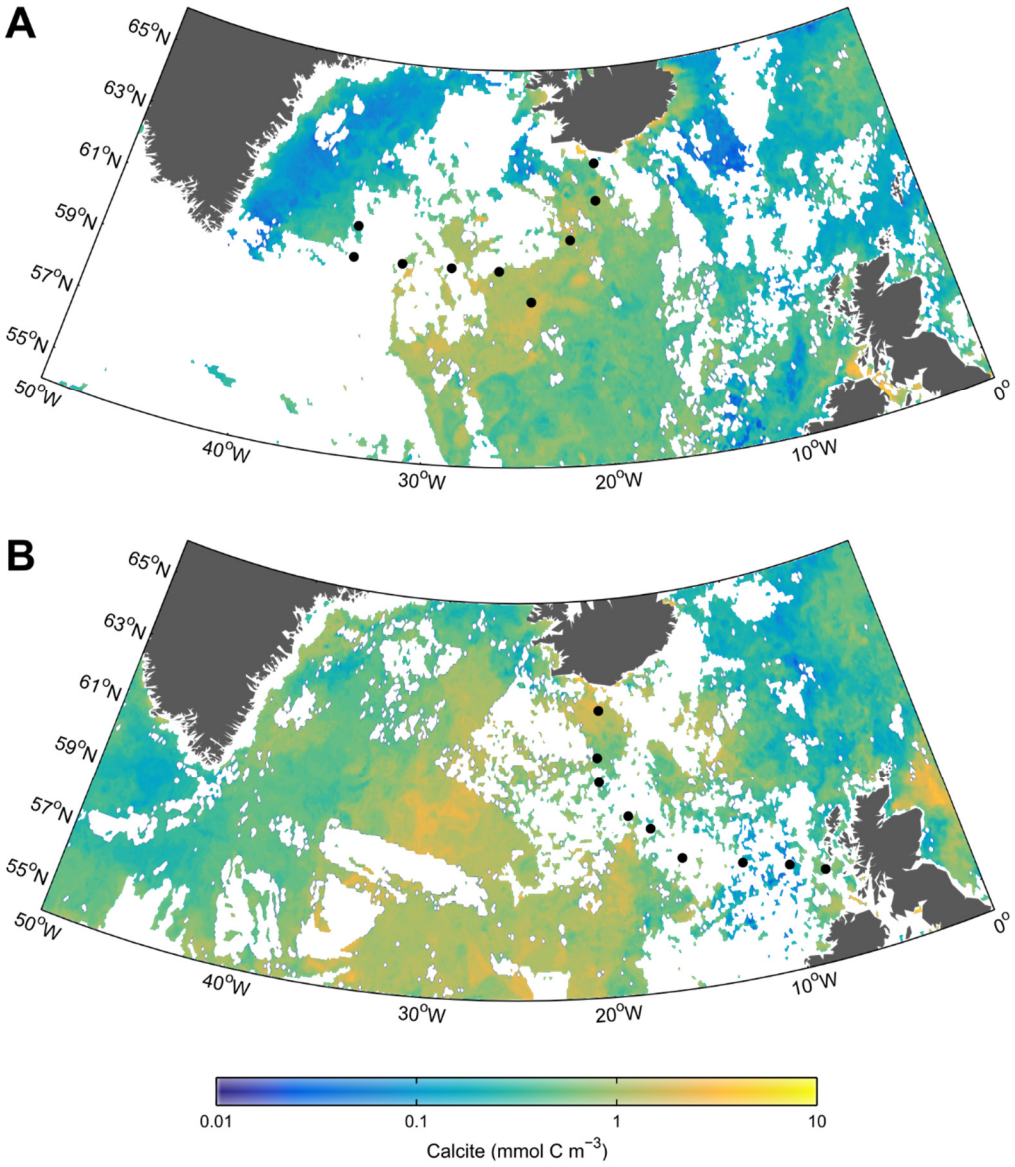

Fig. 5.2: Composites of MODIS particulate inorganic carbon during the period of the cruises A) D350 and B) D351, with station positions superimposed.

Table 5.4 Species-specific contribution to coccolithophore calcite (%) for cruise D351

Station	Species-specific contribution to coccolithophore calcite (%)																		
	Acanthoica quattrospina / Anacanthoica acanthos	*Algirosphaera robusta*	*Alisphaera unicornis*	*Calcidiscus leptoporus*	*Calcidiscus leptoporus* HOL	*Calciopappus caudatus*	*Coccolithus pelagicus*	*Coccolithus pelagicus* HOL	*Coronosphaera mediterranea*	*Coronosphaera mediterranea HOL*	*Emiliania huxleyi*	*Gephyrocapsa muellerae*	*Helicosphaera carteri*	*Michaelsarsia elegans*	*Pontosphaera syracusana*	*Syracosphaera anthos / Syracosphaera corolla*	*Syracosphaera dilatata*	*Syracosphaera pulchra*	*Syracosphaera pulchra* HOL *oblonga*	*Syracosphaera* spp. (small)
4	0.1	0.2	-	0.6	-	0.1	44.1	3.4	1.0	-	47.6	0.9	-	-	-	0.1	0.5	-	-	1.3
10	0.4	0.2	-	-	-	2.3	26.9	9.5	5.5	0.1	24.3	0.9	16.9	-	-	0.3	9.2	-	-	3.3
13	0.1	0.2	-	-	-	2.4	30.2	11.1	11.8	-	17.8	0.3	8.0	-	-	0.4	12.2	-	-	5.6
18	0.3	-	0.1	-	-	1.7	31.6	1.2	2.6	-	51.9	1.4	-	-	-	0.1	6.3	-	-	2.8
22	0.3	0.1	0.1	0.5	-	0.8	10.0	1.2	3.2	-	72.6	1.7	1.2	-	0.5	0.1	3.5	-	-	4.3
27	0.1	-	-	-	-	0.5	91.7	0.2	3.9	-	2.1	0.1	-	-	-	0.1	0.4	0.4	0.1	0.4
34	0.8	-	0.4	-	-	2.4	56.8	0.2	-	-	28.0	0.4	-	-	-	-	0.2	6.8	-	4.1
43	4.3	-	0.4	-	-	-	15.8	-	7.1	-	45.8	15.1	-	-	-	0.5	-	7.6	-	3.4
51	0.9	-	-	-	-	0.3	51.9	2.6	22.5	-	16.0	4.4	-	-	-	-	-	-	-	1.4

Although satellite data indicated a coccolithophore bloom, lower abundances than observed in early spring suggest that the bloom had declined with loose *E. huxleyi* coccoliths causing the satellite to "see" a persisting bloom (Balch et al., 1996b). Therefore, the coccolithophore bloom appears to have occurred alongside the phytoplankton spring bloom. This confirms work by Hopkins et al. (2015) who observed from satellite data that blooms of chlorophyll *a* (phytoplankton) and calcite (coccolithophores) coexisted in the North Atlantic rather than in the traditional theory of succession proposed by Margalef (1978). Furthermore, this has a significant impact when identifying the environmental factors that drive coccolithophore growth, as factors such as high irradiance, shallow mixed layers, high temperatures and reduced grazing (Tyrrell and Merico, 2004; Raitsos et al., 2006) relate to the period in which the highest satellite calcite data are observed. Instead it appears that coccolithophores potentially favour conditions earlier in the season; with lower irradiances, temperatures and when grazing may not be as limiting a factor, such as observed in the early spring bloom in Chapter 3. While the exact factors driving coccolithophore growth cannot be determined here, it demonstrates the lack of knowledge about coccolithophore growth and calcite production in the open ocean. It is likely that calcite production was higher in the spring bloom rather than during the satellite detected "coccolithophore bloom". However, during this transitional period it appears that *C. pelagicus* and *E. huxleyi* remain the major sources of calcite.

5.3.4 Calcite production in summer

The 2007 late summer (July – August) coccolithophore community in the Iceland Basin was dominated by *E. huxleyi* (92 – 98 % abundance), with other species (~20) present in only low relative abundances (Poulton et al., 2010). In contrast, the coccolithophore community in the Iceland and Irminger Basins in the summer (July) of 2010 was not dominated by *E. huxleyi*, which formed only 1 – 43 % of the total coccolithophore abundance (Appendix Table C.4). Abundances (24 – 1030 cells mL^{-1}) were higher than in late spring, with high abundances of holococcolithophores (e.g. *Calyptrolithophora papillifera*, *Calcidiscus leptoporus ssp. leptoporus* HOL and *C. pelagicus* HOL) and small

(< 10 µm) species of *Syracosphaera* (e.g. *Syracosphaera bannockii*, *Syracosphaera marginaporata*, *Syracosphaera molischii* and *Syracosphaera ossa*).

The phytoplankton bloom in 2010 was unusual in that it was much more intense than previously reported (Henson et al., 2013). The Irminger Basin experienced both the potentially iron fertilising tephra fallout from the eruption of the Eyjafjallajökull volcano in Iceland in April/May 2010, and an extremely negative North Atlantic Oscillation in the 2009/2010 winter (Henson et al., 2013). Therefore 2010 may represent an atypical coccolithophore community and its evolution. However, the fact that the community structures in 2010 and 2012 were similar in both spring (D350/D351 and Chapter 3 respectively) and in summer (D354 and Chapter 4 respectively) suggests that this unusual bloom may not have altered the coccolithophore composition. In contrast to 2010, the 2007 late summer phytoplankton community was iron limited (Nielsdóttir et al., 2009; Ryan-Keogh et al., 2013), which may have influenced the coccolithophore community structure (Poulton et al., 2010).

Coccolithus pelagicus was still present and was the major source of calcite in 7 out of 11 stations in late summer, such that *C. pelagicus* remained the major calcifier throughout the different seasons (Table 5.5). Of the other species, *E. huxleyi* was a significant but smaller contributor (12 – 27 %), with significant contributions (18 – 49 %) from the small *Syracosphaera* species. The importance of *Syracosphaera* spp. as a calcite producer was also observed in Chapter 4 where 19 % of the Iceland Basin calcite production was attributed to *Syracosphaera* spp. Furthermore, Poulton et al. (2010) attributed 11 – 32 % of the late summer calcite to a combination of *Syracosphaera molischii*, *Syracosphaera pulchra* and *C. pelagicus* (Poulton, unpub.). While small species of *Syracosphaera* are not heavily calcified (cell calcite estimated to be < 0.4 pmol C cell^{-1}), their relative abundance means they may be major contributors to calcite production. This was observed by Daniels et al. (2014b)(see Appendix D) who as part of a multi-year survey of coccolithophores in the Bay of Biscay identified a bloom (~ 400 cells mL^{-1}) of *S. bannockii* in April 2010, which dominated the coccolithophore community. While *S. bannockii* cellular calcite was estimated to be lower (0.19 pmol

Table 5.5 Species-specific contribution to coccolithophore calcite (%) for cruise D354

Station	Species-specific contribution to coccolithophore calcite (%)																						
	Acanthoica quattrospina / Anacanthoica acanthos	*Algirosphaera robusta*	*Alisphaera unicornis*	*Calcidiscus leptoporus* HOL	*Calciopappus caudatus*	*Calyptrolithina divergens*	*Calyptrolithophora papillifera*	*Coccolithus pelagicus*	*Coccolithus pelagicus* HOL	*Corisphaera gracilis*	*Coronosphaera mediterranea*	*Coronosphaera mediterranea* HOL	*Emiliania huxleyi*	*Gephyrocapsa muellerae*	*Ophiaster formosus*	*Papposphaera* sp.	*Rhabdosphaera clavigera*	*Rhabdosphaera xiphos*	*Syracosphaera anthos / Syracosphaera corolla*	*Syracosphaera dilatata*	*Syracosphaera pulchra*	*Syracosphaera pulchra* HOL *oblonga*	*Syracosphaera* spp. (small)	*Unknown* HOL
4	0.4	0.6	0.3	-	1.2	5.4	-	42.1	-	-	-	-	12.2	3.5	-	-	1.5	-	1.2	-	4.9	-	26.6	-
6	0.5	-	0.1	-	1.0	-	6.4	28.0	2.1	0.1	6.1	2.9	15.8	2.4	0.3	0.2	2.0	0.6	0.4	0.5	9.8	-	20.6	-
12	4.8	-	0.2	-	1.3	-	0.7	33.2	6.8	-	-	-	23.3	-	0.1	-	-	0.2	-	0.7	-	-	28.7	-
14	2.8	-	-	2.0	0.2	-	6.0	39.4	6.0	-	-	-	27.0	-	0.2	-	-	-	-	2.8	-	-	13.5	-
17	0.3	0.1	0.1	0.4	2.4	-	11.3	45.9	6.2	0.1	-	-	2.5	-	0.3	-	0.5	-	1.9	3.3	-	-	24.6	-
19	1.6	-	-	1.5	2.4	-	14.3	34.0	4.0	0.1	-	0.2	3.0	-	0.5	-	0.3	-	1.4	3.5	-	-	33.1	-
20	1.7	-	0.1	5.0	2.0	0.4	19.7	3.8	9.8	-	-	1.5	0.9	-	1.0	-	2.4	-	4.8	1.9	-	-	44.9	-
22	1.3	-	0.1	7.7	1.8	-	13.4	7.9	6.9	0.2	-	3.7	1.1	-	1.0	-	2.3	0.1	0.7	2.6	-	-	49.3	-
23	2.2	0.4	0.1	16.1	4.1	-	16.9	15.7	12.1	-	-	1.6	3.8	-	1.7	-	-	0.1	0.9	1.1	-	-	23.2	-
25	2.0	-	-	4.0	1.9	-	4.0	52.3	3.3	-	-	-	4.9	-	0.4	-	-	-	1.1	-	-	0.7	17.9	7.3
26	0.9	-	0.1	4.5	4.0	-	15.9	12.5	5.1	-	-	-	3.8	-	0.5	-	-	0.2	1.5	7.6	-	-	42.7	0.6

cell^{-1}, Daniels et al., 2014b) than *E. huxleyi*, the relatively high abundances implied that *S. bannockii* would be a major source of calcite in this region at this time.

Coccolithus pelagicus was the only heavily calcified species to persist into summer, while *C. mediterranea* and *H. carteri* disappeared. However, the holococcolith (HOL) life cycle stages of these species were present (e.g. *C. pelagicus* HOL, *C. mediterranea* HOL and *C. leptoporus* HOL). Calcite production and the biogeochemical role of holococcolith bearing coccolithophores is poorly understood; using the estimate for *C. pelagicus* HOL cellular calcite (0.78 pmol C cell^{-1}) made in Chapter 4 results in 5 – 41 % of the coccolithophore calcite in late summer deriving from holococcolithophores. While this is poorly constrained, it provides further evidence for the hypothesis made in Chapter 4 that *C. pelagicus* HOL and other holococcolithophores may be important calcite producers.

The role of and transition between the heterococcolith bearing diploid and the holococcolith bearing haploid life-cycle phases of coccolithophores is poorly understood (Young and Henriksen, 2003). The transition may be driven by biotic pressures (Frada et al., 2008; Von Dassow et al., 2014) or the different phases may inhabit different ecological niches (Houdan et al., 2005; Houdan et al., 2006; Frada et al., 2012). For *C. pelagicus*, I observed both spatial variability in the distribution of *C. pelagicus* and *C. pelagicus* HOL, with *C. pelagicus* more prevalent further north in the Arctic (Chapter 4, Fig. 4.3), and seasonal variability with *C. pelagicus* HOL most abundant in the Iceland and Irminger Basins in spring (D350) and late summer (D354). Such variability may suggest that *C. pelagicus* HOL has a wider ecological niche than *C. pelagicus*. Unlike *C. pelagicus*, *Coccolithus pelagicus* HOL appears mixotrophic, able to ingest bacteria and small (< 5µm) cells (Parke and Adams, 1960; Houdan et al., 2006). This may help *C. pelagicus* HOL to overwinter in the harsh environments of the Arctic and North Atlantic (Brand, 1994). However, despite a potentially narrower niche, *C. pelagicus* may be able to grow faster than *C. pelagicus* HOL during optimum blooming conditions (Houdan et al., 2006).

5.3.5 Summary

Coccolithus pelagicus has been observed in the subpolar North Atlantic throughout early spring (April) to late summer (August). When present, it was often the major source of calcite (in 64 % of the samples considered from D350, D351, D354 and M87/1). Species-specific calcite production estimates in Chapter 4 found *C. pelagicus* was the largest single species source of calcite, responsible for 44 % of calcite production in the Iceland Basin in summer. Estimates of calcite production made here from growth rates and cellular calcite measurements in Chapter 3 estimated *C. pelagicus* to be responsible for 58 % of calcite production in the Iceland Basin in early spring. Therefore, across multiple studies and combining several different types of evidence, I have now shown that *C. pelagicus* is a key biogeochemical species in terms of the production of calcite in the North Atlantic.

5.4 Wider implications

The effect of climate change and ocean acidification on the oceans is significant and widespread. During the 20th century, global ocean sea surface temperature increased by 0.74 °C (IPCC, 2007). Ocean acidification is considered irreversible during our lifetimes; it will take tens of thousands of years for ocean chemistry to return to levels prior to the influence of anthropogenic CO_2 emissions (Society, 2005). Coccolithophores, major contributors to pelagic calcite production and export (Ziveri et al., 2007; Broecker and Clark, 2009), are likely to be impacted by both ocean warming and ocean acidification (Society, 2005; Schluter et al., 2014). If coccolithophores are negatively affected by global warming and climate change, this could significantly reduce both the carbonate pump and calcite ballasted carbon export (Klaas and Archer, 2002), impacting the global carbon cycle. *Emiliania huxleyi* is often considered as a globally important, key pelagic calcifier (Winter et al., 2013; Schluter et al., 2014) and as such the majority of research on coccolithophores has focussed on this species (e.g. Iglesias-Rodriguez et al., 2008; Schluter et al., 2014). In this context, that *C. pelagicus* is the major calcifier in the subpolar North Atlantic and the Arctic rather than

E. huxleyi means that to understand the potential impacts of climate change and ocean acidification on coccolithophores in the North Atlantic from a biogeochemical point of view, studies concerning *C. pelagicus* are essential.

While the North Atlantic, with its large and intensive coccolithophore blooms, is a region of interest for coccolithophore research, coccolithophores are abundant throughout the oceans. With a distribution confined to the Arctic and sub-arctic, (Mcintyre and Bé, 1967; Mcintyre et al., 1970), *C. pelagicus* will not dominate calcite production in other regions. In Chapter 2, the potential for *Coccolithus braarudii*, the temperate sister species of *C. pelagicus* (Baumann et al., 2000b; Cachao and Moita, 2000), to dominate calcite production was demonstrated, yet this species also has a limited range (Giraudeau et al., 1993; Cachao and Moita, 2000; Ziveri et al., 2004) and is unlikely to be a major calcite producer on a global scale.

Other similar relatively heavily calcified species, such as *Calcidiscus leptoporus*, *Helicosphaera carteri* and *Gephyrocapsa oceanica* are more widely distributed (Ziveri et al., 2004) and thus may dominate calcite production in other regions (Ziveri et al., 2007). It is possible that while *E. huxleyi* is globally distributed, on a regional scale a heavily calcified coccolithophore species will dominate calcite production rather than a weakly calcified but abundant species. Therefore, although no one species would dominate global calcite production, *E. huxleyi* is most likely only a small contributor to global calcite production.

One area of research not considered here is the effect of species composition on the ratio of PIC to POC production. Production of POC is a sink of CO_2 while PIC production is a source. The ratio of PIC:POC production therefore will influence whether an individual coccolithophore will behave as a source or sink of CO_2. Furthermore, this will also affect the ratio of PIC:POC in exported material, potentially influencing how much of the material will be exported to depth (Sanders et al., 2010; Hutchins, 2011). More heavily calcified species such as *C. pelagicus* (PIC:POC of 1.2, Chapter 2) and *C. leptoporus* (PIC:POC of ~2, Langer et al., 2006) have a higher PIC:POC than *E. huxleyi* (PIC:POC of ~0.7 when nutrients are replete, Chapter 2), thus these species have a greater potential to impact on air-sea CO_2 exchange.

Beyond the potential influence of heavily calcified species, this study has also demonstrated the potential impact of other less heavily calcified species, such as holococcolithophores and species of *Syracosphaera*. The physiology, ecology and biogeography of these species are poorly understood, yet *Syracosphaera* species have been shown to frequently numerically dominate the coccolithophore community (Leblanc et al., 2009; Daniels et al., 2014b). Therefore, while this study focussed on understanding the key biogeochemical role that *C. pelagicus* plays, it has also demonstrated the need to consider the entire coccolithophore community when considering calcite production, and the role that different species play in producing calcite.

5.5 Limitations and future directions

This study has combined both field observations and laboratory culture experiments in an attempt to understand the biogeochemical role of *C. pelagicus*. This approach has the advantage of combining the benefits of culturing – a precisely controlled environment in which to study individual species, with field studies – natural mixed-species populations of coccolithophores from which in situ observations can be made.

However, as with all studies, there are limitations. Here, the main weakness is that calcite production by *C. pelagicus* cannot be measured directly in situ. To derive species-specific calcite production, estimates of growth rates and cellular calcite, and assumptions that cells are at steady state in terms of the cellular quota (Leynaert et al., 2001) are required. To mitigate these limitations, culture experiments (Chapter 2) were used to constrain growth rates and cellular calcite. However cultures were performed in nutrient replete conditions and the effect of nutrient limitation was not assessed in terms of growth rates and cell calcite.

Cellular variability in *C. pelagicus* and declining growth rates through the onset of a nutrient limiting early stationary phase was examined by Gibbs et al. (2013); through a combination of fossil, culture and field data, a cellular geometry framework was constructed to describe the growth response of coccolithophores. This suggested that

the cellular calcite content of *C. pelagicus* increases under decreased growth rates, with larger cells in the early spring (D350) and late summer. The impact of this on calcite production is currently unclear; while an increased cellular calcite would increase calcite production, decreased growth rates would reduce calcite production rates. However, through using both estimates of cellular calcite from samples and either calcite production rates or growth rates, the cellular variability of *C. pelagicus* should be taken into account when determining species-specific calcite production.

The effect of varying growth rates and cellular calcite contents on calcite production was considered in Chapter 2, while a robustness test on the effect of growth rate variability was performed in Chapter 4. Although this determined that the conclusion that *C. pelagicus* is a key calcifier is robust, significant limitations still remain in the lack of knowledge concerning other species of coccolithophore. With most species not in culture, detailed studies of growth rate and cellular calcite cannot be easily performed. Of those species in culture, few studies have considered those species that this study suggests could be major calcifiers, such as *C. pelagicus*, *C. leptoporus* and *H. carteri*.

Despite these uncertainties, the findings in this thesis demonstrate the importance of *C. pelagicus* as a biogeochemically key calcifier in the North Atlantic and Arctic, and highlight the potential importance of a diverse range of coccolithophore species as potentially important calcite producers. To further understand the role of individual species of coccolithophores in calcite production, the approach of determining species-specific calcite production should be applied to other coccolithophore communities in different locations and environments in the ocean, including more field observations of communities and the isolation and culture of new strains and species of coccolithophore. This will allow for a more global understanding of the key calcite producers and thus a better understanding of how calcite production by coccolithophores will respond in the future as the oceans change.

Appendices

Appendix A: Supplementary data for Chapter 2

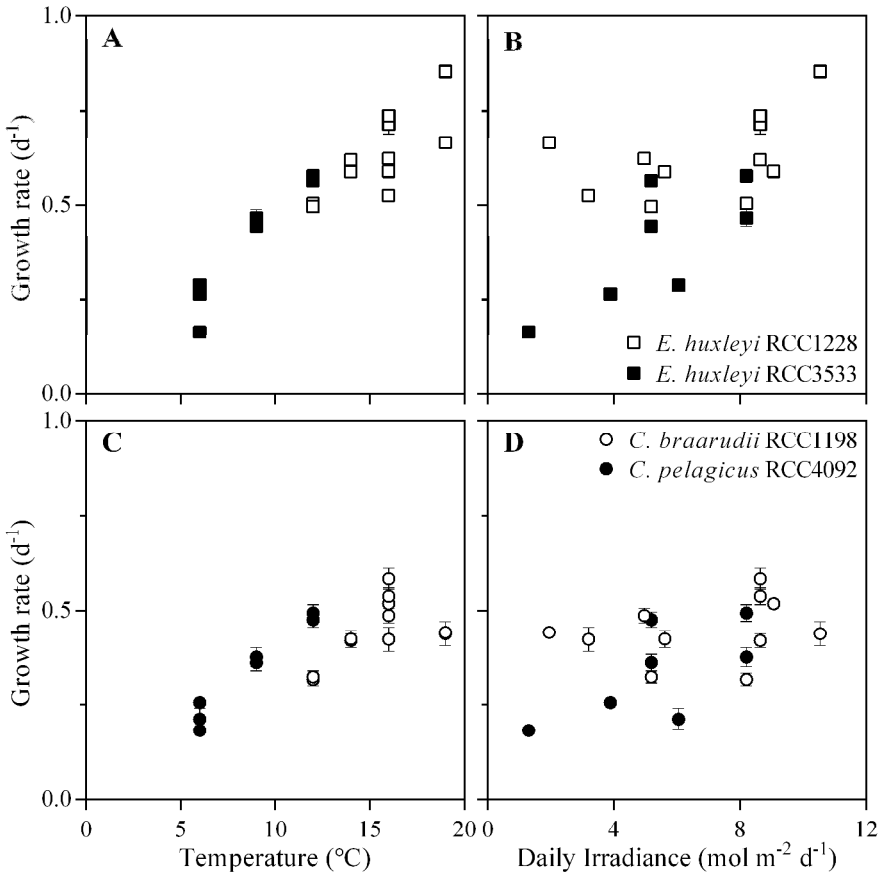

Fig. A.1: Growth rates of A,B) *Emiliania huxleyi* RCC1228 and RCC3533, and C,D) *Coccolithus pelagicus* RCC4092 and *Coccolithus braarudii* RCC1198, against A,C) temperature and B,D) daily irradiance. Error bars are ± 1 standard deviation.

Table A.1: Stations locations and the corresponding abundances (cells mL^{-1}) of *Emiliania huxleyi* and *Coccolithus pelagicus* for three cruises, D350, D351 and D354.

			Coccolithophore abundance (cells mL^{-1})	
Cruise	Latitude (°N)	Longitude (°W)	*E. huxleyi*	*C. pelagicus*
D350	59.01	24.20	68.5	0.4
(26/4 – 9/5)	60.97	34.95	153.0	25.7
	60.02	34.96	171.3	13.5
	60.00	31.98	585.5	22.7
	59.99	29.00	983.7	74.1
	59.94	26.12	390.4	8.7
	60.85	21.75	178.7	9.3
	62.00	20.00	936.3	32.0
	63.13	19.92	701.8	59.9
D351	62.67	19.69	166.4	5.3
(10/5 – 28/5)	61.25	20.00	48.6	1.8
	60.50	20.00	22.9	1.3
	59.40	18.42	101.4	2.1
	58.95	17.19	307.7	1.4
	57.95	15.58	13.4	20.4
	57.51	12.25	22.8	1.6
	57.15	9.70	11.7	0.1
	56.76	7.83	2.4	0.3
	56.67	6.13	0	0
D354	60.00	19.99	7.0	0
(4/7 – 11/8)	61.82	21.02	22.7	2.7
	60.01	19.98	29.4	3.6
	59.99	23.63	33.3	0
	60.01	28.14	10.7	0
	59.98	41.36	128.3	7.1
	60.00	42.67	10.7	0.5
	62.99	35.00	20.3	2.1
	63.00	35.00	19.9	2.2
	63.00	29.98	9.4	1.3
	60.87	31.53	5.4	1.4
	59.24	34.97	7.5	2.1
	58.14	34.98	11.8	3.2
	63.82	35.04	9.6	1.1
	63.82	35.09	5.3	0
	62.48	28.36	0	0
	63.43	23.59	10.7	0
	62.14	24.35	2.1	0

Appendix B: Supplementary data for Chapter 4

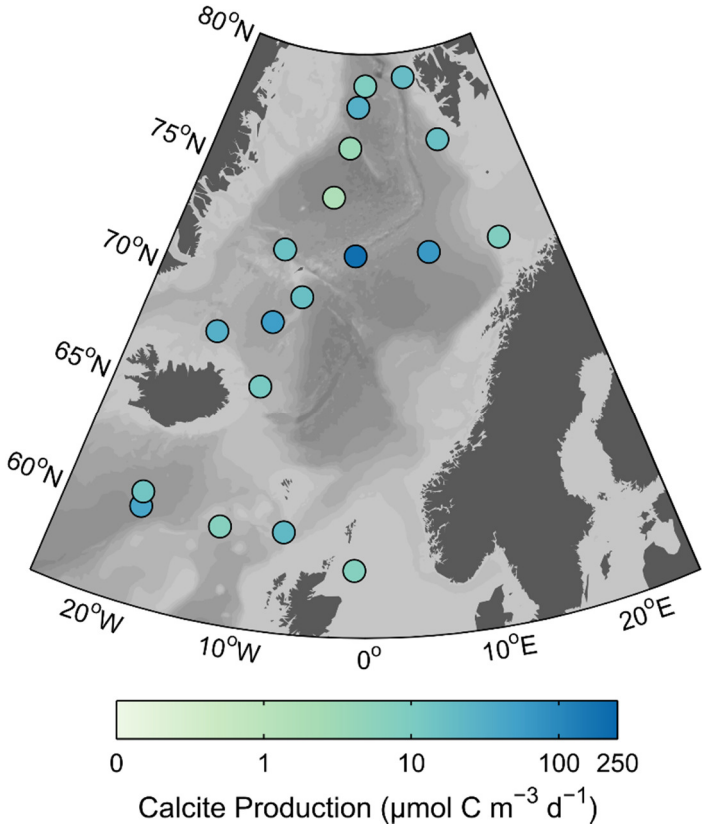

Fig. B.1: The distribution of total calcite production (µmol C m^{-3} d^{-1}).

Appendix C: Supplementary data for Chapter 5

Table C.1: Total calcite production, *Emiliania huxleyi* morphotype-specific calcite production, and species-specific calcite production in early spring (cruise M87/1)

Location	`	Total Calcite Production (µmol C m^{-3} d^{-1})	*E. huxleyi* morphotype-specific calcite production (µmol C m^{-3} d^{-1})			Species-specific calcite production (µmol C m^{-3} d^{-1})			
			E. huxleyi A	*E. huxleyi* B	*E. huxleyi* A over-calcified	Total *E. huxleyi*	*C. pelagicus*	*A. robusta*	*C. caudatus*
ICB	1	0.43	0.08	0.02	0.11	0.22	0.22	-	-
	1	0.40	0.08	0.02	-	0.09	0.31	-	-
	2	0.42	0.06	0.05	0.05	0.16	0.26	-	-
	2	0.37	0.11	0.02	0.02	0.15	0.22	-	-
	3	0.90	0.18	0.06	0.34	0.59	0.31	-	-
	3	1.75	0.21	0.09	0.48	0.78	0.97	-	-
	4	2.08	0.30	0.06	0.58	0.94	1.14	-	-
	4	1.59	0.17	0.07	0.17	0.40	1.19	-	-
	1	0.45	0.11	-	0.04	0.15	0.25	0.03	0.01
NWB	1	1.16	0.08	0.11	0.12	0.31	0.76	0.09	0.00
	2	1.52	0.18	0.06	0.12	0.37	1.10	0.05	0.00
	2	1.77	0.24	0.08	0.18	0.51	1.02	0.23	0.01
	3	8.89	0.41	0.33	0.26	1.00	7.19	0.63	0.07
	3	9.53	0.35	0.32	0.46	1.13	7.56	0.80	0.04

Table C.2: Coccolithophore abundances (cells mL^{-1}) for cruise D350

Station	Coccolithophore abundance (cells mL^{-1})																				
	Acanthoica quattrospina	*Algirophaera robusta*	*Anacanthoica acanthos*	*Calcidiscus leptoporus*	*Calcidiscus leptoporus* HOL	*Calciopappus caudatus*	*Coccolithus pelagicus*	*Coccolithus pelagicus* HOL	*Coronosphaera mediterranea*	*Emiliania huxleyi*	*Gephyrocapsa muellerae*	*Helicosphaera carteri*	*Oolithus fragilis*	*Syracosphaera anthos*	*Syracosphaera bannockii*	*Syracosphaera borealis*	*Syracosphaera corolla*	*Syracosphaera marginaporata*	*Syracosphaera molischii*	*Syracosphaera noroitica*	*Syracosphaera* sp.	*Syracosphaera tumularis*
1	0.4	0.9	1.3	1.3	0.4	11.9	0.4	138.3	7.5	68.5	0.4	3.1	-	0.4	-	-	1.3	-	1.3	0.4	-	6.2
3	0.9	-	0.9	-	-	-	25.7	12.2	-	153	-	-	-	-	-	0.9	-	-	1.3	-	-	-
5	3.1	-	-	-	-	33.6	13.5	32.3	-	171.3	0.9	-	-	-	0.4	1.3	-	10.9	-	-	0.9	2.2
6	1.3	0.4	1.7	1.3	-	27	22.7	176.1	2.6	585.5	-	0.4	-	-	0.4	13.9	0.4	1.3	5.2	-	4.4	13.5
8	7	-	-	0.4	-	7.8	74.1	92	3.9	983.7	1.7	-	-	-	-	1.3	-	-	7.4	-	-	13.9
11	1.1	-	-	-	-	-	8.7	58.6	5.4	390.4	-	1.1	-	-	-	-	-	-	-	-	1.1	-
13	-	-	-	-	-	3.7	9.3	-	-	178.7	-	-	-	-	-	-	-	-	-	-	3.1	-
15	1.2	-	4.1	-	-	2.3	32	121.5	9.3	936.3	8.1	-	1.2	1.7	-	2.3	-	4.6	14.5	-	5.8	19.8
17	2.9	2.3	-	-	-	19.8	59.9	25	-	701.8	12.2	-	-	-	-	1.2	-	22.1	6.4	-	-	5.2

Table C.3: Coccolithophore abundances (cells mL^{-1}) for cruise D351

Station	Coccolithophore abundance (cells mL^{-1})																												
	Acanthoica quattrospina	*Algirosphaera robusta*	*Alisphaera unicornis*	*C. mediterranea* HOL	*Calcidiscus leptoporus*	*Calcidiscus leptoporus* HOL	*Calciopappus caudatus*	*Coccolithus pelagicus*	*Coccolithus pelagicus* HOL	*Coronosphaera mediterranea*	*Emiliania huxleyi*	*Gephyrocapsa muellerae*	*Helicosphaera carteri*	*Michaelsarsia elegans*	*Pontosphaera syracusana*	*Syracosphaera anthos*	*Syracosphaera bannockii*	*Syracosphaera corolla*	*Syracosphaera dilatata*	*Syracosphaera marginaporata*	*Syracosphaera molischii*	*Syracosphaera nana*	*Syracosphaera nodosa*	*Syracosphaera noroitica*	*Syracosphaera ossa*	*Syracosphaera pulchra*	*Syracosphaera pulchra* HOL *oblonga*	*Syracosphaera* sp.	*Syracosphaera tumularis*
4	0.7	0.7	-	-	0.1	-	2.3	5.3	8	0.3	166	1.3	-	-	-	0.1	-	0.3	1.7	1.3	2.9	-	0.1	0.1	-	-	-	0.3	1.3
10	1.6	0.4	0.3	0.1	-	-	25.9	1.8	12.8	0.9	48.6	0.7	0.9	-	-	0.3	-	0.4	17.6	0.1	6.2	-	0.3	0.3	1.0	-	-	0.1	0.6
13	0.3	0.3	0.1	-	-	-	17.2	1.3	9.5	1.2	22.9	0.1	0.3	-	-	-	1.3	0.5	15	0.4	4.4	0.1	-	-	2.9	-	-	-	0.1
18	0.9	-	1.4	-	-	-	18.4	2.1	1.6	0.4	101.0	1.1	-	-	-	0.1	-	-	11.8	-	6.0	-	-	0.1	1.1	-	-	-	-
22	2.3	0.4	2.4	-	0.1	0.1	18.2	1.4	3.5	1.1	308.0	2.9	0.1	0.1	0.1	0.1	0.9	0.1	14.1	1.3	19.7	-	-	-	1.7	-	-	-	-
27	1.3	-	3.1	-	-	0.1	19.4	20.4	0.8	2.0	13.4	0.3	-	-	-	0.7	-	0.1	2.3	1.6	1.5	-	-	0.1	-	0.4	0.3	-	0.3
34	1.2	-	3.2	-	-	-	10.6	1.6	0.1	-	22.8	0.1	-	-	-	-	0.1	-	0.1	3.1	0.9	-	-	-	-	0.8	-	0.1	-
43	2.1	-	1.1	-	-	-	-	0.1	-	0.1	11.7	1.6	-	-	-	0.1	-	-	-	-	1.0	-	-	-	-	0.3	-	0.1	-
51	0.3	-	-	-	-	-	0.3	0.3	0.3	0.3	2.4	0.3	-	-	-	-	-	-	-	-	0.3	-	-	-	-	-	-	-	-

Table C.4: Coccolithophore abundances (cells mL^{-1}) for cruise D354

Station	Coccolithophore abundance (cells mL^{-1})																											
	Acanthoica quattrospina	*Algirosphaera robusta*	*Alisphaera unicornis*	*Calcidiscus leptoporus* HOL	*Calciopappus* sp.	*Calyptrolithina divergens*	*Calyptrolithophora papillifera*	*Coccolithus pelagicus*	*Coccolithus pelagicus* HOL	*Corisphaera gracilis*	*Coronosphaera mediterranea*	*Coronosphaera mediterranea* HOL	*Emiliania huxleyi*	*Gephyrocapsa muellerae*	*Ophiaster formosus*	*Papposphaera* sp.	*Rhabdosphaera clavigera*	*Rhabdosphaera xiphos*	*Syracosphaera bannockii*	*Syracosphaera corolla*	*Syracosphaera dilatata*	*Syracosphaera marginaporata*	*Syracosphaera molischii*	*Syracosphaera ossa*	*Syracosphaera pulchra*	*Syracosphaera pulchra* HOL *oblonga*	*Syracosphaera* sp.	*Syracosphaera tumularis*	*Unknown* HOL
4	1.3	1.3	6.7	-	12.0	6.7	-	-	2.7	-	-	-	22.7	2.7	-	-	1.3	-	-	2.7	-	14.7	20.0	12.0	1.3	-	17.4	-	-
6	1.8	-	2.7	-	9.8	-	8.0	2.7	3.6	3.6	0.9	3.6	29.4	1.8	3.6	1.8	1.8	4.5	6.2	0.9	0.9	7.1	13.4	5.3	2.7	-	17.8	-	-
12	50.8	-	13.4	-	41.0	-	2.7	24.9	7.1	-	-	-	128.0	-	3.6	-	-	3.6	14.3	-	3.6	140.0	18.7	27.6	-	-	4.5	-	-
14	2.1	-	-	0.5	0.5	-	1.6	1.6	0.5	-	-	-	10.7	-	0.5	-	-	-	0.5	-	1.1	3.7	1.6	1.1	-	-	-	-	-
17	5.3	1.1	4.3	2.1	109.0	-	62.0	34.2	2.1	6.4	-	-	20.3	-	15.0	1.1	2.1	1.1	36.3	18.2	25.7	124.0	37.4	53.4	-	-	10.7	-	-
19	21.0	-	2.2	6.6	88.3	-	64.0	17.7	2.2	6.6	-	1.1	19.9	-	18.8	-	1.1	1.1	45.2	11.0	22.1	108.0	55.2	69.5	-	-	4.4	4.4	-
20	34.7	-	6.7	34.7	112.2	2.7	136.3	68.1	1.3	2.7	-	10.7	9.4	-	64.1	1.3	12.0	-	150.0	58.8	18.7	164.0	106.0	166.0	-	-	20.0	-	-
22	12.2	-	2.7	25.7	50.1	-	44.7	23.0	1.4	16.2	-	12.2	5.4	-	29.8	-	5.4	1.4	115.0	4.1	12.2	27.1	114.0	55.5	-	-	8.1	-	-
23	8.6	1.1	1.1	21.4	44.9	-	22.4	16.0	2.1	1.1	-	2.1	7.5	-	20.3	-	-	1.1	25.7	2.1	2.1	6.4	20.3	4.3	-	-	3.2	-	-
25	3.2	-	-	6.4	25.7	-	6.4	5.3	3.2	1.1	-	-	11.8	-	5.3	-	-	-	21.4	3.2	-	4.3	19.2	5.3	-	1.1	5.3	-	11.8
26	4.3	-	3.2	7.5	55.6	-	26.7	8.6	1.1	1.1	-	-	9.6	-	7.5	-	-	2.1	22.4	4.3	18.2	39.5	17.1	52.4	-	-	6.4	1.1	1.1

Appendix D: Reprint of Daniels et al., 2014, JNR

Reprint of: Daniels, C. J., T. Tyrrell, A. J. Poulton, and J. R. Young. 2014. A mixed life-cycle stage bloom of *Syracosphaera bannockii* (Borsetti and Cati, 1976) Cros et al. 2000 (Bay of Biscay, April 2010). Journal of Nannoplankton Research **34:** 31-35

A mixed life-cycle stage bloom of *Syracosphaera bannockii* (Borsetti and Cati, 1976) Cros et al. 2000 (Bay of Biscay, April 2010)

Chris J. Daniels, Toby Tyrrell
Ocean and Earth Sciences, National Oceanography Centre Southampton, University of Southampton, UK; c.daniels@noc.soton.ac.uk

Alex J. Poulton
Ocean Biogeochemistry and Ecosystems, National Oceanography Centre, University of Southampton Waterfront Campus, UK

Jeremy R. Young
Department of Earth Sciences, University College London, London, UK

Abstract: High concentrations (464 cells ml-1) of *Syracosphaera bannockii* have been identified for the first time, in the Bay of Biscay during April 2010. These high concentrations combined with coccolithophore community dominance (~87%) indicated that a bloom of *S. bannockii* had formed. While the bloom consisted mostly of heterococcolith coccospheres, both holococcolith coccospheres and holococcolith-heterococcolith combination coccospheres were observed. This is only the second time that combination coccospheres of *S. bannockii* have been observed.

Keywords: *Syracosphaera bannockii*, coccolithophore bloom, combination coccospheres,

1. Introduction

Syracosphaera is a large and diverse genus of coccolithophores, and forms a significant proportion of the extant coccolithophore community (Young et al., 2003). Despite this, *Syracosphaera* coccolithophores are poorly understood, with only one species, *Syracosphaera pulchra*, maintained and studied in culture (Geisen et al., 2002; Young et al., 2003; Fiorini et al., 2011). Moreover, *S. pulchra* may not be a typical species of this genus since it is significantly larger (~15μm) and appears more heavily calcified than most *Syracosphaera* species.

As part of a multi-year survey of coccolithophores in the Bay of Biscay (Daniels et al., 2012; Smith et al., 2012), high concentrations of *Syracosphaera bannockii* (Borsetti and Cati, 1976) Cros et al. 2000 were observed on one transect in April 2010 (Daniels et al., 2012). *Syracosphaera bannockii* is a coccolithophore with multiple life-cycle stages: a heterococcolith bearing haploid phase, and a holococcolith bearing diploid phase (Cros et al., 2000; Geisen et al., 2002; Young et al., 2003). It has only been relatively recently described by Cros et al. (2000), from combination coccospheres of the holococcolith *Zygosphaera bannockii* and a previously undescribed *Syracosphaera* heterococcolith. This combination was described as *S. bannockii*, since the genus *Syracosphaera* has priority over *Zygosphaera* (Geisen et al., 2002). While this was the first description of *S. bannockii* heterococcoliths, they are very similar to *Syracosphaera orbiculus* and *Syracosphaera delicata*, and may represent intraspecific variation (Young et al., 2003). Little is known about the biogeographical distribution of *S. bannockii*, but it has been reported in communities in both the North and South Atlantic (Balestra et al., 2004; Boeckel and Baumann, 2008; Poulton et al., 2010; Charalampopoulou et al., 2011). Here we present the first evidence that *S. bannockii* can form relatively high cell densities (>400 cells ml^{-1}), in this case consisting of both the heterococcolith and the holococcolith life-cycle phases.

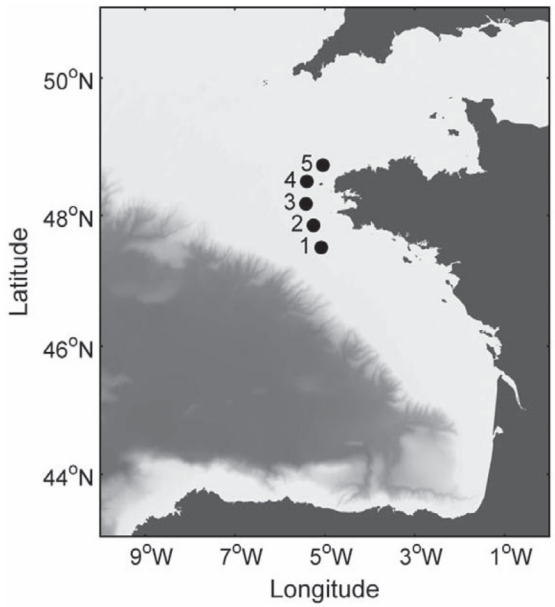

Figure 1. Map of the Bay of Biscay showing the location and station numbers of the 5 stations at which *Syracosphaera bannockii* was found.

2. Material and methods

Samples were collected aboard the MS *Pride of Bilbao* from the Bay of Biscay between 2006 and 2010, with the samples described here collected on the 15th April 2010. Water samples were collected from the ship's seawater intake supply (5m depth) and filtered on to 0.8 μm polycarbonate filters. Samples were collected every 4 hours, corresponding to an approximate resolution of 40 km. Further cruise and sampling details are documented in Daniels et al. (2012). The samples were imaged on a Leo 1450VP scanning electron microscope (SEM). Specimens were initially observed on low resolution automatically captured images, to confirm the identification of *S.*

Plate 1

Syracosphaera bannockii. A–C. Heterococcolith coccospheres with both body coccoliths and circum-flagellar coccoliths with spines. D. Heterococcolith coccosphere with a holococcolith coccosphere next to it. E–F. Holococcolith coccospheres. G–I: Combination coccospheres of both heterococcoliths and holococcoliths, surrounded by exothecal coccoliths. All scale bars are 1μm.

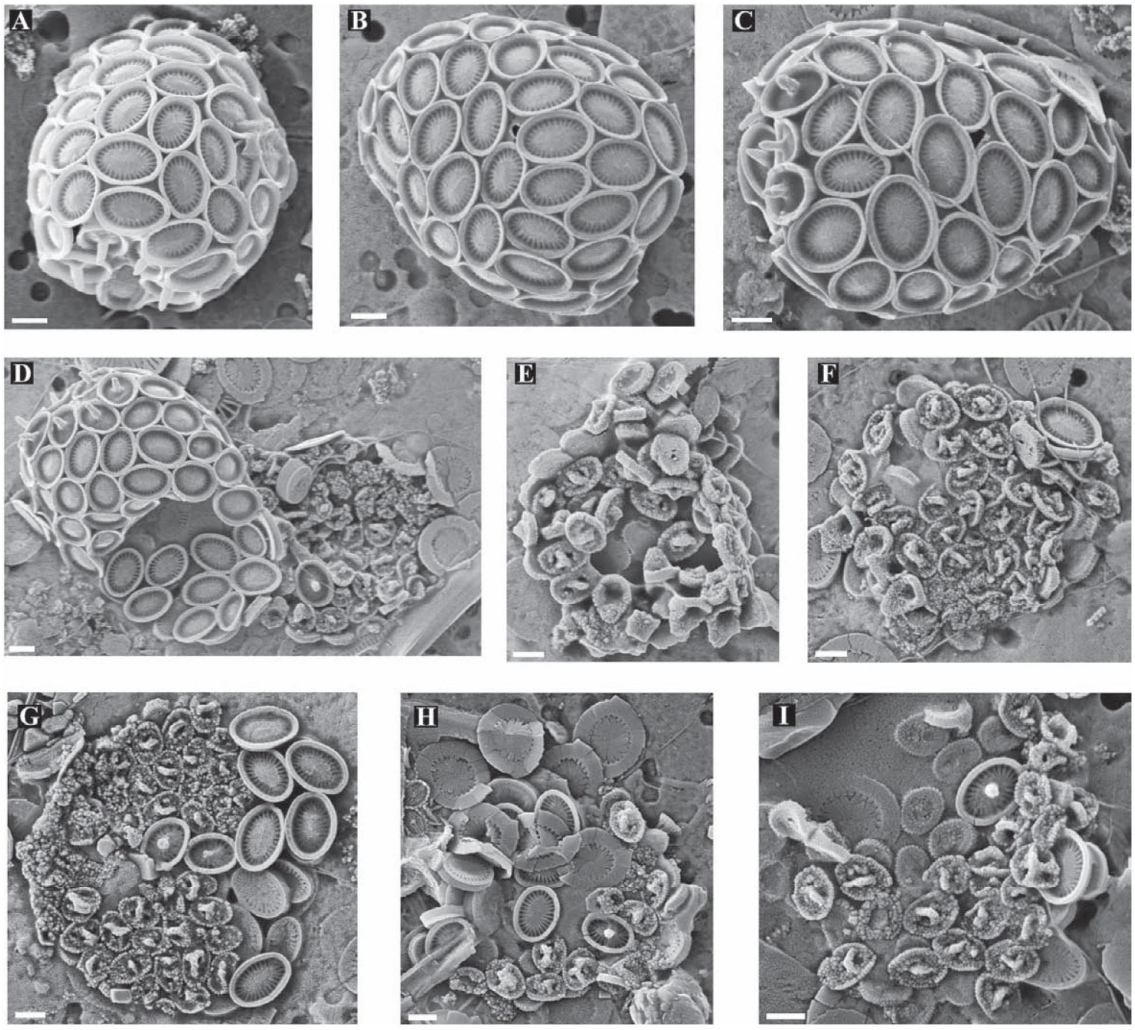

bannockii the sample with the most abundant material was reimaged with manual focussing and image capture. Coccolithophore species were determined following (Young et al., 2003), with cells counted from 225 fields of view (Daniels et al., 2012).

3. A bloom of Syracosphaera bannockii

Analysis of the samples collected in April 2010 identified *S. bannockii* in 5 consecutive samples (Table 1), collected from the Ushant shelf region of the Bay of Biscay (Figure 1), in waters with sea surface temperatures ranging from 10.8–11.1 °C and sea surface salinity 35.0–35.2. Other coccolithophore species observed in relatively low abundances (<37 cells ml^{-1}) in these samples included: *Acanthoica quattrospina*, *Algirosphaera robusta*, *Calciopappus caudatus*, *Coccolithus braarudii* HOL, *Coronosphaera mediterranea*, *Emiliania huxleyi, Pappomonas* sp., *Syracosphaera anthos*, *Syracosphaera molischii*, *Syracosphaera ossa* and *Syracosphaera* sp.

The identification as *S. bannockii* type coccoliths is indicated by the combination of simple murolith body coccoliths and irregular-planolith exothecal coccoliths. Three species are included in this grouping by Young et al. (2003) - *S. bannockii, S. orbiculus* and *S. delicatus*, although it has been suggested that *S. delicatus* is a junior synonym of *S. orbiculus* (Young et al. 2014, Nannotax). The specimens imaged at high resolution (Plate 1) show

Station	Latitude (°N)	Longitude (°W)	S. bannockii (cells ml^{-1})	Life-cycle stage contribution (%)		
				HET	HOL	combination
1	47.52	5.08	8	93	0	7
2	47.85	5.25	464	92	4	4
3	48.17	5.42	369	97	2	1
4	48.50	5.40	88	99	1	0
5	48.74	5.04	16	100	0	0

Table 1. Station locations and the abundance of *Syracosphaera bannockii*, with the percentage contribution from coccospheres of different life-cycle stages. HET – heterococcolith coccospheres. HOL – holococcolith coccospheres. combination – holococcolith-heterococcolith combination coccospheres.

broad rims on the body coccoliths and the exothecal coccoliths do not have ridges, these characteristics indicate that they are *S. bannockii*. There was no evidence from lower resolution images that there was any significant morphological variation within the species. The associated holococcoliths show variable development of a central opening but this variation was previously noted within *S. bannockii* holococcoliths (Cros et al. 2000, Young et al. 2003).

Although *S. bannockii* has been observed in different areas of the North Atlantic (Balestra et al., 2004; Poulton et al., 2010; Charalampopoulou et al., 2011), it has never been reported to dominate the coccolithophore assemblage. Here we observed that in samples 2–4 (Table 1), *S. bannockii* dominated the coccolithophore community with particularly high abundances in samples 2 (464 cells ml^{-1}) and 3 (369 cells ml^{-1}). While these abundances are below the arbitrary 1000 cells ml^{-1} threshold sometimes used to define an *E. huxleyi* bloom (Tyrrell and Merico, 2004), the significant abundances combined with the fact that *S. bannockii* formed ~87% of the total coccolithophore assemblage, suggests that this can be defined as a bloom of *S. bannockii*. Very few coccolithophorids other than *E. huxleyi* have been reported to form blooms; *C. pelagicus* (Milliman, 1980; Tarran et al., 2001) and *Gephyrocapsa oceanica* (Blackburn and Cresswell, 1993) have both been observed in high concentrations (>1000 cells ml^{-1}), while a coccolithophore bloom in southern Benguela waters was attributed to *Syracosphaera pulchra* (Weeks et al., 2003). Therefore we believe that this is the first report of a bloom of *S. bannockii* or any small species of *Syracosphaera*.

Emiliania huxleyi blooms have been observed across multiple years in the Bay of Biscay (Harlay et al., 2010; Harlay et al., 2011; Daniels et al., 2012). However, these blooms occur later in the season (May – June) than this *S. bannockii* bloom, with the 2010 *E. huxleyi* bloom observed in May (Daniels et al., 2012). For high net growth rates associated with bloom formation, conditions must be favourable for high gross growth rates of *S. bannockii*, while mortality through viral lysis or grazing must be low. Factors associated with high *E. huxleyi* abundance include high irradiance, shallow mixed layers, high temperatures and low grazing pressure (Tyrrell and Merico, 2004; Raitsos et al., 2006). However, whilst *S. bannockii* remains absent in culture collections, it is difficult to examine the physiology of this species or the environmental factors which favour faster growth of this species relative to other more renowned bloom forming species (e.g. *E. huxleyi*).

Estimating the areal extent of this bloom from a single transect requires the assumption of a circular distribution and interpolation between samples. With the highest concentrations measured ~40km apart, and lower but significant concentrations spanning a further ~120km, this suggests that the central bloom covered ~1250 km^2, with lower abundances in the surrounding ~18000km^2. While these estimates carry a significant uncertainty, they suggest a bloom of significant magnitude.

The biogeochemical impact of this bloom cannot be easily assessed as we know so little about *S. bannockii*, however using measurements of heterococcolith cellular geometry from SEM images, we can estimate cellular calcite (Young and Ziveri, 2000). Cells of *S. bannockii* had on average, 45 – 46 coccoliths per cell, with an average coccolith length of 2.2 μm. Using a "small *Syracosphaera*" shape factor from Young and Ziveri (2000), we estimate a cellular calcite value of 0.19 pmol C cell^{-1}, which is around half of that found in a (nutrient replete) *E. huxleyi* cell (0.39 – 0.49 pmol C cell^{-1}, Poulton et al., 2010; Daniels et al., 2014). This is a significantly smaller source of calcite, particularly as higher abundances of *E. huxleyi* have been observed in the Bay of Biscay (1000 – 8000 cells mL^{-1}, Harlay et al., 2010; Daniels et al., 2012). However, in terms of its contribution towards standing stocks of organic carbon and chlorophyll *a*, *S. bannockii* is ~8 times larger (~400 μm^3) in terms of cell volume (and hence cellular carbon/chlorophyll content, see Daniels et al., 2014) than *E. huxleyi* (50 μm^3), and on a species-specific level is therefore a potentially more important contributor to primary production and the biological carbon pump.

4. Life-cycle stages of Syracosphaera bannockii

The bloom of *S. bannockii* was comprised of both life-cycle stages. The majority (92 – 100 %) of coccospheres were formed only of heterococcoliths (Plate 1A–D) with an average coccosphere diameter of 9.3 μm (6.9 – 11.9 μm). However, coccospheres formed only of holococcoliths (Plate 1D–F) and combination coccospheres of both heterococcoliths and holococcoliths (Plate 1G–I) were also observed. Combination coccospheres and holococcolith coccospheres were generally collapsed, thus cell size was not measured. Detached exothecal coccoliths of *S. bannockii* (Young et al., 2003) were also found in the samples. The abundance of holococcolith-heterococcolith combination coccospheres observed here confirm the decision by Cros et al. (2000) to describe *S. bannockii* as a single species with multiple life-cycle stages.

The holococcolith bearing diploid life-cycle stage of coccolithophores is generally poorly understood, although it has been suggested that multiple life cycle stages allows for adaptation to different nutrient conditions (Houdan et al., 2006) or to escape viral infection (Frada et al., 2008). That both life-cycle stages are present here suggest that the two stages may have similar ecologies and are both blooming at the same time, or perhaps that a bloom of *S. bannockii* HET is terminating and they are changing into their diploid holococcolith bearing stage to adapt to lower nutrient conditions (Houdan et al., 2006). Without further evidence, this question cannot be answered within this study.

5. Conclusion

A mixed bloom of *S. bannockii*, containing heterococcolith and holococcolith coccospheres, as well as holococcolith-heterococcolith combination coccospheres, was observed in multiple samples in the Bay of Biscay. This is the first time a bloom of *S. bannockii* has been reported, and provides clear confirmation that the life-cycle stage association described by Cros et al. (2000) is correct.

Acknowledgements

The study in which the samples were collected was funded by the European Project on Ocean Acidification (EPOCA) which received funding from the European Community's Seventh Framework Program (FP7/2007-2013) under grant agreement number 211384. This work was also made possible through funding from the European Union to the integrated project CARBOOCEAN (grant EVK2-CT-2000-00088) and through funding from the Department for Environment, Food and Rural Affairs (Defra) for the Defra pH project. C. J. Daniels was supported by a Natural Environmental Research Council studentship.

References

Balestra, B., Ziveri, P., Monechi, S. & Troelstra, S. 2004. Coccolithophorids from the Southeast Greenland Margin (Northern North Atlantic): Production, ecology and the surface sediment record. *Micropaleontology*, **50**(Suppl 1): 23-34, doi:10.2113/50.Suppl_1.23

Blackburn, S. & Cresswell, G. 1993. A coccolithophorid bloom in Jervis Bay, Australia. *Marine and Freshwater Research*, **44**(2): 253-260, doi:10.1071/MF9930253

Boeckel, B. & Baumann, K.H. 2008. Vertical and lateral variations in coccolithophore community structure across the subtropical frontal zone in the South Atlantic Ocean. *Marine Micropaleontology*, **67**(3-4): 255-273, doi:10.1016/j.marmicro.2008.01.014

Borsetti, A.M. & Cati, F. 1976. I1 Nannoplancton calcareo vivente nel Tirreno Centro-meridionale. Parte II. *Giornale di Geologia*, **40**(1): 209-240

Charalampopoulou, A., Poulton, A.J., Tyrrell, T. & Lucas, M.I. 2011. Irradiance and pH affect coccolithophore community composition on a transect between the North Sea and the Arctic Ocean. *Marine Ecology Progress Series*, **431**: 25-43, doi:10.3354/meps09140

Cros, L., Kleijne, A., Zeltner, A., Billard, C. & Young, J. 2000. New examples of holococcolith–heterococcolith combination coccospheres and their implications for coccolithophorid biology. *Marine Micropaleontology*, **39**(1): 1-34, doi:10.1016/S0377-8398(00)00010-4

Daniels, C.J., Poulton, A.J. & Sheward, R.M. 2014. Biogeochemical implications of comparative growth rates of *Emiliania huxleyi* and *Coccolithus* species. *Biogeosciences Discussions*, **11**: 10513-10536, doi:10.5194/bgd-11-10513-2014

Daniels, C.J., Tyrrell, T., Poulton, A.J. & Pettit, L. 2012. The influence of lithogenic material on particulate inorganic carbon measurements of coccolithophores in the Bay of Biscay. *Limnology and Oceanography*, **57**(1): 145-153, doi:10.4319/lo.2012.57.1.0145

Fiorini, S., Middelburg, J.J. & Gattuso, J.P. 2011. Effects of elevated CO_2 partial pressure and temperature on the coccolithophore *Syracosphaera pulchra*. *Aquatic Microbial Ecology*, **64**: 221-232, doi:10.3354/ame01520

Frada, M., Probert, I., Allen, M.J., Wilson, W.H. & De Vargas, C. 2008. The "Cheshire Cat" escape strategy of the coccolithophore *Emiliania huxleyi* in response to viral infection. *Proceedings of the National Academy of Sciences*, **105**(41): 15944-15949, doi:10.1073/pnas.0807707105

Geisen, M., Billard, C., Broerse, A.T.C., Cros, L., Probert, I. & Young, J.R. 2002. Life-cycle associations involving pairs of holococcolithophorid species: Intraspecific variation or cryptic speciation? *European Journal of Phycology*, **37**(4): 531-550, doi:10.1017}S0967026202003852

Harlay, J., Borges, A.V., Van Der Zee, C., Delille, B., Godoi, R.H.M., Schiettecatte, L.S., Roevros, N., Aerts, K., Lapernat, P.E., Rebreanu, L., Groom, S., Daro, M.H., Van Grieken, R. & Chou, L. 2010. Biogeochemical study of a coccolithophore bloom in the

northern Bay of Biscay (NE Atlantic Ocean) in june 2004. *Progress In Oceanography*, **86**(3–4): 317-336, doi:10.1016/j.pocean.2010.04.029

Harlay, J., Chou, L., De Bodt, C., Van Oostende, N., Piontek, J., Suykens, K., Engel, A., Sabbe, K., Groom, S. & Delille, B. 2011. Biogeochemistry and carbon mass balance of a coccolithophore bloom in the northern Bay of Biscay (June 2006). *Deep Sea Research Part I: Oceanographic Research Papers*, **58**(2): 111-127, doi:10.1016/j.dsr.2010.11.005

Houdan, A., Probert, I., Zatylny, C., Véron, B. & Billard, C. 2006. Ecology of oceanic coccolithophores. I. Nutritional preferences of the two stages in the life cycle of *Coccolithus braarudii* and *Calcidiscus leptoporus*. *Aquatic Microbial Ecology*, **44**(3): 291-301, doi:10.3354/ame044291

Milliman, J.D. 1980. Coccolithophorid production and sedimentation, Rockall Bank. *Deep Sea Research Part A. Oceanographic Research Papers*, **27**(11): 959-963, doi:10.1016/0198-0149(80)90007-2

Poulton, A.J., Charalampopoulou, A., Young, J.R., Tarran, G.A., Lucas, M.I. & Quartly, G.D. 2010. Coccolithophore dynamics in non-bloom conditions during late summer in the central Iceland Basin (July–August 2007). *Limnology and Oceanography*, **55**(4): 1601-1613, doi:10.4319/lo.2010.55.4.1601

Raitsos, D.E., Lavender, S.J., Pradhan, Y., Tyrrell, T., Reid, P.C. & Edwards, M. 2006. Coccolithophore bloom size variation in response to the regional environment of the subarctic North Atlantic. *Limnology and Oceanography*, **51**(5): 2122-2130, doi:10.4319/lo.2006.51.5.2122

Smith, H.E.K., Tyrrell, T., Charalampopoulou, A., Dumousseaud, C., Legge, O.J., Birchenough, S., Pettit, L.R., Garley, R., Hartman, S.E., Hartman, M.C., Sagoo, N., Daniels, C.J., Achterberg, E.P. & Hydes, D.J. 2012. Predominance of heavily calcified coccolithophores at low caco3 saturation during winter in the bay of biscay. *Proceedings of the National Academy of Sciences*, **109**(23): 8845-8849, doi:10.1073/pnas.1117508109

Tarran, G.A., Zubkov, M.V., Sleigh, M.A., Burkill, P.H. & Yallop, M. 2001. Microbial community structure and standing stocks in the NE Atlantic in June and July of 1996. *Deep Sea Research Part II: Topical Studies in Oceanography*, **48**(4–5): 963-985, doi:10.1016/S0967-0645(00)00104-1

Tyrrell, T. & Merico, A. 2004. *Emiliania huxleyi*: bloom observations and the conditions that induce them. *In*: H. R. Thierstein & J. R. Young (Eds.), *Coccolithophores: From Molecular Processes to Global Impact*. Springer-Verlag: 75-90.

Weeks, S.J., Pitcher, G.C. & Bernard, S. 2003. Satellite monitoring of the evolution of a coccolithophorid bloom in the Southern Benguela upwelling system. *Oceanography*, **17**(1): 83-89, doi:10.5670/oceanog.2004.70

Young, J.R., Geisen, M., Cros, L., Kleijne, A., Sprengel, C., Probert, I. & Ostergaard, J. 2003. A guide to extant coccolithophore taxonomy. *Journal of Nannoplankton Research Special Issue*, **1**: 1-132.

Young, J.R. & Ziveri, P. 2000. Calculation of coccolith volume and its use in calibration of carbonate flux estimates. *Deep Sea Research Part II*, **47**(9-11): 1679-1700, doi:10.1016/S0967-0645(00)00003-5.

References

ACIA: Arctic Climate Impact and Assessment, Cambridge, UK, 2004.

Andruleit, H.: Coccolithophore fluxes in the Norwegian-Greenland Sea: Seasonality and assemblage alterations, Marine Micropaleontology, 31, 45-64, doi:10.1016/S0377-8398(96)00055-2, 1997.

Armstrong, R. A., Lee, C., Hedges, J. I., Honjo, S., and Wakeham, S. G.: A new, mechanistic model for organic carbon fluxes in the ocean based on the quantitative association of POC with ballast minerals, Deep Sea Research Part II: Topical Studies in Oceanography, 49, 219-236, doi:10.1016/S0967-0645(01)00101-1, 2001.

Backhaus, J. O., Hegseth, E. N., Wehde, H., Irigoien, X., Hatten, K., and Logemann, K.: Convection and primary production in winter, Marine Ecology Progress Series, 251, 1-14, doi:10.3354/meps251001, 2003.

Baines, S. B., Twining, B. S., Brzezinski, M. A., Nelson, D. M., and Fisher, N. S.: Causes and biogeochemical implications of regional differences in silicification of marine diatoms, Global Biogeochemical Cycles, 24, GB4031, doi:10.1029/2010GB003856, 2010.

Balch, W. M., Kilpatrick, K., Holligan, P. M., and Cucci, T.: Coccolith production and detachment by *Emiliania huxleyi* (Prymnesiophyceae), Journal of Phycology, 29, 566-575, doi:10.1111/j.0022-3646.1993.00566.x, 1993.

Balch, W. M., Kilpatrick, K. A., Holligan, P., Harbour, D., and Fernandez, E.: The 1991 coccolithophore bloom in the central North Atlantic. 2. Relating optics to coccolith concentration, Limnology and Oceanography, 41, 1684-1696, doi:10.4319/lo.1996.41.8.1684, 1996a.

Balch, W. M., Kilpatrick, K. A., and Trees, C. C.: The 1991 coccolithophore bloom in the central North Atlantic. 1. Optical properties and factors affecting their distribution,

Limnology and Oceanography, 41, 1669-1683, doi:10.4319/lo.1996.41.8.1669, 1996b.

Balch, W. M., Drapeau, D. T., and Fritz, J. J.: Monsoonal forcing of calcification in the Arabian Sea, Deep Sea Research Part II, 47, 1301-1337, doi:10.1016/S0967-0645(99)00145-9, 2000.

Balch, W. M.: Re-evaluation of the physiological ecology of coccolithophores. In: Coccolithophores: from molecular processes to global impact, Thierstein, H. R. and Young, J. R. (Eds.), Springer, Berlin, 165-190, 2004.

Balch, W. M. and Utgoff, P. E.: Potential interactions among ocean acidification, coccolithophores, and the optical properties of seawater, Oceanography, 22, 146-159, doi:10.5670/oceanog.2009.104, 2009.

Barber, R. T. and Hiscock, M. R.: A rising tide lifts all phytoplankton: Growth response of other phytoplankton taxa in diatom-dominated blooms, Global Biogeochemical Cycles, 20, GB4S03, doi:10.1029/2006gb002726, 2006.

Baumann, K., Andruleit, H., and Samtleben, C.: Coccolithophores in the Nordic Seas: Comparison of living communities with surface sediment assemblages, Deep Sea Research Part II, 47, 1743-1772, doi:10.1016/S0967-0645(00)00005-9, 2000a.

Baumann, K. H., Young, J. R., Cachao, M., and Ziveri, P.: Biometric study of *Coccolithus pelagicus* and its paleoenvironmental utility, Journal of Nannoplankton Research, 22, 82, 2000b.

Baumann, K. H., Böckel, B., and Frenz, M.: Coccolith contribution to South Atlantic carbonate sedimentation. In: Coccolithophores: from molecular processes to global impact, Thierstein, H. R. and Young, J. R. (Eds.), Springer, Berlin, 367-402, 2004.

Behrenfeld, M. J.: Abandoning Sverdrup's Critical Depth Hypothesis on phytoplankton blooms, Ecology, 91, 977-989, doi:10.1890/09-1207.1, 2010.

Behrenfeld, M. J. and Boss, E. S.: Resurrecting the ecological underpinnings of ocean plankton blooms, Annual Review of Marine Science, 6, 167-194, doi:10.1146/annurev-marine-052913-021325, 2014.

Bellerby, R., Olsen, A., Johannessen, T., and Croot, P.: A high precision continuous spectrophotometric method for seawater pH measurements: The automated marine pH sensor (AMpS), Talanta, 56, 61-69, doi:10.1016/S0039-9140(01)00541-0, 2002.

Bellerby, R. G. J.: Discrete carbonate chemistry measured during the M87/1 cruise in April 2012, PANGAEA, doi:http://doi.pangaea.de/10.1594/PANGAEA.830294, 2014.

Bibby, T. S. and Moore, C. M.: Silicate:nitrate ratios of upwelled waters control the phytoplankton community sustained by mesoscale eddies in sub-tropical North Atlantic and Pacific, Biogeosciences, 8, 657-666, doi:10.5194/bg-8-657-2011, 2011.

Billard, C. and Inouye, I.: What is new in coccolithophore biology? In: Coccolithophores: from molecular processes to global impact, Thierstein, H. R. and Young, J. R. (Eds.), Springer, Berlin 1-29, 2004.

Blasco, D., Estrada, M., and Jones, B.: Relationship between the phytoplankton distribution and composition and the hydrography in the northwest African upwelling region near Cabo Corbeiro, Deep Sea Research Part A. Oceanographic Research Papers, 27, 799-821, doi:10.1016/0198-0149(80)90045-X, 1980.

Bown, P. R., Lees, J. A., and Young, J. R.: Calcareous nannoplankton evolution and diversity through time. In: Coccolithophores: from molecular processes to global impact, Thierstein, H. R. and Young, J. R. (Eds.), Springer, Berlin, 481-508, 2004.

Boyd, P. and Newton, P.: Evidence of the potential influence of planktonic community structure on the interannual variability of particulate organic carbon flux, Deep Sea Research Part I: Oceanographic Research Papers, 42, 619-639, doi:10.1016/0967-0637(95)00017-Z, 1995.

Boyd, P. W. and Trull, T. W.: Understanding the export of biogenic particles in oceanic waters: Is there consensus?, Progress In Oceanography, 72, 276-312, doi:10.1016/j.pocean.2006.10.007, 2007.

Braarud, T.: The temperature range of the non-motile stage of *Coccolithus pelagicus* in the North Atlantic region, British Phycological Journal, 14, 349-352, doi:10.1080/00071617900650391, 1979.

Bradshaw, A. L., Brewer, P. G., Shafer, D. K., and Williams, R. T.: Measurements of total carbon dioxide and alkalinity by potentiometric titration in the GEOSECS program, Earth and Planetary Science Letters, 55, 99-115, doi:10.1016/0012-821X(81)90090-X, 1981.

Brand, L. E.: Physiological ecology of marine coccolithophores. In: Coccolithophores, Winter, A. and Siesser, W. G. (Eds.), Cambridge University Press, Cambridge, 39-49, 1994.

Brody, S. R. and Lozier, M. S.: Changes in dominant mixing length scales as a driver of subpolar phytoplankton bloom initiation in the North Atlantic, Geophysical Research Letters, 41, 3197-3203, doi:10.1002/2014GL059707, 2014.

Broecker, W. and Clark, E.: Ratio of coccolith $CaCO_3$ to foraminifera $CaCO_3$ in late holocene deep sea sediments, Paleoceanography, 24, PA3205, doi:10.1029/2009PA001731, 2009.

Broecker, W. S. and Peng, T. H.: The role of $CaCO_3$ compensation in the glacial to interglacial atmospheric CO_2 change, Global Biogeochemical Cycles, 1, 15-29, doi:10.1029/GB001i001p00015, 1987.

Broerse, A. T. C., Ziveri, P., van Hinte, J. E., and Honjo, S.: Coccolithophore export production, species composition, and coccolith-$CaCO_3$ fluxes in the NE Atlantic (34°N 21°W and 48°N 21°W), Deep Sea Research Part II, 47, 1877-1905, doi:10.1016/S0967-0645(00)00010-2, 2000.

Brown, L., Sanders, R., Savidge, G., and Lucas, C. H.: The uptake of silica during the spring bloom in the Northeast Atlantic Ocean, Limnology and Oceanography, 48, 1831-1845, doi:10.4319/lo.2003.48.5.1831, 2003.

Brown, S. L., Landry, M. R., Selph, K. E., Jin Yang, E., Rii, Y. M., and Bidigare, R. R.: Diatoms in the desert: Plankton community response to a mesoscale eddy in the subtropical North Pacific, Deep Sea Research Part II: Topical Studies in Oceanography, 55, 1321-1333, doi:10.1016/j.dsr2.2008.02.012, 2008.

Brownlee, C. and Taylor, A. R.: Calcification in coccolithophores: A cellular perspective. In: Coccolithophores: from molecular processes to global impact, Thierstein, H. R. and Young, J. R. (Eds.), Springer, Berlin, 31-50, 2004.

Buitenhuis, E. T., Pangerc, T., Franklin, D. J., Le Quéré, C., and Malin, G.: Growth rates of six coccolithophorid strains as a function of temperature, Limnology and Oceanography, 53, 1181-1185, doi:10.4319/lo.2008.53.3.1181, 2008.

Cabeçadas, L. and Oliveira, A.: Impact of a *Coccolithus braarudii* bloom on the carbonate system of Portuguese coastal waters, Journal of Nannoplankton Research, 27, 141-147, 2005.

Cachao, M. and Moita, M.: *Coccolithus pelagicus*, a productivity proxy related to moderate fronts off Western Iberia, Marine Micropaleontology, 39, 131-155, doi:10.1016/S0377-8398(00)00018-9, 2000.

Charalampopoulou, A., Poulton, A. J., Tyrrell, T., and Lucas, M. I.: Irradiance and pH affect coccolithophore community composition on a transect between the North Sea and the Arctic Ocean, Marine Ecology Progress Series, 431, 25-43, doi:10.3354/meps09140, 2011.

Chisholm, S. W.: Oceanography: Stirring times in the Southern Ocean, Nature, 407, 685-687, doi:10.1038/35037696, 2000.

Ciais, P., Sabine, C., Bala, G., Bopp, L., Brovkin, V., Canadell, J., Chhabra, A., DeFries, R., Galloway, J., Heimann, M., Jones, C., Le Quéré, C., Myneni, R. B., Piao, S., and Thornton, P.: Carbon and other biogeochemical cycles. In: Climate change 2013: the

physical science basis. Contribution of working group I to the fifth assessment report of the intergovernmental panel on climate change, Stocker, T. F., Qin, D., Plattner, G.-K., Tignor, M., Allen, S. K., Boschung, J., Nauels, A., Xia, Y., Bex, V., and Midgley, P. M. (Eds.), Cambridge University Press, Cambridge, United Kingdom and New York, NY, USA, 2013.

Clarke, K. R.: Non-parametric multivariate analyses of changes in community structure, Australian Journal of Ecology, 18, 117-143, doi:10.1111/j.1442-9993.1993.tb00438.x, 1993.

Cottier, F., Hwang, P., and Drysdale, L.: JR271 physical oceanography analysis for ocean acidification cruise, SAMS Internal Report, 290, 31, 2014.

Cubillos, J. C., Henderiks, J., Beaufort, L., Howard, W. R., and Hallegraeff, G. M.: Reconstructing calcification in ancient coccolithophores: Individual coccolith weight and morphology of *Coccolithus pelagicus* (sensu lato), Marine Micropaleontology, 92-93, 29-39, doi:10.1016/j.marmicro.2012.04.005, 2012.

Dale, T., Rey, F., and Heimdal, B. R.: Seasonal development of phytoplankton at a high latitude oceanic site, Sarsia, 84, 419-435, doi:10.1080/00364827.1999.10807347, 1999.

Daniels, C. J., Tyrrell, T., Poulton, A. J., and Pettit, L.: The influence of lithogenic material on particulate inorganic carbon measurements of coccolithophores in the Bay of Biscay, Limnology and Oceanography, 57, 145-153, doi:10.4319/lo.2012.57.1.0145, 2012.

Daniels, C. J. and Poulton, A. J.: Chlorophyll-a, primary production rates, carbon concentrations and cell counts of coccolithophores, diatoms and microzooplankton measured in water samples from the North Atlantic during the M87/1 cruise in April 2012, PANGAEA, doi:http://doi.pangaea.de/10.1594/PANGAEA.823595, 2013.

Daniels, C. J., Mirza, J., and Poulton, A. J.: Coccolithophore abundances from CTD niskin samples in the North Atlantic Ocean on cruises D350, D351 and D354, British

Oceanographic Data Centre - Natural Environment Research Council, UK, doi:10/wqr, 2014a.

Daniels, C. J., Tyrrell, T., Poulton, A. J., and Young, J. R.: A mixed life-cycle stage bloom of *Syracosphaera bannockii* (Borsetti and Cati, 1976) Cros et al. 2000 (Bay of Biscay, April 2010), Journal of Nannoplankton Research, 34, 31-35, 2014b.

de Vargas, C., Aubry, M., Probert, I., and Young, J. R.: Origin and evolution of coccolithophores: From coastal hunters to oceanic farmers. In: Evolution of Primary Producers in the Sea, Falkowski, P. G. and Knoll, A. H. (Eds.), Academic Press, Burlington, 251-285, 2007.

Dickson, A. G. and Millero, F. J.: A comparison of the equilibrium constants for the dissociation of carbonic acid in seawater media, Deep Sea Research, 34, 1733-1743, doi:10.1016/0198-0149(87)90021-5, 1987.

Dickson, A. G.: Thermodynamics of the dissociation of boric acid in synthetic sea water from 273.15 to 318.15 K, Deep Sea Research, 37, 755-766, doi:10.1016/0198-0149(90)90004-F, 1990a.

Dickson, A. G.: Standard potential of the reaction: AgCl(s) + 1/2H_2(g) = Ag(s) + HCl(aq), and the standard acidity constant of the ion HSO_4^- in synthetic seawater from 273.15 to 318.15 K, Journal of Chemical Themodynamics, 22, 113-127, doi:10.1016/0021-9614(90)90074-Z, 1990b.

Dickson, A. G., Sabine, C. L., and Christian, J. R.: Guide to best practices for ocean CO_2 measurements, PICES Special Publication 3, 2007.

Dickson, A. G.: Standards for ocean measurements, Oceanography, 23, 34-47, doi:10.5670/oceanog.2010.22, 2010.

Doney, S., Fabry, V., Feely, R., and Kleypas, J.: Ocean acidification: The other CO_2 problem, Annual Review of Marine Science, 1, 169-192, doi:10.1146/annurev.marine.010908.163834, 2009.

Eilertsen, H. C.: Spring blooms and stratification, Nature, 363, 24-24, doi:10.1038/363024a0, 1993.

Eppley, R. W.: Temperature and phytoplankton growth in the sea, Fishery Bulletin, 70, 1063-1085, 1972.

Esposito, M. and Martin, A. P.: Nutrient concentrations of water samples collected by CTD-rosettes during the cruise M87/1 in April 2012, PANGAEA, doi:10.1594/PANGAEA.823681, 2013.

Falkowski, P., Scholes, R. J., Boyle, E., Canadell, J., Canfield, D., Elser, J., Gruber, N., Hibbard, K., Högberg, P., Linder, S., Mackenzie, F. T., Moore III, B., Pedersen, T., Rosenthal, Y., Seitzinger, S., Smetacek, V., and Steffen, W.: The global carbon cycle: A test of our knowledge of Earth as a system, Science, 290, 291-296, doi:10.1126/science.290.5490.291, 2000.

Falkowski, P. G. and Raven, J. A.: Aquatic photosynthesis, Princeton University Press, 2007.

Fernandez, E., Boyd, P., Holligan, P. M., and Harbour, D. S.: Production of organic and inorganic carbon within a large-scale coccolithophore bloom in the northeast Atlantic Ocean, Marine Ecology Progress Series, 97, 271-285, doi:10.3354/meps097271, 1993.

Finkel, Z. V., Beardall, J., Flynn, K. J., Quigg, A., Rees, T. A. V., and Raven, J. A.: Phytoplankton in a changing world: Cell size and elemental stoichiometry, Journal of Plankton Research, 32, 119-137, doi:10.1093/plankt/fbp098, 2009.

Fiorini, S., Middelburg, J. J., and Gattuso, J. P.: Effects of elevated CO_2 partial pressure and temperature on the coccolithophore *Syracosphaera pulchra*, Aquatic Microbial Ecology, 64, 221-232, doi:10.3354/ame01520, 2011.

Fischer, A. D., Moberg, E. A., Alexander, H., Brownlee, E. F., Hunter-Cevera, K. R., Pitz, K. J., Rosengard, S. Z., and Sosik, H. M.: Sixty years of Sverdrup: A retrospective of progress in the study of phytoplankton blooms, Oceanography, 27, 222-235, doi:10.5670/oceanog.2014.26, 2014.

Frada, M., Probert, I., Allen, M. J., Wilson, W. H., and de Vargas, C.: The "Cheshire Cat" escape strategy of the coccolithophore *Emiliania huxleyi* in response to viral infection, Proceedings of the National Academy of Sciences, 105, 15944-15949, doi:10.1073/pnas.0807707105, 2008.

Frada, M., Young, J. R., Cachao, M., Lino, S., Martins, A., Narciso, A., Probert, I., and de Vargas, C.: A guide to extant coccolithophores (Calcihaptophycidae, Haptophyta) using light microscopy, Journal of Nannoplankton Research, 31, 58-112, 2010.

Frada, M. J., Bidle, K. D., Probert, I., and de Vargas, C.: In situ survey of life cycle phases of the coccolithophore *Emiliania huxleyi* (Haptophyta), Environmental Microbiology, 14, 1558-1569, doi:10.1111/j.1462-2920.2012.02745.x, 2012.

Fritz, J. J. and Balch, W. M.: A light-limited continuous culture study of *Emiliania huxleyi*: Determination of coccolith detachment and its relevance to cell sinking, Journal of Experimental Marine Biology and Ecology, 207, 127-147, doi:10.1016/s0022-0981(96)02633-0, 1996.

Geisen, M., Billard, C., Broerse, A. T. C., Cros, L., Probert, I., and Young, J. R.: Life-cycle associations involving pairs of holococcolithophorid species: Intraspecific variation or cryptic speciation?, European Journal of Phycology, 37, 531-550, doi:10.1017/S0967026202003852, 2002.

Geisen, M., Young, J. R., Probert, I., Sáez, A. G., Baumann, A., Sprengel, C., Bollmann, J., Cros, L., De vargas, C., and Medlin, L. K.: Species level variation in coccolithophores. In: Coccolithophores: from molecular processes to global impact, Thierstein, H. R. and Young, J. R. (Eds.), Springer, Berlin, 313-352, 2004.

Gerecht, A. C., Šupraha, L., Edvardsen, B., Probert, I., and Henderiks, J.: High temperature decreases the PIC / POC ratio and increases phosphorus requirements in *Coccolithus pelagicus* (Haptophyta), Biogeosciences, 11, 3531-3545, doi:10.5194/bg-11-3531-2014, 2014.

Gibbs, S. J., Poulton, A. J., Bown, P. R., Daniels, C. J., Hopkins, J., Young, J. R., Jones, H. L., Thiemann, G. J., O'Dea, S. A., and Newsam, C.: Species-specific growth response

of coccolithophores to Palaeocene-Eocene environmental change, Nature Geoscience, 6, 218-222, doi:10.1038/ngeo1719, 2013.

Giering, S. L., Sanders, R., Lampitt, R. S., Anderson, T. R., Tamburini, C., Boutrif, M., Zubkov, M. V., Marsay, C. M., Henson, S. A., and Saw, K.: Reconciliation of the carbon budget in the ocean's twilight zone, Nature, 507, 480-483, doi:10.1038/nature13123, 2014.

Giering, S. L. C., Sanders, R., Martin, A. P., Lindemann, C., Daniels, C. J., Mayor, D. J., and St. John, M. A.: High export via small particles before the onset of the North Atlantic spring bloom, Global Biogeochemical Cycles, *in review*.

Giraudeau, J., Monteiro, P., and Nikodemus, K.: Distribution and malformation of living coccolithophores in the northern Benguela upwelling system off Namibia, Marine Micropaleontology, 22, 93-110, doi:10.1016/0377-8398(93)90005-I, 1993.

Guiry, M. D.: How many species of algae are there?, Journal of Phycology, 48, 1057-1063, doi:10.1111/j.1529-8817.2012.01222.x, 2012.

Hallegraeff, G.: Coccolithophorids (calcareous nanoplankton) from Australian waters, Botanica marina, 27, 229-248, doi:10.1515/botm.1984.27.6.229, 1984.

Henson, S. A., Dunne, J. P., and Sarmiento, J. L.: Decadal variability in North Atlantic phytoplankton blooms, Journal of Geophysical Research, 114, C04013, doi:10.1029/2008JC005139, 2009.

Henson, S. A., Sanders, R., Madsen, E., Morris, P. J., Le Moigne, F., and Quartly, G. D.: A reduced estimate of the strength of the ocean's biological carbon pump, Geophysical Research Letters, 38, L04606, doi:10.1029/2011GL046735, 2011.

Henson, S. A., Painter, S. C., Penny Holliday, N., Stinchcombe, M. C., and Giering, S. L. C.: Unusual subpolar North Atlantic phytoplankton bloom in 2010: Volcanic fertilization or North Atlantic Oscillation?, Journal of Geophysical Research: Oceans, 118, 4771-4780, doi:10.1002/jgrc.20363, 2013.

Hinz, D. J., Poulton, A. J., Nielsdóttir, M. C., Steigenberger, S., Korb, R. E., Achterberg, E. P., and Bibby, T. S.: Comparative seasonal biogeography of mineralising nannoplankton in the scotia sea: *Emiliania huxleyi*, *Fragilariopsis* spp. and *Tetraparma pelagica*, Deep Sea Research Part II: Topical Studies in Oceanography, 59–60, 57-66, doi:10.1016/j.dsr2.2011.09.002, 2012.

Hoffman, R., Kirchlechner, C., Langer, G., Wochnik, A. S., Griesshaber, E., Schmahl, W. W., and Scheu, C.: Insight into *Emiliania huxleyi* coccospheres by focused ion beam sectioning, Biogeosciences, 12, 825-834, doi:10.5194/bg-12-825-2015, 2015.

Holligan, P. M., Viollier, M., Harbour, D. S., Camus, P., and Champagne-Philippe, M.: Satellite and ship studies of coccolithophore production along a continental shelf edge, Nature, 304, 339-342, doi:10.1038/304339a0, 1983.

Holligan, P. M., Fernandez, E., Aiken, J., Balch, W. M., Boyd, P., Burkill, P. H., Finch, M., Groom, S. B., Malin, G., Muller, K., Purdie, D. A., Robinson, C., Trees, C. C., Turner, S. M., and Vanderwal, P.: A biogeochemical study of the coccolithophore, *Emiliania huxleyi*, in the North Atlantic, Global Biogeochemical Cycles, 7, 879-900, doi:10.1029/93GB01731, 1993.

Hopkins, J., Henson, S. A., Painter, S. C., Tyrrell, T., and Poulton, A. J.: Phenological characteristics of global coccolithophore blooms, Global Biogeochemical Cycles, 29, 239-253, doi:10.1002/2014GB004919, 2015.

Hoppe, C., Langer, G., and Rost, B.: *Emiliania huxleyi* shows identical responses to elevated pCO_2 in TA and DIC manipulations, Journal of Experimental Marine Biology and Ecology, 406, 54-62, doi:10.1016/j.jembe.2011.06.008, 2011.

Houdan, A., Billard, C., Marie, D., Not, F., Sáez, A. G., Young, J. R., and Probert, I.: Holococcolithophore-heterococcolithophore (Haptophyta) life cycles: Flow cytometric analysis of relative ploidy levels, Systematics and Biodiversity, 1, 453-465, doi:10.1017/S1477200003001270, 2004.

Houdan, A., Probert, I., Van Lenning, K., and Lefebvre, S.: Comparison of photosynthetic responses in diploid and haploid life-cycle phases of *Emiliania*

huxleyi (Prymnesiophyceae), Marine Ecology Progress Series, 292, 139-146, doi:10.3354/meps292139, 2005.

Houdan, A., Probert, I., Zatylny, C., Véron, B., and Billard, C.: Ecology of oceanic coccolithophores. I. Nutritional preferences of the two stages in the life cycle of *Coccolithus braarudii* and *Calcidiscus leptoporus*, Aquatic Microbial Ecology, 44, 291-301, doi:10.3354/ame044291, 2006.

Huisman, J., van Oostveen, P., and Weissing, F. J.: Critical depth and critical turbulence: Two different mechanisms for the development of phytoplankton blooms, Limnology and Oceanography, 44, 1781-1787, doi:10.4319/lo.1999.44.7.1781, 1999.

Hurst, J.: Phytoplankton community composition and export in the Irminger and Iceland Basins, MSc, Ocean and Earth Sciences, University of Southampton, 79 pp., 2011.

Hutchins, D. A.: Oceanography: Forecasting the rain ratio, Nature, 476, 41-42, doi:10.1038/476041a, 2011.

Hutchinson, G. E.: The paradox of the plankton, American Naturalist, 137-145, 1961.

Iglesias-Rodriguez, M. D., Halloran, P. R., Rickaby, R. E. M., Hall, I. R., Colmenero-Hidalgo, E., Gittins, J. R., Green, D. R. H., Tyrrell, T., Gibbs, S. J., and Von Dassow, P.: Phytoplankton calcification in a high-CO_2 world, Science, 320, 336, doi:10.1126/science.1154122, 2008.

IPCC: Contribution of Working Group I to the Fourth Assessment Report of the Intergovernmental Panel on Climate Change, 2007. Solomon, S., Qin, D., Manning, M., Chen, Z., Marquis, M., Averyt, K. B., Tignor, M., and Miller, H. L. (Eds.), Cambridge University Press, Cambridge, United Kingdom and New York, NY, USA, 2007.

Johannessen, O. M.: Brief overview of the physical oceanography. In: The Nordic Seas, Hurdle, B. G. (Ed.), Springer, Berlin, 103-127, 1986.

Johnson, K. M., Sieburth, J. M., Williams, P. J., and Brandström, L.: Coulometric total carbon analysis for marine studies: Automation and calibration, Marine Chemistry, 21, 117-133, doi:10.1016/0304-4203(93)90201-X, 1987.

Joint, I., Pomroy, A., Savidge, G., and Boyd, P.: Size-fractionated primary productivity in the northeast Atlantic in May–July 1989, Deep Sea Research Part II: Topical Studies in Oceanography, 40, 423-440, doi:10.1016/0967-0645(93)90025-i, 1993.

Kara, A. B., Rochford, P. A., and Hurlburt, H. E.: An optimal definition for ocean mixed layer depth, Journal of Geophysical Research: Oceans, 105, 16803-16821, doi:10.1029/2000JC900072, 2000.

Keller, M. D., Selvin, R. C., Claus, W., and Guillard, R. R. L.: Media for the culture of oceanic ultraphytoplankton, Journal of Phycology, 23, 633-638, doi:10.1111/j.1529-8817.1987.tb04217.x, 1987.

Kenitz, K., Williams, R. G., Sharples, J., Selsil, Ö., and Biktashev, V. N.: The paradox of the plankton: species competition and nutrient feedback sustain phytoplankton diversity, Marine Ecology Progress Series, 490, 107-119, doi:10.3354/meps10452, 2013.

Kirk, J. T. O.: Light and photosynthesis in aquatic ecosystems, Cambridge University Press, Cambridge, 1994.

Klaas, C. and Archer, D. E.: Association of sinking organic matter with various types of mineral ballast in the deep sea: Implications for the rain ratio, Global Biogeochemical Cycles, 16, 1116, doi:10.1029/2001GB00176510.1029/2001GB001765, 2002.

Kleijne, A.: Holococcolithophorids from the Indian Ocean, Red Sea, Mediterranean Sea and North Atlantic Ocean, Marine Micropaleontology, 17, 1-76, doi:10.1016/0377-8398(91)90023-Y, 1991.

Krug, S., Schulz, K., and Riebesell, U.: Effects of changes in carbonate chemistry speciation on *Coccolithus braarudii*: A discussion of coccolithophorid sensitivities, Biogeosciences, 8, 771-777, doi:10.5194/bg-8-771-2011, 2011.

Langer, G., Geisen, M., Baumann, K., Kläs, J., Riebesell, U., Thoms, S., and Young, J.: Species-specific responses of calcifying algae to changing seawater carbonate chemistry, Geochemistry Geophysics Geosystems, 7, Q09006, doi:10.1029/2005GC001227, 2006.

Langer, G., Nehrke, G., Probert, I., Ly, J., and Ziveri, P.: Strain-specific responses of *Emiliania huxleyi* to changing seawater carbonate chemistry, Biogeosciences, 6, 2637-2646, doi:10.5194/bg-6-2637-2009, 2009.

Langer, G., Oetjen, K., and Brenneis, T.: Coccolithophores do not increase particulate carbon production under nutrient limitation: A case study using *Emiliania huxleyi* (PML B92/11), Journal of Experimental Marine Biology and Ecology, 443, 155-161, doi:10.1016/j.jembe.2013.02.040, 2013.

Leblanc, K., Hare, C. E., Feng, Y., Berg, G. M., DiTullio, G. R., Neeley, A., Benner, I., Sprengel, C., Beck, A., Sanudo-Wilhelmy, S. A., Passow, U., Klinck, K., Rowe, J. M., Wilhelm, S. W., Brown, C. W., and Hutchins, D. A.: Distribution of calcifying and silicifying phytoplankton in relation to environmental and biogeochemical parameters during the late stages of the 2005 North East Atlantic Spring Bloom, Biogeosciences, 6, 2155-2179, doi:10.5194/bg-6-2155-2009, 2009.

Lee, K., Kim, T.-W., Byrne, R. H., Millero, F. J., Feely, R. A., and Liu, Y.-M.: The universal ratio of boron to chlorinity for the North Pacific and North Atlantic oceans, Geochimica et Cosmochimica Acta, 74, 1801-1811, doi:10.1016/j.gca.2009.12.027, 2010.

Legendre, L. and Gosseline, M.: Estimation of N and C uptake rates by phytoplankton using ^{15}N or ^{13}C: revisiting the usual computation formulae, Journal of Plankton Research, 19, 263-271, doi:10.1093/plankt/19.2.263, 1996.

Lewis, E. and Wallace, D. W. R.: Program developed for CO_2 system calculations. ORNL/CDIAC-105. Carbon Dioxide Information Analysis Center, O. R. N. L., U.S. Department of Energy, Oak Ridge, Tennessee (Ed.), 1998.

Lewis, W. M.: Surface/volume ratio: implications for phytoplankton morphology, Science, 192, 885-887, doi:10.1126/science.192.4242.885, 1976.

Leynaert, A., Tréguer, P., Lancelot, C., and Rodier, M.: Silicon limitation of biogenic silica production in the Equatorial Pacific, Deep Sea Research Part I: Oceanographic Research Papers, 48, 639-660, doi:10.1016/S0967-0637(00)00044-3, 2001.

Lindemann, C. and St. John, M. A.: A seasonal diary of phytoplankton in the North Atlantic, Frontiers in Marine Science, 1, 37, doi:10.3389/fmars.2014.00037, 2014.

Lochte, K., Ducklow, H. W., Fasham, M. J. R., and Stienen, C.: Plankton succession and carbon cycling at 47°N 20°W during the JGOFS North Atlantic Bloom Experiment, Deep Sea Research Part II: Topical Studies in Oceanography, 40, 91-114, doi:10.1016/0967-0645(93)90008-b, 1993.

Lohbeck, K. T., Riebesell, U., and Reusch, T. B.: Adaptive evolution of a key phytoplankton species to ocean acidification, Nature Geoscience, 5, 346-351, doi:10.1038/ngeo1441, 2012.

Lueker, T. J., Dickson, A. G., and Keeling, C. D.: Ocean pCO2 calculated from dissolved inorganic carbon, alkalinity, and equations for K_1 and K_2: validation based on laboratory measurements of CO_2 in gas and seawater at equilibrium, Marine Chemistry, 70, 1801-1811, 2000.

Mahadevan, A., D'Asaro, E., Lee, C., and Perry, M. J.: Eddy-driven stratification initiates North Atlantic spring phytoplankton blooms, Science, 337, 54-58, doi:10.1126/science.1218740, 2012.

Malin, G., Turner, S., Liss, P., Holligan, P., and Harbour, D.: Dimethylsulphide and dimethylsulphoniopropionate in the Northeast Atlantic during the summer coccolithophore bloom, Deep Sea Research Part I: Oceanographic Research Papers, 40, 1487-1508, doi:10.1016/0967-0637(93)90125-m, 1993.

Margalef, R.: Life-forms of phytoplankton as survival alternatives in an unstable environment, Oceanologica acta, 1, 493-509, 1978.

Martin, A.: The kaleidoscope ocean, Philosophical Transactions of the Royal Society A: Mathematical, Physical and Engineering Sciences, 363, 2873-2890, doi:10.1098/rsta.2005.1663, 2005.

McIntyre, A. and Bé, A. W. H.: Modern coccolithophoridae of the Atlantic Ocean—I. Placoliths and cyrtoliths, Deep Sea Research and Oceanographic Abstracts, 14, 561-597, doi:10.1016/0011-7471(67)90065-4, 1967.

McIntyre, A., Bé, A., and Roche, M.: Modern pacific coccolithophorida: A paleontological thermometer, Transactions of the New York Academy of Sciences, 32, 720-731, doi:10.1111/j.2164-0947.1970.tb02746.x, 1970.

McQuoid, M. R. and Godhe, A.: Recruitment of coastal planktonic diatoms from benthic versus pelagic cells: Variations in bloom development and species composition, Limnology and Oceanography, 49, 1123-1133, doi:10.4319/lo.2004.49.4.1123, 2004.

Menden-Deuer, S. and Lessard, E. J.: Carbon to volume relationships for dinoflagellates, diatoms, and other protist plankton, Limnology and Oceanography, 45, 569-579, doi:10.4319/lo.2000.45.3.0569, 2000.

Miller, C. B.: Biological Oceanography, Wiley-Blackwell, Oxford, 2003.

Milliman, J. D.: Coccolithophorid production and sedimentation, Rockall Bank, Deep Sea Research Part A. Oceanographic Research Papers, 27, 959-963, doi:10.1016/0198-0149(80)90007-2, 1980.

Mitchell-Innes, B. and Winter, A.: Coccolithophores: A major phytoplankton component in mature upwelled waters off the Cape Peninsula, South Africa in March, 1983, Marine Biology, 95, 25-30, doi:10.1007/BF00447481, 1987.

Moore, C. M., Lucas, M. I., Sanders, R., and Davidson, R.: Basin-scale variability of phytoplankton bio-optical characteristics in relation to bloom state and community structure in the Northeast Atlantic, Deep Sea Research Part I: Oceanographic Research Papers, 52, 401-419, doi:10.1016/j.dsr.2004.09.003, 2005.

Moore, C. M., Mills, M. M., Milne, A., Langlois, R., Achterberg, E. P., Lochte, K., Geider, R. J., and La Roche, J.: Iron limits primary productivity during spring bloom development in the central North Atlantic, Global Change Biology, 12, 626-634, doi:10.1111/j.1365-2486.2006.01122.x, 2006.

Moore, C. M., Mills, M. M., Achterberg, E. P., Geider, R. J., LaRoche, J., Lucas, M. I., McDonagh, E. L., Pan, X., Poulton, A. J., and Rijkenberg, M. J.: Large-scale distribution of Atlantic nitrogen fixation controlled by iron availability, Nature Geoscience, 2, 867-871, doi:10.1038/ngeo667, 2009.

Nielsdóttir, M. C., Moore, C. M., Sanders, R., Hinz, D. J., and Achterberg, E. P.: Iron limitation of the postbloom phytoplankton communities in the Iceland Basin, Global Biogeochemical Cycles, 23, GB3001, doi:10.1029/2008GB003410, 2009.

O'Dea, S. A., Gibbs, S. J., Bown, P. R., Young, J. R., Poulton, A. J., Newsam, C., and Wilson, P. A.: Coccolithophore calcification response to past ocean acidification and climate change, Nature Communications, 5, doi:10.1038/ncomms6363, 2014.

Okada, H. and McIntyre, A.: Seasonal distribution of modern coccolithophores in the western North Atlantic Ocean, Marine Biology, 54, 319-328, doi:10.1007/BF00395438, 1979.

Olson, M. B. and Strom, S. L.: Phytoplankton growth, microzooplankton herbivory and community structure in the southeast Bering Sea: insight into a formation and persistence of an *Emiliania huxleyi* bloom, Deep Sea Research Part II: Topical Studies in Oceanography, 49, 5969-5990, doi:10.1016/S0967-0645(02)00329-6, 2002.

Paasche, E.: Marine plankton algae grown with light-dark cycles. 1. *Coccolithus huxleyi*, Physiologia Plantarum, 20, 946-956, doi:10.1111/j.1399-3054.1967.tb08382.x, 1967.

Paasche, E. and Brubak, S.: Enhanced calcification in the coccolithophorid *Emiliania huxleyi* (Haptophyceae) under phosphorus limitation, Phycologia, 33, 324-330, doi:10.2216/i0031-8884-33-5-324.1, 1994.

Paasche, E.: A review of the coccolithophorid *Emiliania huxleyi* (Prymnesiophyceae), with particular reference to growth, coccolith formation, and calcification-photosynthesis interactions, Phycologia, 40, 503-529, doi:10.2216/i0031-8884-40-6-503.1, 2002.

Parekh, P., Dutkiewicz, S., Follows, M. J., and Ito, T.: Atmospheric carbon dioxide in a less dusty world, Geophysical Research Letters, 33, L03610, doi:10.1029/2005GL025098, 2006.

Parke, M. and Adams, I.: The motile (*Crystallolithus hyalinus* Gaarder & Markali) and non-motile phases in the life history of *Coccolithus pelagicus* (Wallich) Schiller, Journal of the Marine Biological Association of the United Kingdom, 39, 263-274, doi:10.1017/S002531540001331X, 1960.

Paulsen, M. L., Riisgaard, K., and Nielsen, T. G.: Abundance of pico- and nanophytoplankton during the Meteor cruise M87/1, PANGAEA, doi:http://doi.pangaea.de/10.1594/PANGAEA.839416, 2014.

Pei, S. and Laws, E. A.: Does the ^{14}C method estimate net photosynthesis? Implications from batch and continuous culture studies of marine phytoplankton, Deep Sea Research Part I: Oceanographic Research Papers, 82, 1-9, doi:10.1016/j.dsr.2013.07.011, 2013.

Poulton, A. J., Sanders, R., Holligan, P. M., Stinchcombe, M. C., Adey, T. R., Brown, L., and Chamberlain, K.: Phytoplankton mineralization in the tropical and subtropical Atlantic Ocean, Global Biogeochemical Cycles, 20, GB4002, doi:10.1029/2006GB002712, 2006.

Poulton, A. J., Adey, T. R., Balch, W. M., and Holligan, P. M.: Relating coccolithophore calcification rates to phytoplankton community dynamics: Regional differences and implications for carbon export, Deep Sea Research Part II, 54, 538-557, doi:10.1016/j.dsr2.2006.12.003, 2007.

Poulton, A. J., Charalampopoulou, A., Young, J. R., Tarran, G. A., Lucas, M. I., and Quartly, G. D.: Coccolithophore dynamics in non-bloom conditions during late

summer in the central Iceland Basin (July–August 2007), Limnology and Oceanography, 55, 1601-1613, doi:10.4319/lo.2010.55.4.1601, 2010.

Poulton, A. J., Young, J. R., Bates, N. R., and Balch, W. M.: Biometry of detached *Emiliania huxleyi* coccoliths along the patagonian shelf, Marine Ecology Progress Series, 443, 1-17, doi:10.3354/meps09445, 2011.

Poulton, A. J., Painter, S. C., Young, J. R., Bates, N. R., Bowler, B., Drapeau, D., Lyczsckowski, E., and Balch, W. M.: The 2008 *Emiliania huxleyi* bloom along the patagonian shelf: Ecology, biogeochemistry, and cellular calcification, Global Biogeochemical Cycles, 27, 2013GB004641, doi:10.1002/2013GB004641, 2013.

Poulton, A. J., Stinchcombe, M. C., Achterberg, E. P., Bakker, D. C. E., Dumousseaud, C., Lawson, H. E., Lee, G. A., Richier, S., Suggett, D. J., and Young, J. R.: Coccolithophores on the north-west European shelf: calcification rates and environmental controls, Biogeosciences, 11, 3919-3940, doi:10.5194/bg-11-3919-2014, 2014.

Probert, I. and Houdan, A.: The laboratory culture of coccolithophores. In: Coccolithophores: from molecular processes to global impact, Thierstein, H. R. and Young, J. R. (Eds.), Springer, Berlin, 217-250, 2004.

Probert, I., Fresnel, J., Billard, C., Geisen, M., and Young, J. R.: Light and electron microscope observations of *Algirosphaera robusta* (Prymnesiophyceae), Journal of Phycology, 43, 319-332, doi:10.1111/j.1529-8817.2007.00324.x, 2007.

Putt, M.: Abundance, chlorophyll content and photosynthetic rates of ciliates in the Nordic Seas during summer, Deep Sea Research Part A. Oceanographic Research Papers, 37, 1713-1731, doi:10.1016/0198-0149(90)90073-5, 1990.

Ragueneau, O. and Tréguer, P.: Determination of biogenic silica in coastal waters: applicability and limits of the alkaline digestion method, Marine Chemistry, 45, 43-51, doi:10.1016/0304-4203(94)90090-6, 1994.

Raitsos, D. E., Lavender, S. J., Pradhan, Y., Tyrrell, T., Reid, P. C., and Edwards, M.: Coccolithophore bloom size variation in response to the regional environment of

the subarctic North Atlantic, Limnology and Oceanography, 51, 2122-2130, doi:10.4319/lo.2006.51.5.2122, 2006.

Raven, J. A. and Crawfurd, K.: Environmental controls on coccolithophore calcification, Marine Ecology Progress Series, 470, 137-166, doi:10.3354/meps09993, 2012.

Redfield, A. C.: The biological control of chemical factors in the environment, American Scientist, 46, 205-221, 1958.

Rees, A. P., Joint, I., and Donald, K. M.: Early spring bloom phytoplankton-nutrient dynamics at the Celtic Sea Shelf Edge, Deep Sea Research Part I: Oceanographic Research Papers, 46, 483-510, doi:10.1016/s0967-0637(98)00073-9, 1999.

Richier, S., Achterberg, E. P., Dumousseaud, C., Poulton, A. J., Suggett, D. J., Tyrrell, T., Zubkov, M. V., and Moore, C. M.: Phytoplankton responses and associated carbon cycling during shipboard carbonate chemistry manipulation experiments conducted around Northwest European shelf seas, Biogeosciences, 11, 4733-4752, doi:10.5194/bg-11-4733-2014, 2014.

Riebesell, U., Zondervan, I., Rost, B., Tortell, P. D., Zeebe, R. E., and Morel, F. M. M.: Reduced calcification of marine plankton in response to increased atmospheric CO_2, Nature, 407, 364-367, doi:10.1038/35030078, 2000.

Rost, B. and Riebesell, U.: Coccolithophores and the biological pump: responses to environmental changes. In: Coccolithophores: from molecular processes to global impact, Springer, 99-125, 2004.

Ryan-Keogh, T. J., Macey, A. I., Nielsdóttir, M. C., Lucas, M. I., Steigenberger, S. S., Stinchcombe, M. C., Achterberg, E. P., Bibby, T. S., and Moore, C. M.: Spatial and temporal development of phytoplankton iron stress in relation to bloom dynamics in the high-latitude North Atlantic Ocean, Limnology and Oceanography, 58, 533-545, doi:10.4319/lo.2013.58.2.0533, 2013.

Rynearson, T., Richardson, K., Lampitt, R., Sieracki, M., Poulton, A., Lyngsgaard, M., and Perry, M.: Major contribution of diatom resting spores to vertical flux in the sub-

polar North Atlantic, Deep Sea Research Part I: Oceanographic Research Papers, 82, 60-71, doi:10.1016/j.dsr.2013.07.013, 2013.

Sabine, C. L., Feely, R. A., Gruber, N., Key, R. M., Lee, K., Bullister, J. L., Wanninkhof, R., Wong, C. S., Wallace, D. W. R., and Tilbrook, B.: The oceanic sink for anthropogenic CO_2, Science, 305, 367, doi:10.1126/science.1097403, 2004.

Sáez, A. G., Probert, I., Geisen, M., Quinn, P., Young, J. R., and Medlin, L. K.: Pseudo-cryptic speciation in coccolithophores, Proceedings of the National Academy of Sciences, 100, 7163, doi:10.1073/pnas.1132069100, 2003.

Sanders, R., Brown, L., Henson, S., and Lucas, M.: New production in the Irminger Basin during 2002, Journal of Marine Systems, 55, 291-310, doi:10.1016/j.jmarsys.2004.09.002, 2005.

Sanders, R., Morris, P. J., Stinchcombe, M., Seeyave, S., Venables, H., and Lucas, M.: New production and the *f* ratio around the Crozet Plateau in austral summer 2004–2005 diagnosed from seasonal changes in inorganic nutrient levels, Deep Sea Research Part II: Topical Studies in Oceanography, 54, 2191-2207, doi:10.1016/j.dsr2.2007.06.007, 2007.

Sanders, R., Morris, P., Poulton, A., Stinchcombe, M., Charalampopoulou, A., Lucas, M., and Thomalla, S.: Does a ballast effect occur in the surface ocean?, Geophysical Research Letters, 37, L08602, doi:10.1029/2010GL042574, 2010.

Sanders, R., Henson, S. A., Koski, M., De La Rocha, C. L., Painter, S. C., Poulton, A. J., Riley, J., Salihoglu, B., Visser, A., Yool, A., Bellerby, R., and Martin, A.: The biological carbon pump in the North Atlantic, Progress In Oceanography, 129, 200-218, doi:10.1016/j.pocean.2014.05.005, 2014.

Sarthou, G., Timmermans, K. R., Blain, S., and Tréguer, P.: Growth physiology and fate of diatoms in the ocean: a review, Journal of Sea Research, 53, 25-42, doi:10.1016/j.seares.2004.01.007, 2005.

Sato, T., Yuguchi, S., Takayama, T., and Kameo, K.: Drastic change in the geographical distribution of the cold-water nannofossil *Coccolithus pelagicus* (Wallich) Schiller at

2.74 Ma in the late Pliocene, with special reference to glaciation in the Arctic Ocean, Marine Micropaleontology, 52, 181-193, doi:10.1016/j.marmicro.2004.05.003, 2004.

Savidge, G., Boyd, P., Pomroy, A., Harbour, D., and Joint, I.: Phytoplankton production and biomass estimates in the northeast Atlantic Ocean, May–June 1990, Deep Sea Research Part I: Oceanographic Research Papers, 42, 599-617, doi:10.1016/0967-0637(95)00016-Y, 1995.

Schiebel, R., Brupbacher, U., Schmidtko, S., Nausch, G., Waniek, J. J., and Thierstein, H.-R.: Spring coccolithophore production and dispersion in the temperate eastern North Atlantic Ocean, Journal of Geophysical Research, 116, C08030, doi:10.1029/2010jc006841, 2011.

Schluter, L., Lohbeck, K. T., Gutowska, M. A., Groger, J. P., Riebesell, U., and Reusch, T. B. H.: Adaptation of a globally important coccolithophore to ocean warming and acidification, Nature Climate Change, 4, 1024-1030, doi:10.1038/nclimate2379, 2014.

Sheward, R. M., Daniels, C. J., and Gibbs, S. J.: Growth rates and biometric measurements of coccolithophores (*Coccolithus pelagicus*, *Coccolithus braarudii*, *Emiliania huxleyi*) during experiments, PANGAEA, doi:http://doi.pangaea.de/10.1594/PANGAEA.836841, 2014.

Siegel, D., Doney, S., and Yoder, J.: The North Atlantic spring phytoplankton bloom and Sverdrup's Critical Depth Hypothesis, Science, 296, 730, doi:10.1126/science.1069174, 2002.

Sieracki, M. E., Verity, P. G., and Stoecker, D. K.: Plankton community response to sequential silicate and nitrate depletion during the 1989 North Atlantic spring bloom, Deep Sea Research Part II: Topical Studies in Oceanography, 40, 213-225, doi:10.1016/0967-0645(93)90014-E, 1993.

Silva, A., Palma, S., and Moita, M. T.: Coccolithophores in the upwelling waters of portugal: Four years of weekly distribution in Lisbon bay, Continental Shelf Research, 28, 2601-2613, doi:10.1016/j.csr.2008.07.009, 2008.

Smetacek, V. S.: Role of sinking in diatom life-history cycles: ecological, evolutionary and geological significance, Marine Biology, 84, 239-251, doi:10.1007/BF00392493, 1985.

Smith, H. E. K., Tyrrell, T., Charalampopoulou, A., Dumousseaud, C., Legge, O. J., Birchenough, S., Pettit, L. R., Garley, R., Hartman, S. E., Hartman, M. C., Sagoo, N., Daniels, C. J., Achterberg, E. P., and Hydes, D. J.: Predominance of heavily calcified coccolithophores at low $CaCO_3$ saturation during winter in the Bay of Biscay, Proceedings of the National Academy of Sciences of the United States of America, 109, 8845-8849, doi:10.1073/pnas.1117508109, 2012.

Smyth, T. J., Allen, I., Atkinson, A., Bruun, J. T., Harmer, R. A., Pingree, R. D., Widdicombe, C. E., and Somerfield, P. J.: Ocean net heat flux influences seasonal to interannual patterns of plankton abundance, PLoS ONE, 9, e98709, doi:10.1371/journal.pone.0098709, 2014.

Society, R.: Ocean acidifcation due to increasing atmospheric carbon dioxide, The Royal Society, London, 2005.

Stoecker, D. K.: Mixotrophy among dinoflagellates, Journal of Eukaryotic Microbiology, 46, 397-401, doi:10.1111/j.1550-7408.1999.tb04619.x, 1999.

Stoll, H. M., Klaas, C. M., Probert, I., Ruiz Encinar, J., and Garcia Alonso, J. I.: Calcification rate and temperature effects on Sr partitioning in coccoliths of multiple species of coccolithophorids in culture, Global and Planetary Change, 34, 153-171, doi:10.1016/S0921-8181(02)00112-1, 2002.

Sverdrup, H.: On conditions for the vernal blooming of phytoplankton, Journal du Conseil International pour l'Exploration de la Mer, 18, 287-295, 1953.

Tarran, G. A., Zubkov, M. V., Sleigh, M. A., Burkill, P. H., and Yallop, M.: Microbial community structure and standing stocks in the NE Atlantic in June and July of 1996,

Deep Sea Research Part II: Topical Studies in Oceanography, 48, 963-985, doi:10.1016/S0967-0645(00)00104-1, 2001.

Taylor, A. R., Russell, M. A., Harper, G. M., Collins, T. f. T., and Brownlee, C.: Dynamics of formation and secretion of heterococcoliths by *Coccolithus pelagicus* ssp. *braarudii*, European Journal of Phycology, 42, 125-136, doi:10.1080/09670260601159346, 2007.

Taylor, J. R. and Ferrari, R.: Shutdown of turbulent convection as a new criterion for the onset of spring phytoplankton blooms, Limnology and Oceanography, 56, 2293, doi:10.4319/lo.2011.56.6.2293, 2011a.

Taylor, J. R. and Ferrari, R.: Ocean fronts trigger high latitude phytoplankton blooms, Geophysical Research Letters, 38, doi:10.1029/2011GL049312, 2011b.

Tett, P. and Barton, E.: Why are there about 5000 species of phytoplankton in the sea?, Journal of Plankton Research, 17, 1693-1704, doi:10.1093/plankt/17.8.1693, 1995.

Townsend, D. W., Keller, M. D., Sieracki, M. E., and Ackleson, S. G.: Spring phytoplankton blooms in the absence of vertical water column stratification, Nature, 360, 59-62, doi:10.1038/360059a0, 1992.

Townsend, D. W., Cammen, L. M., Holligan, P. M., Campbell, D. E., and Pettigrew, N. R.: Causes and consequences of variability in the timing of spring phytoplankton blooms, Deep Sea Research Part I: Oceanographic Research Papers, 41, 747-765, doi:10.1016/0967-0637(94)90075-2, 1994.

Tyrrell, T. and Merico, A.: *Emiliania huxleyi*: bloom observations and the conditions that induce them. In: Coccolithophores: from molecular processes to global impact, Thierstein, H. R. and Young, J. R. (Eds.), Springer, Berlin, 75-90, 2004.

Tyrrell, T. and Young, J. R.: Coccolithophores. In: Encylopedia of Ocean Sciences, Steele, J. H., Turekian, K. K., and Thorpe, S. A. (Eds.), Academic Press, Oxford, 606-614, 2009.

Van Heuven, S., Pierrot, D., Rae, J. W. B., Lewis, E., and Wallace, D. W. R.: CO2SYS v 1.1, MATLAB program developed for CO_2 system calculations. ORNL/CDIAC-105b. Carbon Dioxide Information Analysis Center, O. R. N. L., U.S DoE, Oak Ridge, TN (Ed.), 2011.

Volk, T. and Hoffert, M. I.: Ocean carbon pumps: Analysis of relative strengths and efficiencies in ocean-driven atmospheric CO_2 changes. In: The carbon cycle and atmospheric CO_2: Natural variations archean to present, American Geophysical Union, 99-110, 1985.

von Dassow, P., John, U., Ogata, H., Probert, I., Bendif, E. M., Kegel, J. U., Audic, S., Wincker, P., Da Silva, C., Claverie, J.-M., Doney, S., Glover, D. M., Flores, D. M., Herrera, Y., Lescot, M., Garet-Delmas, M.-J., and de Vargas, C.: Life-cycle modification in open oceans accounts for genome variability in a cosmopolitan phytoplankton, ISME J, doi:10.1038/ismej.2014.221, 2014.

Weiss, R. F.: Carbon dioxide in water and seawater: the solubility of a non-ideal gas, Marine Chemistry, 2, 203-215, doi:10.1016/0304-4203(74)90015-2, 1974.

Winter, A., Jordan, R. W., and Roth, P. H.: Biogeography of living coccolithophores in ocean waters. In: Coccolithophores, Winter, A. and Siesser, W. G. (Eds.), Cambridge University Press, Cambridge, 161-177, 1994.

Winter, A., Henderiks, J., Beaufort, L., Rickaby, R. E. M., and Brown, C. W.: Poleward expansion of the coccolithophore *Emiliania huxleyi*, Journal of Plankton Research, 36, 316-325, doi:10.1093/plankt/fbt110, 2013.

Wolf-Gladrow, D. A., Zeebe, R. E., Klaas, C., Körtzinger, A., and Dickson, A. G.: Total alkalinity: The explicit conservative expression and its application to biogeochemical processes, Marine Chemistry, 106, 287-300, doi:10.1016/j.marchem.2007.01.006, 2007.

Young, J. R.: Functions of coccoliths. In: Coccolithophores, Winter, A. and Siesser, W. G. (Eds.), Cambridge University Press, Cambridge, 63-82, 1994.

Young, J. R. and Ziveri, P.: Calculation of coccolith volume and its use in calibration of carbonate flux estimates, Deep Sea Research Part II, 47, 1679-1700, doi:10.1016/S0967-0645(00)00003-5, 2000.

Young, J. R., Geisen, M., Cros, L., Kleijne, A., Sprengel, C., Probert, I., and Ostergaard, J.: A guide to extant coccolithophore taxonomy, Journal of Nannoplankton Research Special Issue, 1, 1-132, 2003.

Young, J. R. and Henriksen, K.: Biomineralization within vesicles: the calcite of coccoliths, Reviews in mineralogy and geochemistry, 54, 189-215, 2003.

Young, J. R., Poulton, A. J., and Tyrrell, T.: Morphology of *Emiliania huxleyi* coccoliths on the northwestern European shelf – is there an influence of carbonate chemistry?, Biogeosciences, 11, 4771-4782, doi:10.5194/bg-11-4771-2014, 2014.

Ziveri, P., Broerse, A. T. C., van Hinte, J. E., Westbroek, P., and Honjo, S.: The fate of coccoliths at 48°N 21°W, northeastern Atlantic, Deep Sea Research Part II, 47, 1853-1875, doi:10.1016/S0967-0645(00)00009-6, 2000.

Ziveri, P., Baumann, K. H., Böckel, B., Bollmann, J., and Young, J. R.: Biogeography of selected holocene coccoliths in the Atlantic Ocean. In: Coccolithophores: from molecular processes to global impact, Thierstein, H. R. and Young, J. R. (Eds.), Springer, Berlin, 403-428, 2004.

Ziveri, P., de Bernardi, B., Baumann, K. H., Stoll, H. M., and Mortyn, P. G.: Sinking of coccolith carbonate and potential contribution to organic carbon ballasting in the deep ocean, Deep Sea Research Part II, 54, 659-675, doi:10.1016/j.dsr2.2007.01.006, 2007.

Zondervan, I.: The effects of light, macronutrients, trace metals and CO_2 on the production of calcium carbonate and organic carbon in coccolithophores—A review, Deep Sea Research Part II: Topical Studies in Oceanography, 54, 521-537, doi:10.1016/j.dsr2.2006.12.004, 2007.

Zubkov, M. V., Burkill, P. H., and Topping, J. N.: Flow cytometric enumeration of DNA-stained oceanic planktonic protists, Journal of Plankton Research, 29, 79-86, doi:10.1093/plankt/fbl059, 2007.